DEVELOPMENT OF A FLEXIBLE IMAGE-BASED APPROACH FOR STUDYING SIGNAL TRANSDUCTION IN ISOLATED ARTERIOLES

A Thesis
presented to
the Faculty of the Graduate School
at the University of Missouri-Columbia

In Partial Fulfillment
of the Requirements for the Degree

Master of Science

---

by
SRIKANTH R. ELLA

Dr. Michael A. Hill, Thesis Supervisor

AUGUST 2007

The undersigned, appointed by the dean of the Graduate School, have examined the thesis entitled

DEVELOPMENT OF A FLEXIBLE IMAGE-BASED APPROACH FOR STUDYING SIGNAL TRANSDUCTION IN ISOLATED ARTERIOLES

presented by Srikanth Ella,

a candidate for the degree of Master of Science,

and hereby certify that, in their opinion, it is worthy of acceptance.

Dr. Michael Hill, Biological Engineering,
Medical Pharmacology and Physiology

Dr. Michael Davis, Biological Engineering,
Medical Pharmacology and Physiology

Dr. Gerald Meininger, Medical Pharmacology and Physiology,
Dalton Cardiovascular Research Center

ACKNOWLEDGEMENTS

I thank all the people who helped me, in my project and encouraged me in completing my thesis. Firstly, I would like to thank Prof. Michael A. Hill for all his support, direction, motivation and encouragement all through my Masters. I express my gratitude to him for providing me an excellent opportunity to work and learn under his guidance. He took me on when I was in trouble and dealt with patience in teaching me the basics. I feel I have committed all the possible errors in my biological preparations and he has helped me learn from the mistakes and not repeat them. Without his guidance and assistance, this work wouldn't have been possible. I express my gratitude to the Dalton Cardiovascular Research Center and all its staff members for all their support.

I would like to thank Prof. Michael Davis, who first introduced me to Dr. Hill. He has also been a great co-supervisor for me and helped shaped both my project and thesis. I thank Prof. Gerald Meininger for helping me analyzing the data acquired in the experiments. Group meetings conducted by his lab each week have helped me in developing laboratory techniques, insight into solving practical problems and learning new biological concepts.

Jun Dong, a technician in Dr. Hill's lab was of great help to me in the performance of experiments. I thank her for her uncanny ability of cannulating arterioles onto glass pipettes. She maintained the lab in great shape keeping everything accessible, when I was engaged with my coursework. Since leaving the laboratory, her absence is certainly felt by all, and she is genuinely missed. I sincerely thank Priyanka Pasam, graduate research assistant in Dr. Hill's lab for providing me freshly isolated cerebral and cremaster smooth muscle cells from her experimental preparations. I also thank Dr. Zhe Sun, Research Assistant Professor in Dr. Meininger's lab for providing his experience when needed for my experiments. It is a pleasure for me to be a part of such a great team in the field of cardiovascular sciences. I also mention my thanks to Dr. Rick Heil-Chapdelaine, Hitschfield Instruments, St. Louis for educating me in the current trends in optical microscopy.

I am very grateful to my parents, siblings and friends for their words of wisdom and for instilling confidence in me. I dedicate all the success to my parents.

TABLE OF CONTENTS

LIST OF FIGURES

Figure Page

LIST OF TABLES

Table Page

DEVELOPMENT OF A FLEXIBLE IMAGE-BASED APPROACH FOR STUDYING SIGNAL TRANSDUCTION IN ISOLATED ARTERIOLES

Srikanth Ella

Dr. Michael Hill, Thesis Supervisor

ABSTRACT

Arterioles exhibit myogenic responsiveness, where the diameter of the blood vessel changes in response to changes in intraluminal pressure. In particular, within a physiological pressure range, an increase in intraluminal pressure causes vasoconstriction while a decrease in pressure causes vasodilation. The relevance of this mechanism relates to local control of blood flow and pressure and providing a level of constriction or tone on which vasodilator factors can act. Consequently, understanding the exact underlying signaling mechanisms in the arteriolar myogenic response is of basic physiological interest and is a requisite for understanding several pathological conditions including hypertension and diabetes mellitus.

A complete understanding of the transient signaling events which result from a change in intraluminal pressure subsequently triggering a mechanical response still remain to be defined. When pressure is increased changes in smooth muscle membrane potential (depolarization) are associated with increased intracellular calcium and contraction.

However, technical limitations with measurements of transient changes in membrane potential have made it difficult to establish an exact causative relationship between these variables. In this report, a novel approach is described that would permit questions regarding the mechanisms of mechanotransduction in arterioles. Ultimately this will allow the hypothesis that membrane depolarization is a necessary and causative factor in myogenic constriction.

The basis for our studies lies in improved availability of sensitive voltage sensing probes and the implementation of Fluorescence Resonance Energy Transfer (FRET) to cell systems. In particular, it was hypothesized that such approaches provides an approach for detecting membrane potential changes occurring in stimulated arteriolar smooth muscle cells. FRET is a technique, where non-radiative transfer of energy takes place between two fluorochromes which are very close to each other (<10 Angstroms). In these studies Coumarin- labeled phospholipid (CC2-DMPE) is used as a FRET donor at the plasma membrane. The non- polar nature of the CC2-DMPE's acrylic chain does not allow the probe to enter into the cell, anchoring it in the outer leaflet of the membrane. $DisBAC_4(3)$ was used as the mobile FRET acceptor translocating across the membrane with changes in membrane potential of the cell. Excitation (405nm) of the donor molecule leads to emission of the acceptor via FRET which decreases on membrane depolarization. Hence a ratiometric technique (Donor Emission: Acceptor Emission) can be employed to detect changes in membrane potential.

To perform the FRET-based studies of smooth muscle membrane potential in either freshly isolated smooth muscle cells or cannulated arterioles it was necessary to custom design an optical microscope. Additional capability was introduced into the system by enabling the measurement of intracellular calcium and object dimensions. The system utilized an inverted microscope to which was coupled both laser and brightfield illumination. Appropriate fluorescent excitation light was directed to the tissue/cells via dichroic mirrors and a high speed confocal spinning disk unit (Solamere Technologies, Utah). Reflected emission signals were separated using a Quadview (Optical Insigths, Arizona) equipped with appropriate dichroic mirrors and emission filters. The resulting signals were then passed to the face of an intensified CCD, XR Mega10-S30 (Stanford Photonics). 80% of brightfield illumination was passed directly to a second CCD positioned on the bottom port of the microscope. The remaining 20% was directed through the Quadview to the intensified CCD.

Initial experiments were performed on cultured smooth muscle cells and cannulated arterioles to test for possible toxic effects of the fluorochromes. Vessel responses to vasoagonists and pressure step changes were largely unaffected by the FRET fluorochromes, indicating that the dyes have little apparent toxicity effect on the arterioles. Toxicity studies were extended to examine triple loading of the vessels, with the FRET dyes plus Fluo4- AM, a calcium ion indicator. A lack of nuclear propridium iodide staining confirmed that the dyes did not have toxic effects on the cells.

Several tests were performed on the developed system to check for correct level of fluorescence detection. Fluorescent beads were used initially to estimate the level of fluorescence and to examine optimal intensity and resolution. Fluorescent slides of Fluo-loaded cells, Alexa-488, brain slices from rat were available to align the Quadview optics, while continuing to check the chromatic parfocality.

As initial 'proof of principle' the ability of the system to detect changes in membrane potential was examined in freshly isolated cerebral and cremaster muscle arteriolar smooth muscle cells. Cells were depolarized by adding KCl (60mM) and fluorescence changes were observed in both the donor and acceptor emission channels. A ratiometric signal was calculated to normalize the changes in different cells. A graded depolarization signal was observed when KCl (30+30mM) was added. In regard to fluorescence changes, a significant ratiometric signal was detected when the cells were depolarized by a 60mM KCl stimulus, which is much greater than the single ratiometric dye di-8-ANEPPS (5-6% Fluorescence change per 100mV Em change).

A customized optical microscope was installed and is ready for studies on single cells and cannulated arteriole preparations. Implementation of FRET to measure Em changes, along with parallel use of other indicators to measure the role of the basic physiological ions such as Ca^{2+} will aid in a better understanding of signaling mechanisms. Importantly, a temporal relationship can be drawn between intraluminal pressure, Em, global cytosolic calcium and arteriolar dimensions on cells and arterioles. The proposed

approach will become a significant tool for future studies on arteriolar mechanotransduction processes.

The fundamental significance of these studies will lead to answering a major remaining question in the understanding of the myogenic signaling pathway of the arterioles. More importantly the system enables the study of effects of a number of vasoactive factors or stimulus that affect the Em of the arterioles.

CHAPTER 1

HYPOTHESIS AND AIMS OF THE PROJECT

Arterioles respond to changes (increase or decrease) in intraluminal pressure with changes (decrease or increase) in diameter. This phenomenon is referred to as the myogenic response and allows such vessels to exhibit a tonic contraction known as myogenic tone. The myogenic response of blood vessels assists in the setting of peripheral vascular resistance, local blood flow autoregulation, sets the capillary pressure [1-3]. Importantly, myogenic tone in a vessel, allows vasoactive factors (for example vasodilator metabolites) to induce changes in diameter such that local hemodynamics can be matched to metabolic needs [4, 5]. Changes in the myogenic responsiveness of arterioles have been reported to contribute to vascular complications in hypertension and diabetes mellitus.

The precise underlying signaling mechanisms still remain unclear though the importance of the myogenic response is clearly understood. This is because the transduction processes involved and the transducers involved in the process are not fully identified. An early event that occurs in the smooth muscle is membrane depolarization, leading to opening of the voltage dependent calcium channels and entry of Ca^{2+} ions through these

channels ultimately causing contraction [6-8]. The exact relationships among the application of intraluminal pressure, changes in smooth muscle cell membrane potential, dimensions of the arteriole, and intracellular calcium concentration in the transient state have not been defined. Glass electrode recording of membrane potential in intact arterioles are largely limited to the steady state as the vessel wall moves and constricts upon application of pressure [9, 10]. Early attempts to measure changes in membrane potential with fluorescent techniques have lacked either the time resolution or a proper signal to noise ratio [11].

Fluorescence (Fŏrster) Resonance Energy Transfer (F.R.E.T) is a relatively new technique to be employed in cells to measure membrane potential [12]. We therefore ***hypothesized*** that improvements in systems for studying isolated and cannulated arterioles and implementation of FRET to measure Em in arterioles provides a means to determine transient relationships among Em, global intracellular calcium and arteriolar dimensions following a change in intraluminal pressure. To exploit this potential we have collaborated with optical specialists to design a laser-based microscope system that will allow the simultaneous use of multiple fluorophores in both wide field and high-speed confocal modes. On the basis of the above the proposed studies ***aimed*** to:

i. Develop imaging-based methods that allow simultaneous measurements of Em (via FRET), intracellular Ca^{2+} and vessel diameter in isolated smooth muscle cells and single cannulated arterioles.

ii. Perform toxicity studies for the loading of the dyes on cannulated vessels and isolated cells.

iii. Perform utility tests of the FRET- based Em measurements in both isolated cells and cannulated arterioles.

It was anticipated that complex transient state signaling pathways in the arteriolar myogenic response, still remaining obscure, can be understood by the proposed project. The technique and optical setup explained here can become a major tool in the ongoing research for studying the signaling mechanisms in cultured and fresh cremaster smooth muscle cells and the arteriolar myogenic response. Changes in the membrane potential of the cells in response to depolarizing and hyperpolarizing agents can be detected through the ratiometric approach provided by FRET. The method has the potential to explore the transient state relationship among membrane potential, intracellular calcium, and arteriolar dimensions. Data obtained through the studies will also contribute towards pathophysiological situations and pharmacological therapies.

CHAPTER 2

INTRODUCTION

All essential metabolites, nutrients and by-products of metabolism are transported to/ from various parts of the body by the circulatory system. Transport mechanisms are provided by the cardiovascular system, and its essential constituents are the heart, blood vessels, and the capillaries. Blood is delivered to various organs and tissues through arteries and the smaller arterioles.

Arterioles are critical in providing friction to blood flow, and maintaining a physiological blood pressure through their inherent myogenic tone [2, 3]. These vessels regulate the blood flow through their intricate contractile mechanisms and help maintain the appropriate blood pressure in the system [2]. Blood flows through high pulsatile pressure from the heart, and through the arteries, and this pressure must be regulated before entering into the organs [1]. Effective functioning of arterioles is a requisite for proper maintenance of blood pressure across the entire network and organs.

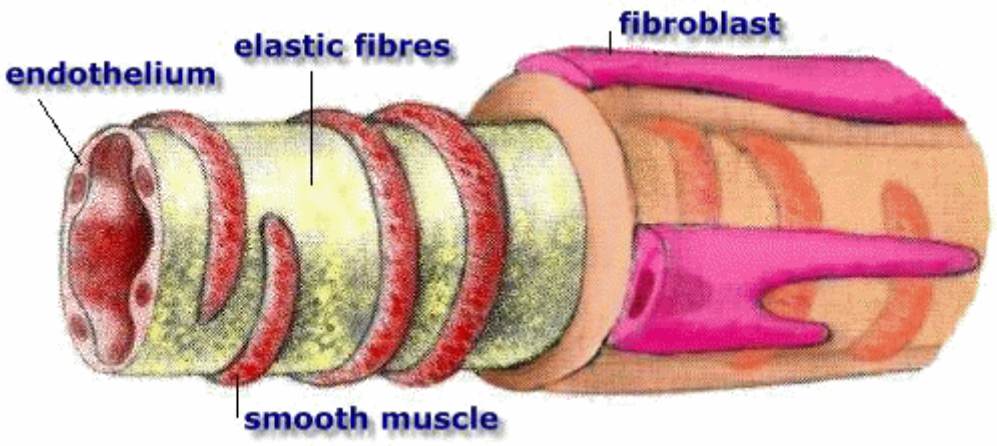

Figure 1: Cross section of an arteriole. Smooth muscle cells wrap around the arterioles and respond to changes in intraluminal pressure and vasoagonists and modulate the diameter of the lumen of the vessel.

Arterioles are a tubular network consisting of two main types of cells- endothelial and smooth muscle as shown in Figure 1. The endothelial cells are lined longitudinally in the inner lumen of the vessel and the smooth muscle cells are 1 or 2 transversely layered structures [13]. Contractile force developed in the smooth muscle cells controls the diameter of the arterioles [14]. The contractile or relaxation force in smooth muscle cells is caused by a multitude of factors and the accurate underlying signaling mechanisms involved in this process are still to be determined [15]. Arterioles are said to exhibit myogenic tone if they develop active forces during changes in transmural pressure. Increased intraluminal pressure of an arteriole contracts the smooth muscle cells by activating classes of non-selective cation channels leading to membrane depolarization and opening of the voltage dependent calcium ion channels. This subsequently leads to an increase in the intracellular calcium concentration and contraction [8].

A transient relationship among the membrane potential, intracellular calcium and arteriolar dimensions is still to be determined and is the major motivation for the project. The described method/approach for simultaneously estimating all the physiological parameters can become a major tool for studying the arteriolar myogenic responses. Developments in the field of optics, and improvements in Fluorescence Resonance Energy Transfer technique enabled the detection of membrane potential in cells using fluorochromes. Studies are basically done on freshly isolated cremaster and cerebral cells and will later be integrated onto vessels. Toxicity effects of these fluorophores on cells and arterioles should be determined to examine if there was any subsequent change in their functioning. The optimal concentration of the dyes used for labeling the cells is estimated while continuing to monitor the toxicity effects at these concentrations.

Development of a novel imaging station on an Olympus IX-71 microscope to perform FRET is described in this report. Introduction to the concept of FRET and its implementation on arterioles and smooth muscle cells is explained in depth. A provision for near simultaneous detection of global cytosolic calcium using the popular Ca^{2+} indicator Fluo4-AM is employed. A customized optical path is defined by using 2 laser lines and a quadview to separate the specimen's illumination based on wavelength. Future improvements and up gradation of the microscope can be done by adding additional laser lines and modifying the optical paths, by insertion of new dichroics and filters in the well defined optical path.

2.1 Cardiovascular System:

The cardiovascular system is composed of the heart, blood vessels or vasculature, and the cells and plasma that form the blood. From an anatomical point of view there are three main categories of blood vessel:

• Veins - the efferent blood vessels that return deoxygenated blood to the heart;

• Arteries - the afferent blood vessels that carry oxygenated blood away from the heart;

• Capillaries - narrow, thin-walled blood vessels that form networks within the tissues.

The blood vessels of the body represent a closed delivery system, which function to transport blood around the body, circulating supplying substances such as oxygen, nutrients, and hormones, while facilitating removal of waste products. In addition to transport functions arterial vessels act to control blood flow and pressure through their contractile properties while the venous circulation, or capacitance vessels, can act as a blood reservoir. The capillary bed represents the main site for exchange due to their walls being only a single endothelial cell in thickness.

Control of blood flow through the circulation occurs through both extrinsic mechanisms (neurohumoral) and intrinsic responses to local changes in mechanical and metabolic factors [16]. As an example of local control, arterioles (small arterioles with diameter less than approximately 150 μm) respond to increases or decreases in intra luminal pressure with contraction or relaxation, respectively, and this phenomenon is referred as the ***Myogenic Response***. Myogenic response is also seen in arteries, venules, veins and

lymphatics, but it is more pronounced in arterioles [1]. Following an increase in intralumenal pressure arterioles respond with a large passive distention, followed by active contraction - often decreasing their steady-state intraluminal diameter below that observed prior to the pressure increase. Similarly, they respond to decrease in pressure with a transient passive collapse, followed by relaxation to increase their diameter [17]. While the exact events that are sensed by the arteriolar wall when pressure changes current evidence suggests that changes in tension may trigger the subsequent vasomotor responses. Candidate mechanisms are discussed in more detail in following sections.

There is an immense physiological significance of the myogenic response in arterioles. The cardiovascular system pumps blood to various parts of the body by circulating through arteries, arterioles, capillaries, venules and veins. Arteriolar network is vital in the system and releases the blood into the capillaries. Blood flow into the tissues from these arterioles is also regulated by several neuroharmonal factors [14]. Change in the intraluminal diameter controls the blood flow across the network. So understanding the underlying signaling mechanisms involved in the arterioles is very important for the cardiovascular system. Physiological disorders in the system changes the signaling, and is a major cause of pathological conditions in the system [18]. So, efficient knowledge in the signaling mechanism at cellular level is important for curing the routine heart diseases.

2.2 History of the Myogenic Response:

Sir William Bayliss in 1902 first reported that there are measurable increases in the volume of the dog handlimb following transient aortic occlusions. Bayliss felt that these changes in the handlimb might not be occurring secondary to the accumulation of vasoactive metabolites, but rather to the myogenic properties, or pressure sensitivity of the arterial vessels [19]. Later Anrep argued against Bayliss' views by declaring that the handlimb response was a result of metabolic factors. However, his arguments were largely indirect as there was relatively little work on myogenic response. Later, Folkow was the first to assess that vascular tone depends on the intralumenal pressure developed in the vessel bed [20, 21]. Later, Selkurt and Johnson developed techniques in-vivo to measure the vascular resistance changes [20]. Johnson and Wiederhielm devised many techniques for clearly defining myogenic response in arterioles [22]. Implementation of isolated vessel techniques led to more insight in the signaling mechanism underlying the vascular mechanotransduction [23].

2.3 Definition of Myogenic Response:

A strict definition of the arteriolar myogenic response has proved problematic, in part, because arterioles exhibit several behaviors which have loosely been attributed to their myogenic properties. These include myogenic responsiveness, steady-state myogenic tone and vasomotoin [17, 24]. As stated above an acute increase in intralumenal pressure

leads to transient distention followed by sustained active vasoconstriction. Conversely a decrease in pressure leads to vasodilatation. For the context of the following discussion these responses will form the definition of the '*myogenic response*'.

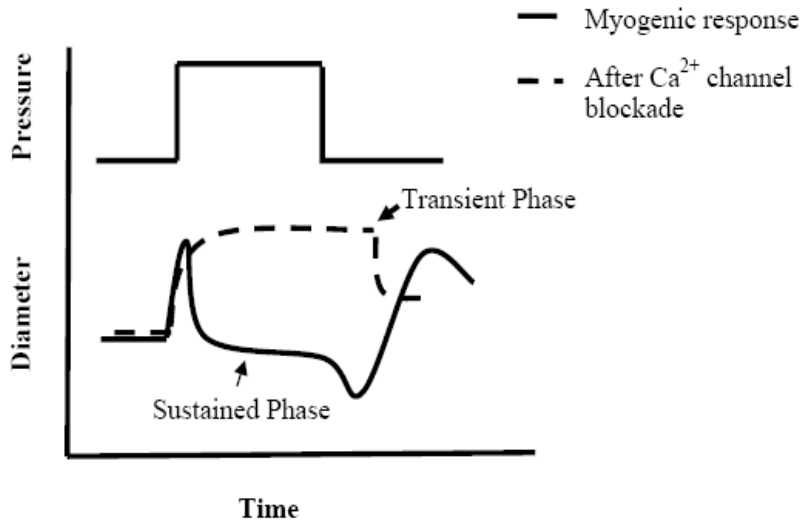

Figure 2(a):

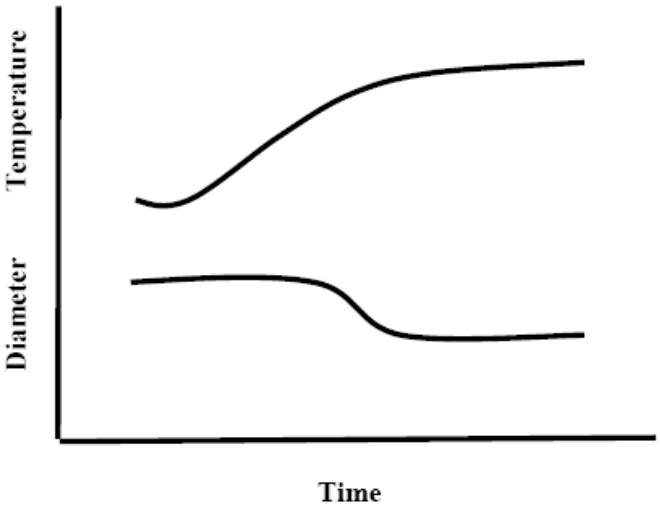

Figure 2(b):

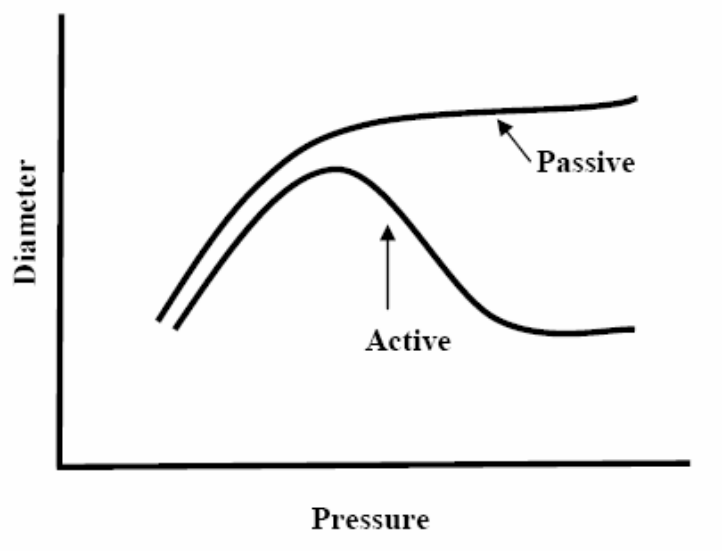

Figure 2(c):

Figure 2: Examples of myogenic behavior in arterioles. 2(a) signifies the change in the diameter of an active and passive vessel in response to a pressure step. 2(b), 2(c) represents a vessel gaining spontaneous myogenic tone (bottom curve) over a period

Source: Davis, Hill. *Physiol Rev* 1999

Examples of myogenic behavior are shown in Figure 2. In Figure 2(a) change in the intralumenal pressure of the arterioles causes a transient and steady state in diameter. In Figure 2(b), vascular tone is attained when the vessel is continuously pressurized and the temperature raised to physiological conditions (34°C). The vessel constricts from its initial passive diameter over time (~1hour). Figure 2(c): Myogenic tone can also be seen in vessels superfused with Calcium bicarbonate buffer over time, provided proper pressure and temperature conditions are maintained. In a buffer with zero calcium concentration, arteriole is subjected to be in passive conditions and would not constrict and not exhibit myogenic responsiveness. Hence the arteriole under these conditions would be under maximal relaxation.

2.4 Signaling Mechanisms Underlying the Arteriolar Myogenic Response:

Blood vessels maintain a level of tone in-vivo to maintain physiological balance in the system. The physiological significance of the vascular tone is to set the peripheral vascular resistance, local blood flow autoregulation and a contribution towards the control of capillary pressure. Vascular smooth muscle cells integrate signals from hormones, neurotransmitters, endothelium derived factors, and blood pressure, and determine the activity of contractile apparatus of muscle cells. Ca^{2+} ions play a pivotal role in the underlying signaling events and thus crucial to maintaining a level of tone [8]. Ions moving across the ion channels present in the plasma membrane of the cell to regulate the membrane potential and intracellular Ca^{2+}.

Vascular tone is regulated by the 4 different types of major ions in the smooth muscle cell. Early events in the myogenic signaling mechanism is the depolarization of the smooth muscle and entry of the extracellular Ca^{2+} into the cell through the L-type Voltage dependent Ca^{2+} channels (VDCC) and leads to contraction of the arteriole as depicted in the Figure 3. The signaling events involved in the arteriolar myogenic response and of main interest in the current project are shown in the Figure 4. This

increase in cytosolic Ca^{2+} activates the

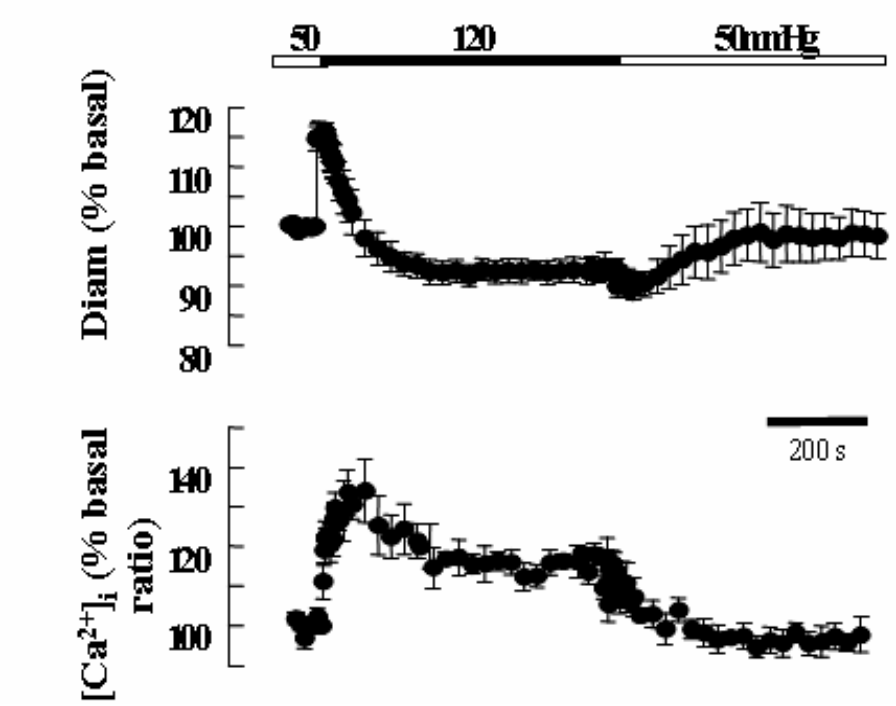

Figure 3: Pressure induced depolarization in the arterioles leads to opening of VDCC's and global rise in the intracellular calcium. Calcium entering the cells through the ion channels exponentially decays in the steady state.

Source: Zou, Ratz, Hill. *Am J Physiol.* 1995

ryanodine sensitive Ca^{2+} channels in the Sarcoplasmic Reticulum (SR), and thence Ca^{2+} from the stores is released into the cytoplasm [11]. These localized Ca^{2+} release events are called as Ca^{2+} sparks. This global release in the Ca^{2+} activates the large conductance Ca^{2+} activated K^+ channels and outflow of K^+ ions occurs leading to cell hyperpolarization. The latter event is therefore viewed as a negative-feedback regulation of the initial depolarization- induced contraction [25, 26]. Figure 5 shows a flow chart of the signaling mechanisms involved in the arteriolar mechanotransduction process.

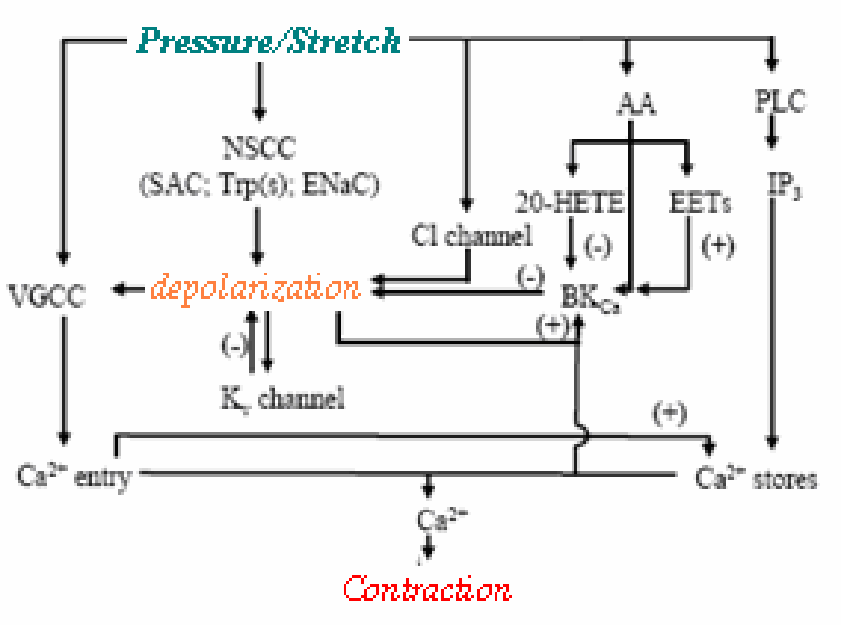

Figure 4: Figure represents the multiple signaling events involved in the pressure induced constriction of the arteriole. Increase in pressure or stretch in the arteriole leads to depolarization of the smooth muscle cells, and opening of the VDCC's to increase the intracellular calcium leading to development of contractile force

Source: Davis, Hill & co. *in press. 2007*

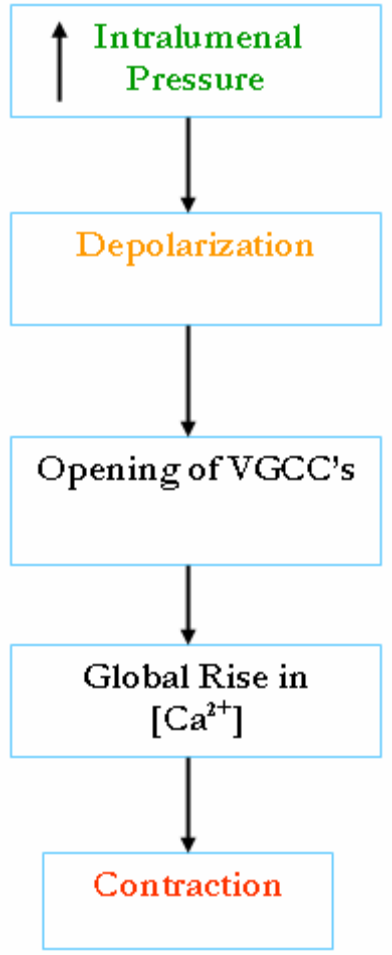

Figure 5: Flow chart of the signaling mechanisms involved in the arteriolar myogenic response. Increase in the intraluminal pressure leads to development of contractile force in the smooth muscle cells wrapped around the arteriole.

Resting membrane potential in unpressurized vessels ranges from -60 to -75mV, and the membrane potential is depolarized when the intralumenal pressure is raised. Membrane Potential is estimated to be around -40 to -60mV at physiological pressures [27, 28]. Figure 6 shows the relationship between intralumenal pressure, membrane potential [9]. Figure 6 clearly depicts the pressure induced depolarization. Similar results have been

obtained in rat, rabbit, cats [29-31]. All the measurements and conclusions were made under steady state. A generalization was made that an approximate 20-30mV graded depolarization would occur at pressures between 30mm Hg – 110mmHg. Transient state measurements using glass electrode measurements were not possible here because of the vasomotion and constriction of the vessels when the pressure was changed Despite of much work being done on the vascular smooth muscle cells, a complete intricate relationship in the pressure induced mechanotransduction process could not be revealed [1].

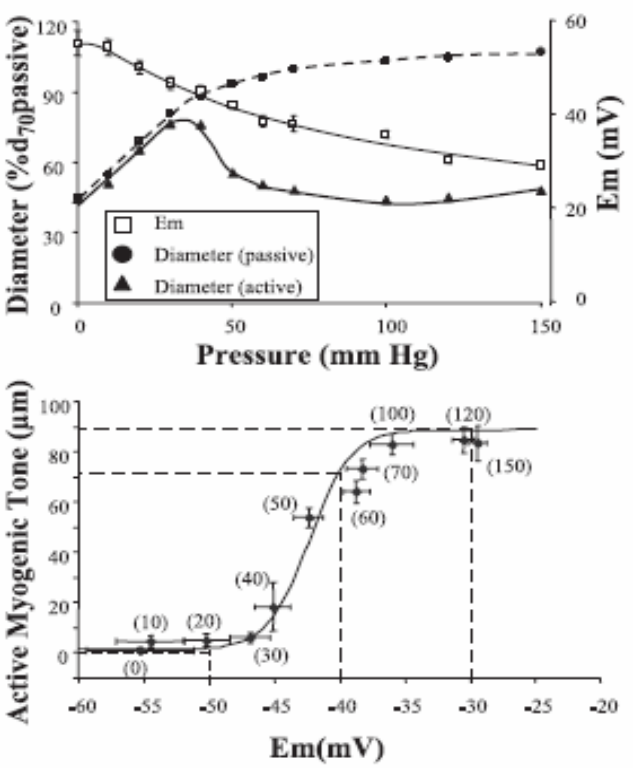

Figure 6: Central role of depolarization in pressure induced Ca^{2+} mobilization and contraction. Fig depicts a change in the membrane potential due to the change in the pressure for vessels exhibiting myogenic tone (top). Increase in pressure leads to depolarization in the arteriolar smooth muscle. Membrane potential of the smooth muscle bears a sigmoidal relationship with the active myogenic constriction (bottom). Values in the parenthesis depict the intraluminal pressure of the vessel.

Source: Kotecha, Hill. *Am J Physiol Heart Circ Physiol*- 289:1326-1334, 2005**.**

2.4.1 Regulation of Vascular Tone by K^+ Channels and VDCC:

K^+ ions play a pivotal role in determining and regulating the membrane potential and vascular tone. Potassium ions cause membrane hyperpolarization by flowing out when their respective channels are open and leads to dilation or relaxation of the cells. Ca^{2+} ions mainly enter the cells through voltage gated calcium channels and depolarize the cell and cause constriction. Conversely outward flow of these ions from the cells causes membrane hyperpolarization and dilation. Of all the different types of Ca channels present, dihydropyridine-sensitive L-type Voltage dependent Ca^{2+} channels (VDCC) are the major regulators of the vascular tone and membrane potential [7, 8].

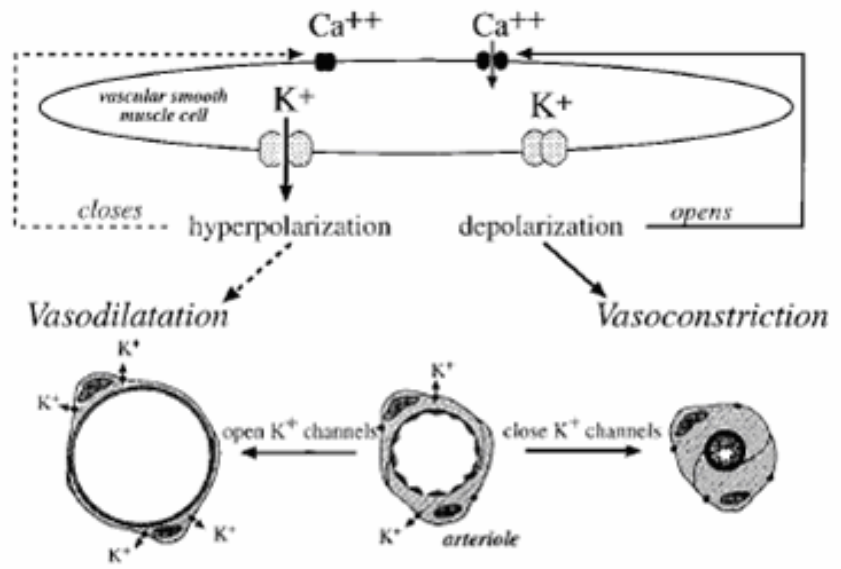

Figure 6: Relationship between K^+ channels and myogenic tone. Influx of calcium through the VDCC's by the depolarization of the cells leads to contraction of the cells. Calcium released from the stores activates the large conductance calcium activated potassium channels, leading to efflux of K^+ ions and hyperpolarization and relaxation of the cells.

Source: William Jackson, Hypertension. 2000;35: 173-18

The VDCC's are controlled by vasoconstrictors and vasodilators. Hence these ion channels are modulated by several neural, humoral, and vascular tone. As discussed earlier electrical potential of the cell also influences the Sarcoplasmic Reticulum and releases Ca^{2+} from the stores, by activating the Inositol 1,4,5- triphosphate (IP3) [32, 33]. Ca^{2+} released from the stores activates the large conductance Ca^{2+} activated K^{+} channels (BKCa) leading to outward flow of the K^{+} ions and hence membrane hyperpolarization as shown in the Figure 7 [34, 35]. This balance of the cell potential is needed for the regulation of vascular tone. Likewise there are a number of other channels present in the cells, which regulate the electrical activity and hence the myogenic tone.

2.4.2 Other Types of Ion Channels:

K_{ATP} channels are important in the regulation of resting electric potential and the vascular tone [36]. Vasoagonists including Adenosine and prostacyclin act on the K_{ATP} channels and causing them to open, leading to outward K^+ flow and membrane hyperpolarization [25, 37]. Other channels like K_V, K_{IR}, Cl- also participate in the modulation of the tone [25, 38-42]. Figure 8 depicts the possible effects of all the important channels and their regulation.

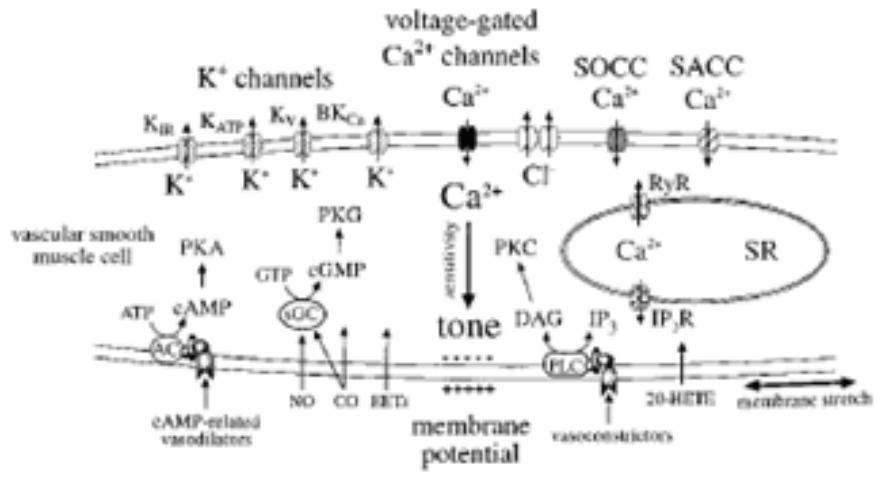

Figure 7: Ion channels and vascular tone. Schematic of a vascular smooth muscle cell showing all the important defined ion channels, SOC, SAC, SR etc.

Source: Jackson Review, 2000;35 (173-178)

CHAPTER 3

INTRODUCTION TO MICROSCOPY

3.1 History of Confocal Microscopy:

Confocal microscopy was first developed by Marvin Minsky in the mid 1950's at Harvard University [43]. Its initial popularity was however limited because of requirement for precision lasers and sophisticated computers. Dutch physicist G. Fred Brakenhoff made the concept of confocal a reality, by developing a scanning confocal station in 1979 [44]. Later many other physicists using advanced high efficiency mirror units, high throughput fiber optics, better dielectric coatings, precision lasers, and better quality cameras, brought confocal microscopy into life science imaging.

The modern day approach for confocal microscopy remains similar to Minsky's technique. His technique was to perform a point by point image construction by scanning light across a specimen and collecting the emitted light. This avoided continually exposing the entire specimen to the light. Minsky scanned the stage instead of scanning the light across the specimen. He used a solenoid coil to move the stage in the XY at various frequencies and managed low frame rate collecting 1 image for every 10 sec.

3.2 Principle:

The confocal microscope works by the point by point illumination of a sample and eliminating the out of focus light [43]. To accomplish the process, light from a highly directional source is focused through a pinhole and then passed through a system of lenses to illuminate the sample at a single point. A pair of lenses, shown in Figure 8 modifies the light path to the specimen. Lens B focuses the coherent light through lens A onto the specimen. According to basic physics, the fluoresced or reflected light need not be at the same focal point of the lens to form an image. Hence the light traverses in a different path through the lens and reaches the screen with a pinhole [43]. Only the light from the focal plane at the specimen will be able to reach the pinhole and other light will be obstructed by the screen as shown in the Figure 8. Hence the pinhole reduces the background haze which is a major limitation of wide field fluorescence. Images produced likewise are highly resolved and sharper. The focal point of the objective lens and the point of pinhole position are said to be conjugate to each other and are called as conjugate points. Their respective planes are called as conjugate planes, and thence the name was given as confocal [45]. A schematic diagram illustrating a basic confocal setup is also shown in Figure 9.

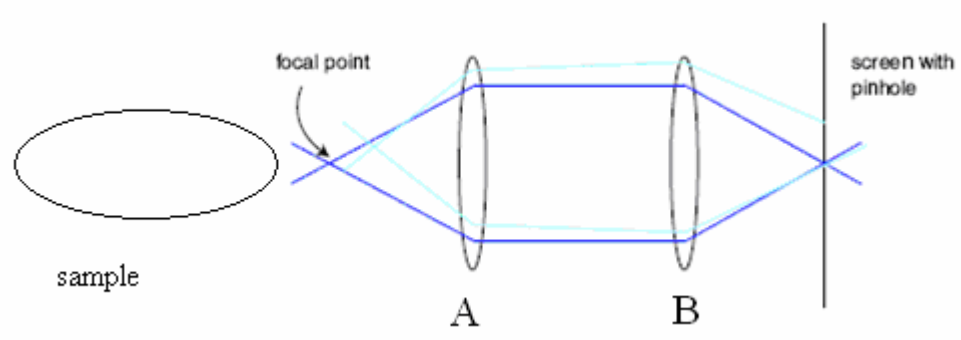

Figure 8: Light from the source passes through the pinhole and illuminates the sample at a focal point by traversing through the lens setup. The fluoresced or reflected light in focus of the objective traverses through the lens and passes through the pinhole to a detector.

Source: Semwogerere, Confocal Microscopy, 2005

At a given time, confocal microscopy can obtain useful information from only a point on the specimen. Thus, a fast scanning mirror raster scans the light across the specimen repeatedly in a 2D plane to obtain an image of an optical section. Computer algorithms have been developed which can collect the data from the photodetector and allow meaningful images to be reproduced. For 3D imaging, the optical 'Z'axis is shifted at intervals after scanning the optical section in XY (2D) [46].

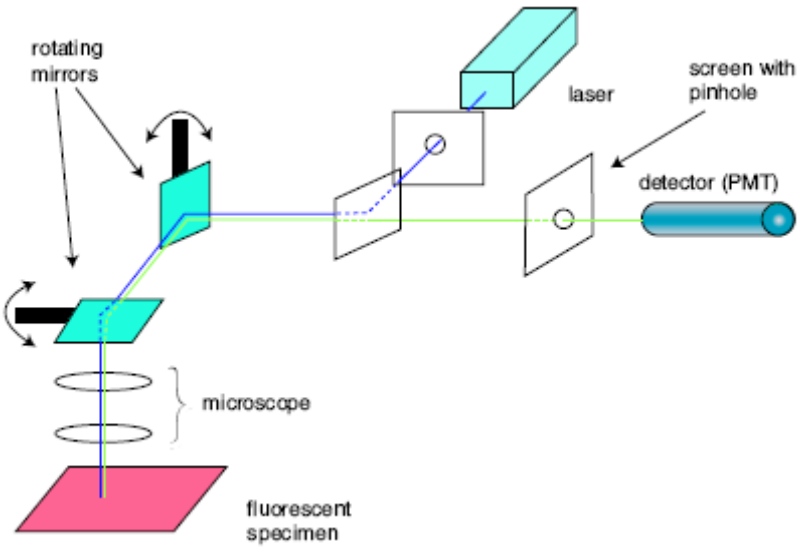

Figure 9: A light path of a fundamental confocal setup for a fluorescent specimen.

Source: Semwogerere, Confocal Microscopy, 2005

For a more exhaustive consideration of the principles of confocal microscopy the reader is referred to 'Confocal microscopy' 2005 by Semwogerere.

3.3 Limitations of Confocal Microscopy:

1. Though the resolution of confocal microscope is improved compared with the widefield microscopy, it has its own limitations. The point of light produced on the specimen appears like an "airy disk". The diameter of the airy disk depends on the wavelength of the exciting light and NA of the objective lens used. Hence maximum resolution is limited because of the airy disks [47].

2. The size of the pinhole used on the screen is a trade off for optical sectioning. Pinhole size cannot be made as small as possible as it places a limitation on the

number of photons reaching the photodetector [48]. Further, in trying to counteract, this increased intensity of the light source would endanger the specimen. For optimal results the pinhole size would be made approximately equal to the size of the airy disk.

3. High intensity of excitation light, illuminating the specimen, results in loss of fluorescence over a period of time. This occurs due to indefinite stay of the molecules in the excited state and a decrease in the population in the ground state (Photobleaching) [34].

4. Confocal microscopy is restricted to illuminate a point on the specimen. However, the exciting light causes a cone of out of focus light above and below the focal point, hence leading to damage of tissues (photodamage) throughout the area of these cones [49].

CHAPTER 4

FLUORESCENCE (FÖRSTER) RESONANCE ENERGY TRANSFER (FRET)

4.1 Introduction:

Light microscopy initiated understanding of cellular structure and function; molecular biological studies show the cellular events such as signal transduction gene transcription requiring the assembly of proteins into specific macromolecular complexes. Traditional biophysical or biochemical methods do not provide direct access to the interactions of these protein partners in their natural environment. New imaging technologies, coupled with the development of new genetically encoded fluorescent labels and sensors and the increasing capability of computer software for image acquisition and analysis, have permitted increasingly sophisticated studies of protein functions and processes like gene expression, intracellular signaling etc. Intensity-based measurements like FRET microscopy were developed for the analysis of these interactions inside intact living cells.

FRET is a process in which energy is transferred non-radiatively (via dipole-dipole coupling) from a fluorophore in an electronic excited state acting as donor, to another fluorophore or acceptor. For FRET to occur, the acceptor need not be a fluorescent molecule. The energy transfer rate varies inversely with the 6^{th} power of the donor-

acceptor separation over a minute range of 1-100 Angstorms [50]. The transfer rate also depends on three parameters (1) The overlap of the donor emission and acceptor absorption spectra, (2) the relative angular orientation of the donor absorption and acceptor transitions moments and (3) the refractive index of the solution in which the fluorophores are dissolved. For FRET, excitation light induces an oscillating field in the donor. The donor's oscillating emission dipole can then potentially influence the absorption dipole of an acceptor to oscillate in synchrony (if their spectra overlap) [50-52]. FRET can be compared to two musical tuning forks which have the same tone. If one fork is excited, a characteristic tone is produced. Bringing a second fork close to the first one will start to give a tone even they do not touch. This is resonance energy transfer [12].

4.2 Conditions for FRET:

There are three spsecific conditions that must be met for FRET to occur.

1. The emission spectrum of the Donor should overlap the absorption spectrum of the acceptor molecule. Hence exciting the donor molecule alone would result in emissions from the donor and the acceptor.

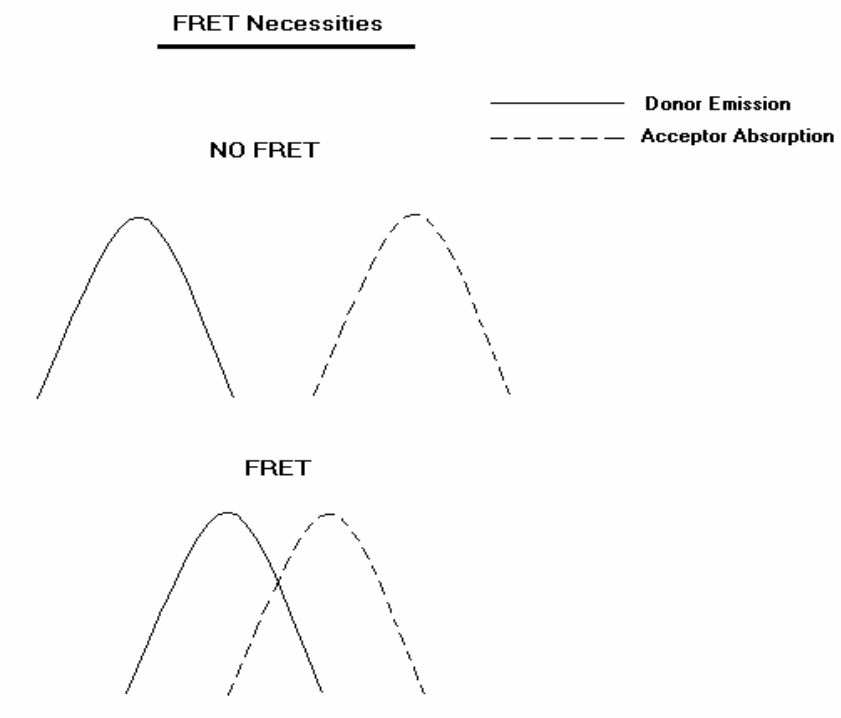

Figure 10: Spectral overlap of the donor emission and the acceptor absorption, a necessary constraint for FRET to occur.

2. The orientation of the donor's emission dipole and the acceptor's absorption dipole should not be perpendicular. In FRET, an oscillating field is induced in the donor by the donor excitation light. This oscillating field then potentially influences the acceptor's dipole to oscillate in synchrony provided the spectra overlap.

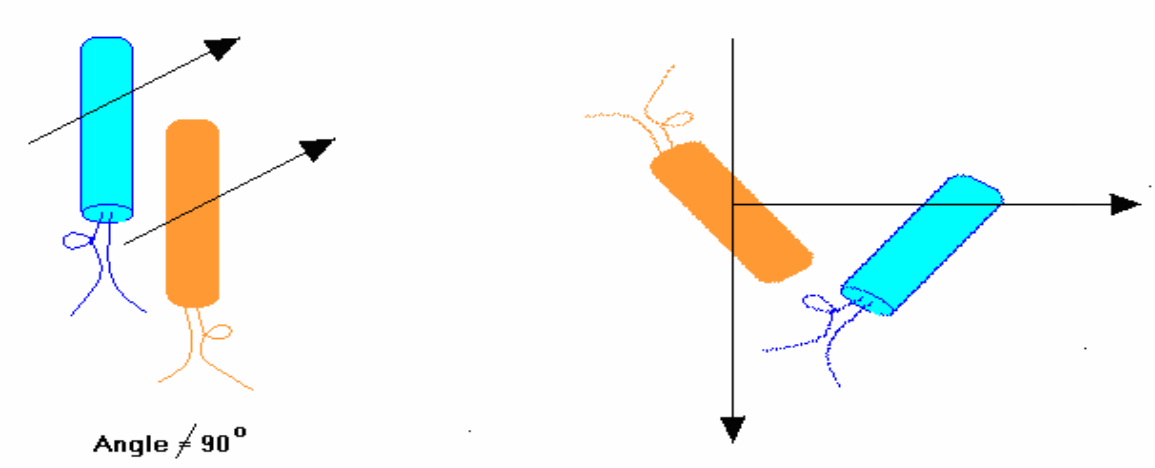

Figure 11: Relative angular orientation of the FRET probes should not be perpendicular for FRET to occur.

3. The distance between the donor and acceptor molecules must be less than 10nm (100 Angstorms).

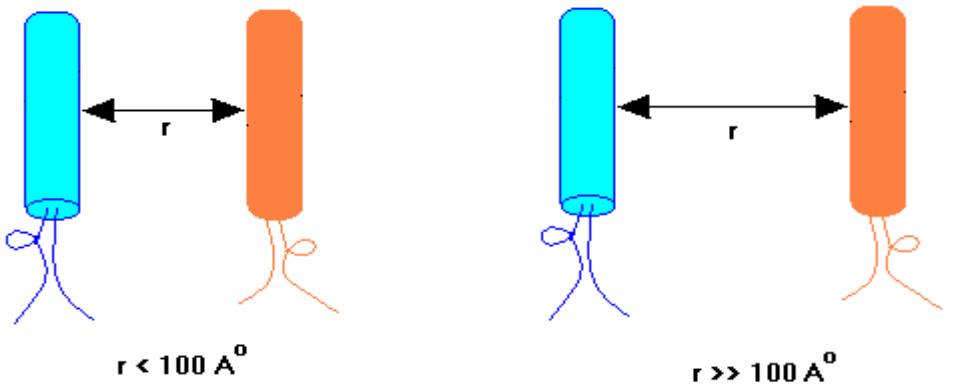

Figure 12: Distance of separation between the fluorophores should be less than 100 Angstorms for FRET to occur.

Source: Vogel Fanciful FRET 2006.

Efficiency of FRET depends on the 6^{th} power relationship on the separation distance between the donor and the acceptor molecules [50].

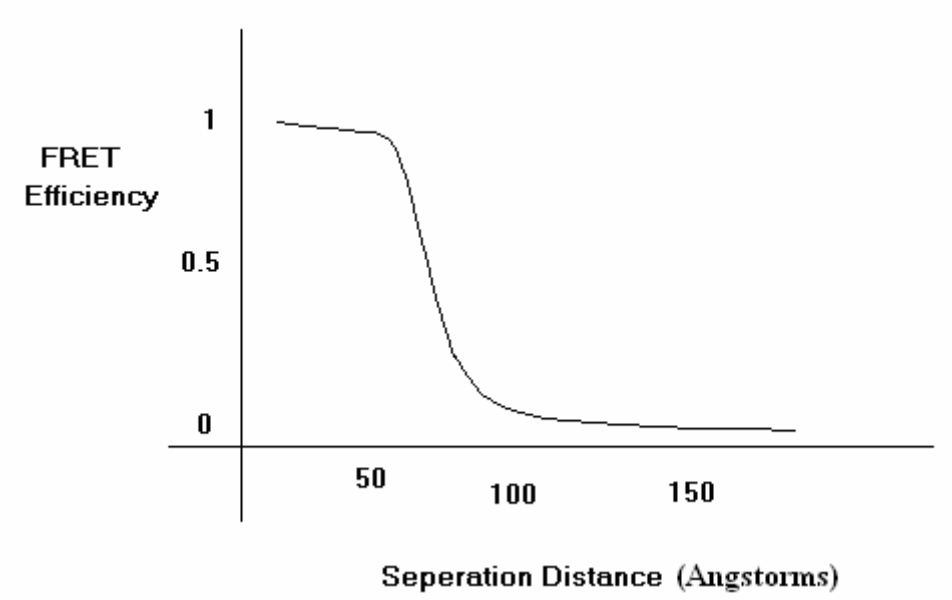

Figure 13: FRET efficiency decreases if the separation distances between the probes increases.

4.3 Mechanisms of FRET:

The donor fluorophore in its excited electronic state transfers its excitation energy to a nearby acceptor fluorophore non-radiatively through dipole-dipole interactions. The excited fluorophore oscillates at a given frequency, and energy transfer takes place if the acceptor dipole also oscillates at the frequency exhibited by the donor dipole. This process yields a significant amount of structural information concerning the donor-acceptor pair [10, 53].

As stated above for FRET to occur the acceptor molecule need not be a fluorophore, and hence the energy transfer is not mediated through photon emission. However, in most biological applications of FRET, both the molecules are fluorophores. Several methods to measure the FRET between the fluorophores have been designed [54]. Quenching of donor fluorescence, reduction of fluorescence lifetime, and increase in acceptor fluorescence emission are the most popular methods [55]. In the current project, quenching of donor fluorescence was used. The efficiency of energy transfer between the 2 molecules depends on the distance between them. Efficiency and distance are related as,

$$E = \frac{R_o^6}{R_o^6 + r^6}$$

Here R0 is termed the Forster distance and r is the actual distance between the molecules. R0 depends on several factors such as fluorescence quantum yield of the donor, refractive index of the solution, dipole angular orientation of the molecules, and the spectral overlap of the molecules [50].

Figure 14 explains the quantum mechanics of fluorescence. The fluorescent molecule's electrons are excited from resting state S0 to a higher vibrational state. Subsequently these excited electrons spend very little time, in the order of pico seconds, in that state before traversing to lower energy states releasing energy in the form of heat. Then the excited electrons decay to ground state within nano seconds emitting energy in the form of photons resulting in the normal fluorescence as shown in Figure 15. This process

occurs when the electrons are in their singlet state of vibration. If the electrons enter into their triplet state of vibration, they undergo intersystems crossing as shown in Figure 15. Intersystems crossing is a photophysical process in which, an isoenergetic non-radiative transition between two electronic states takes place. Such electrons oscillate at a particular frequency and eventually deactivate to a lower energy level. A Resonance energy transfer takes place between two molecules, if their respective electrons oscillate (vibrate) at such frequency. Hence FRET occurs if the energy emitted by a donor molecule is transferred non-radiatively to another molecule. Then as for the donor molecule, the acceptor will also be excited and emit energy as shown in Figure (16) [56].

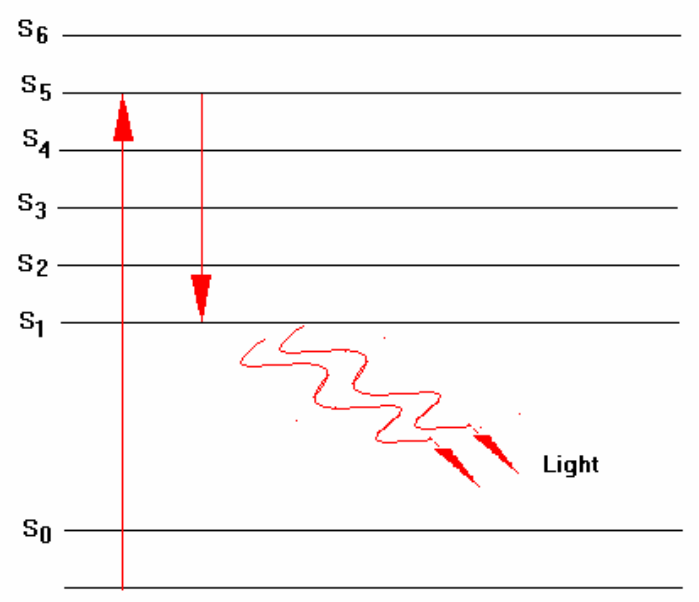

Figure 14: Electronic transitions during optical Fluorescence. Energy released by the electron when it jumps from higher energy state to ground state will be in the form of light of higher wavelength than the wavelength of the photon exciting the electron.

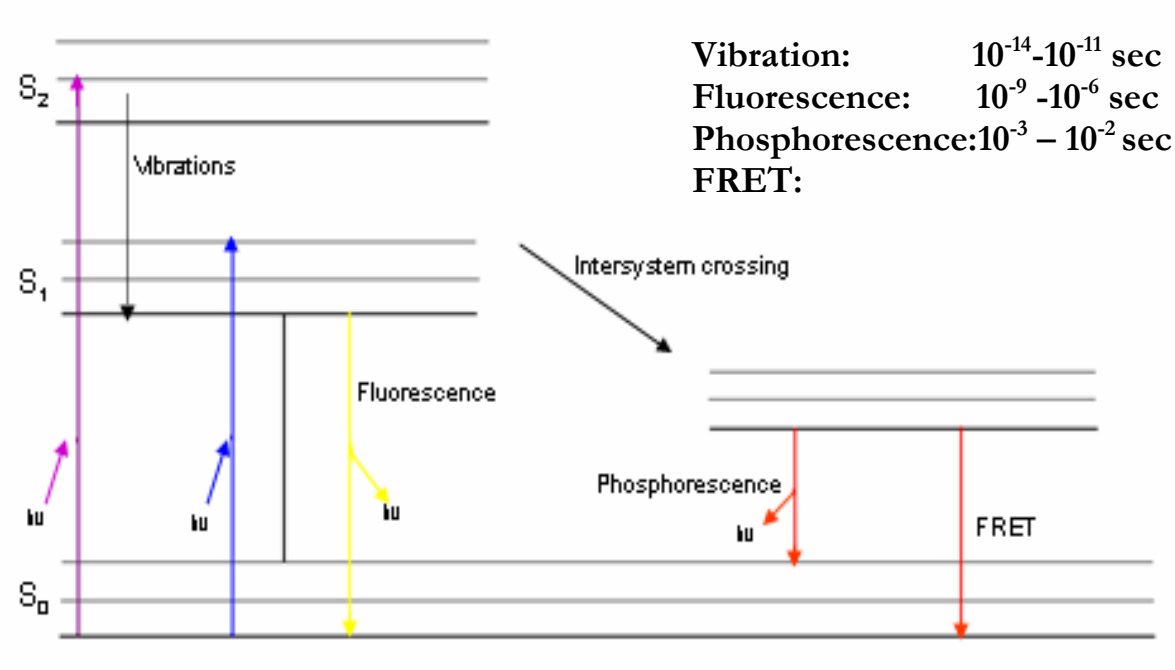

Figure 15: Jablonski's Energy Diagram showing all the basic electronic transitions involved in Fluorescence, phosphorescence, FRET along with the time scale of the events occurring.

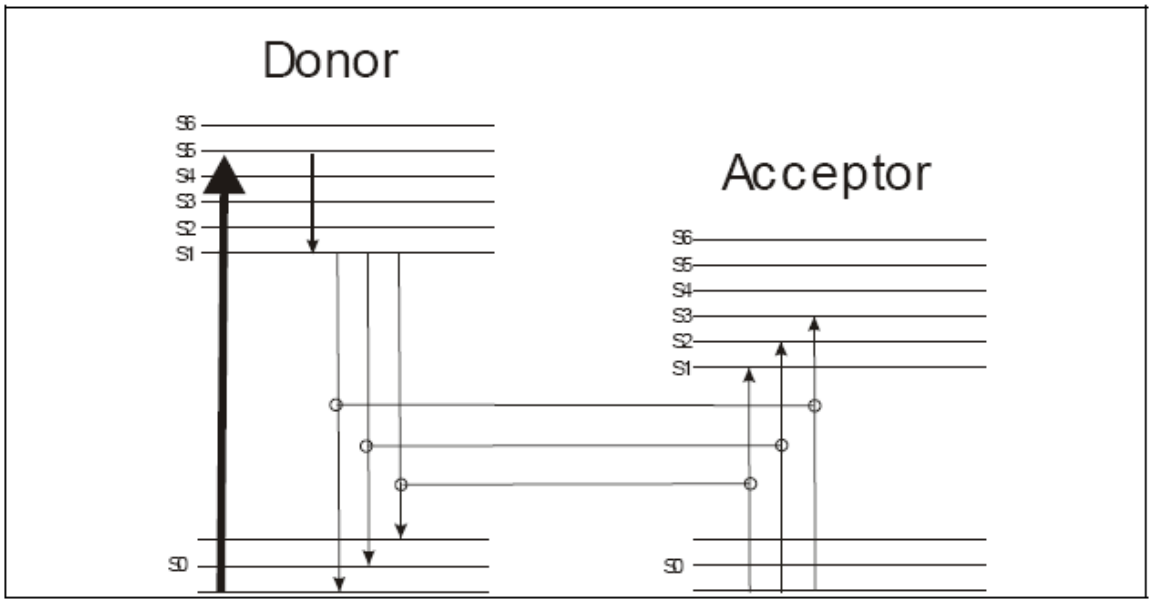

Figure 16: Excited electrons undergo intersystems crossing and this phenomenon leads to resonance energy transfer between the fluorophores.

4.4 FRET Measurement Techniques:

There are numerous approaches to measuring FRET. These can be classified under 4 fundamental categories

1. Detecting change in donor fluorescence.
2. Detecting change in acceptor fluorescence.
3. Detecting both donor and acceptor fluorescence.
4. Detecting change in the orientation of the fluorophores.

FLIM – FRET (Fluorescence life time imaging) is a commonly used direct method. Here FRET is measured by detecting donor's fluorescence lifetime. It is a measure of the time taken for the population of fluorophores emitting light after an excitation. Data analysis uses curve fitting algorithms, to calculate the ratio of the donor's fluorescent exponential decay constants in the presence and absence of acceptor. Many assumptions are made in the algorithm, and this method also needs precise instrumentation for detecting numerous emitted photons for accuracy. This might lead to photobleaching of the fluorophores, phototoxicity and damage of the tissue [51].

Another popular method for measuring FRET is detecting donor's fluorescence by acceptor photobleaching. Donor's fluorescence increases when the acceptor is photobleached during FRET. This needs simple wide field optics to perform, and photobleaching of acceptors can be done easily within a few mins without even affecting

the donor. This method requires a 'three-cube filter setup' in which the donor is excited and the acceptor's emission is detected. Also using precise filter cubes, it is possible to simultaneously detect the donor, and acceptor emissions. Many correction algorithms are available to correct for changes in background fluorescence as well as donor and acceptor spectral bleed through. This method appears highly accurate and precise, if proper experimental conditions (objectives, exposure time, light source intensity, etc.) are met [57].

4.5 Description of Em-Indicators: CC2-DMPE and $DisBAC_4(3)$

FRET membrane potential probes can be classified into 2 types. Electrochromic probes are the dyes capable of detecting microsecond voltage changes. Their limitation is the sensitivity, which can be approximated to 1-10% F/F0 per 100mV [58]. The other type of probes are environment sensitive probes which redistribute between cytoplasm based on the ionic forces developed due to changes in membrane potential [10, 12, 53, 56, 59].

Voltage sensor probes have recently been used in high throughput screening applications [53]. This approach has emanated from the studies of Gonzalez and Tsien using the donor-acceptor pair of coumarin and oxonol. Coumarin labeled phospholipid binds onto the outer leaflet of the cell membrane and acts as a FRET donor. Negatively charged hydrophobic oxonol ($DisBAC_2(3)$ or $DisBAC_4(3)$) is a FRET acceptor and resides on

either side of the plasma membrane in response to changes in membrane potential [59, 60]. A potential advantage of using 2 dyes is, they reduce errors arising from cell to cell based on ratiometric approach. Data acquired using these probes are precise and is as rapid as the patch clamp technique. The sensitivity of the approach can detect 5mV changes in Em, with 1-2% change in emission ratio [53]. CC2-DMPE has two negative charges from the coumarin and phosphate groups and hence does not leave the plasma membrane. CC2-DMPE has an excitation peak at 405nm and emission peak at 460nm. The DisBAC series has an emission peak at 560nm as shown in the Figure 17. Because of the large spectral separation of the indicators, these dyes can be detected efficiently.

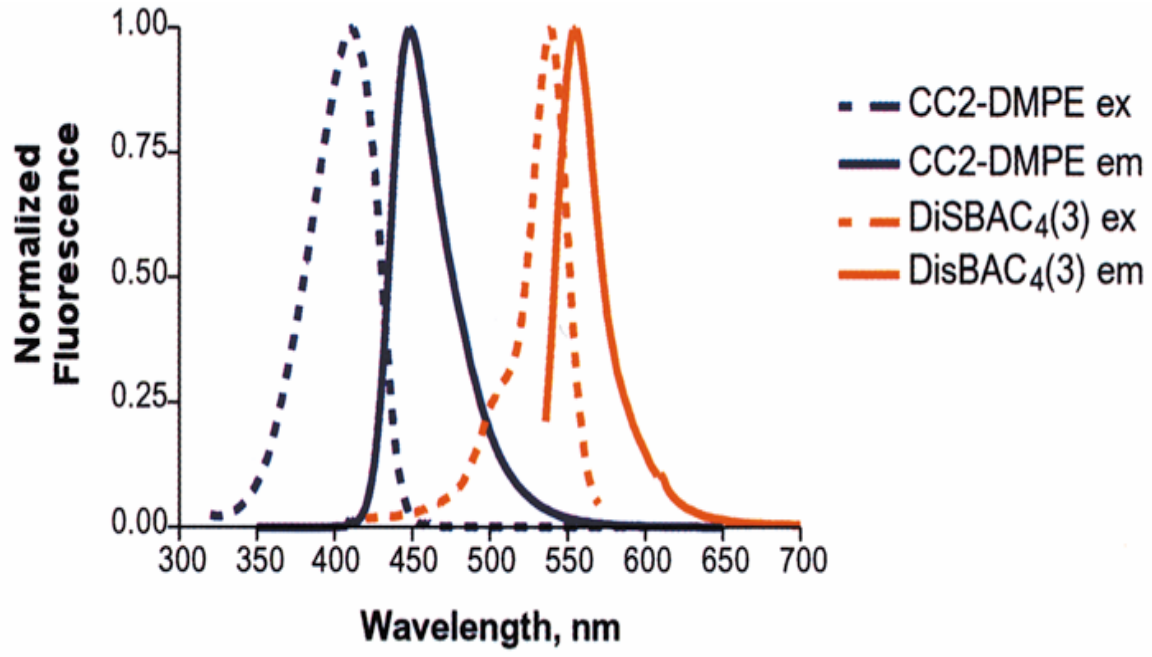

Figure 17: Spectral characteristics of the FRET based indicators, FRET donor (CC2-DMPE) and FRET acceptor ($DisBAC_2(3)$). The emission spectrum of CC2-DMPE overlaps with the absorption spectrum of the DisBAC2(3) resulting in the Fluorescence Resonance Energy Transfer.

Source: Gonzalez, Maher. Receptors and Channels. 8: 283-295, 2002.

4.5.1 Membrane Potential Sensing in Cells:

Techniques for Em measurement are devised earlier. Glass electrode impalements on cannulated arterioles for Em measurement were successful on arterioles in myogenic tone. These measurements were restricted to steady state, as the impalements had no stability during vasomotion, contraction and relaxation of the vessels. Fluorescent dyes were also examined for Em measurements, but these dyes either lacked desired signal to noise ratio or time responsiveness. For instance, the di-8-ANEPPS have a response of 1% change in fluorescence signal for 100mV Em change. Thence a need for an efficient method for measurement of Em is desperate to investigate the signaling mechanisms in arterioles.

FRET is a fast ratiometric method varying the fluorescence of two probes in accordance with the charge gradient [12]. The basic principle lies in the membrane potential-dependent movement of the hydrophobic acceptor anions from the outer leaflet of the plasma membrane toward the cell interior. In contrast, the donor molecule remains stationary in the outer leaflet of the membrane due to its phospholipid component.. At hyperpolarized potentials these probes lie in close proximity such that FRET can occur and fluorescence emission from the acceptor approaches its maximum. When depolarization occurs, the mobile anionic fluorophore is displaced leading to a decrease in acceptor emission fluorescence and a relative increase in fluorescence from the donor molecule [61]. Consequently, the responsiveness of the technique to voltage changes depends on the rate and magnitude of movement of the acceptor molecules from one site

to the other. Oxonol dyes which act as the acceptor molecule have to meet many molecular requirements. There should be a delocalized charge which has a low Born charging energy and can rapidly move within the cytoplasm based on the electrostatic forces from a hydrophilic to a hydrophobic area. Cations are less responsive to anions, because the ester groups in the membranes generate dipole potential which prevents the cations from entering the membrane [62].

Contraction in smooth muscle cells of the arterioles occurs due to many physiological causes including, mechanical stretch, electrical depolarization, and chemical effects. Depolarization of the smooth muscle cells causes their contraction by opening the L-type voltage dependent calcium channels allowing Ca^{2+} ions to enter the cell via a favorable ionic concentration gradient [56]. Increases and decreases in membrane potential are termed as hyperpolarization and depolarization. Changes in the membrane potential are very critical in several processes such as nerve signal transmission, muscle contraction and relaxation, and ion gating events. FRET technique can be employed successfully to most of the cell types for the membrane potential detection. A number of voltage sensitive fluorescent probes have been prepared which vary in their sensitivity and speed of response [60].

4.5.2 Application of FRET in the Measurement of Em:

The initial description of the aforementioned FRET dyes for the measurement of membrane potential was provided by Gonzales et al. [10]. Later studies of Em measurement on cells were extended using the FRET based assays, and implementation of high throughput screening to describe the ion channel activity simplified the approach as shown in Figure 18 [53]. They have also been used for a limited number of cell physiology studies including agonist stimulation of keratinocytes [59]; examination of the relationship between Em and intracellular Ca^{2+} in Islets of Langerhans and isolated cells and neuronal activity in cortical tissue.

Importantly, the studies referred to above, demonstrate that FRET-based Em measurements can be performed on a time base that is relevant to the study of vascular smooth muscle. For instance, it was shown in keratinocytes that measurements could be collected at a frequency of 2 measurements per second using a photometry detection system [60].

Using this approach these investigators were able to demonstrate rapid phasic responses of keratinocytes to stimuli, depolarizing the cells, followed by a sustained

hyperpolarization [60].

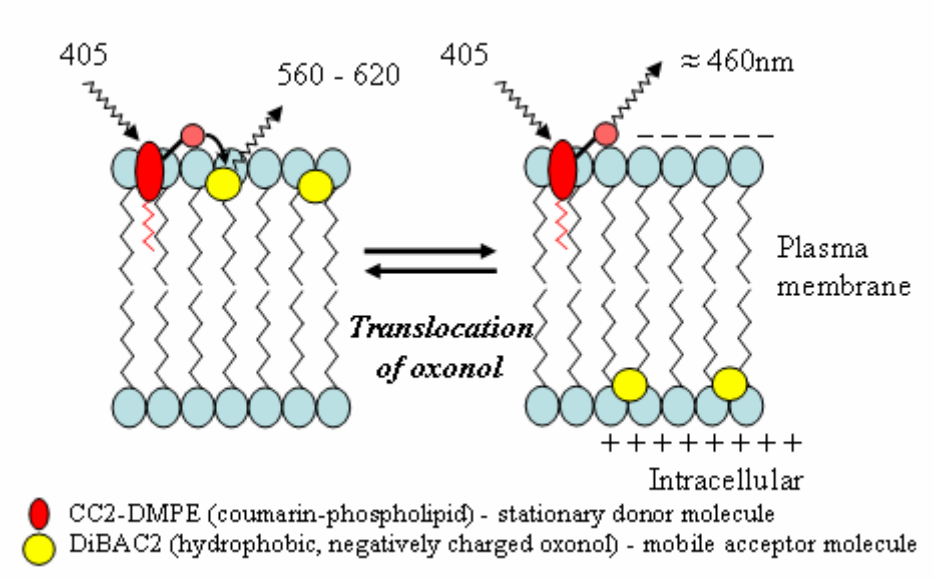

Figure 18: Depolarization assay principle. During depolarized state of the cell, because of the translocation of the FRET acceptor to the more positive face of the membrane, emission of CC2-DMPE increases and emission of the oxonol dye decreases.

Source: Gonzalez, Maher. *Receptors and Channels*. 8: 283-295, 2002.

Similar results were shown using an image-based detection system [59]. An image based approach was developed to perform FRET on pancreatic beta cells of Islet of Langerhans along with simultaneous measurement of intracellular Calcium. Results obtained showed a tight coupling between Em oscillations and Ca^{2+} recordings, although the recordings were on done a slower time course. By using an oxonol acceptor dye with a longer alkyl side chain it is conceivable that frequency of collection could be increased (for example DiSBAC2 has a reported time constant of 500ms compared to DiSBAC4 20ms), however, this would be at the expense of sensitivity (1-3 compared to 0.6-1%ΔR/mV) [63]. Despite this, the level of sensitivity would still be expected to remain substantially

above that for single fast dye approaches such as using di-8-Anepps. Hence compared to these fluorescent methods of Em measurement, FRET based approach has higher speed and sensitivity, and importantly has better temporal resolution.

4.5.3. Advantages of FRET Dye-based Em Measurements in Vascular Studies

1. The FRET based phenomenon occurs relatively with greater sensitivity compared to the previous fluorescence methods used for Em measurements (Ex: Di-8-ANEPPS).
2. FRET based Em measurement avoids difficulties associated with tissue movement, such as those observed during glass microelectrode impalement for Em measurements on arterioles. Hence the FRET based sensors can be used for transient state studies.
3. FRET approach has potential for improved ability to obtain spatial data, which was not possible using glass microelectrode because of the measurements being restricted to single cell.
4. Can be used in combination with other measurement approaches, for instance changes in intracellular Ca^{2+} using a Ca^{2+} indicator Fluo4-AM.
5. Ratiometric approach of the FRET probes reduces potential artifacts due to variation in excitation intensity, optical path length, cell number in a given field, cell loading.

In due consideration to all the potential advantages of the FRET based sensors, they were introduced into the cardiovascular studies for the first time for better understanding of the signaling mechanisms.

CHAPTER 5

MATERIALS AND METHODS

5.1 Isolated Vessel Studies:

For all experiments male Sprague-Dawley rats weighing in the range 150-250 gms were used. Prior to use rats were housed in the environmentally controlled facilities of the Dalton Cardiovascular Research Center animal facility. All protocols were approved by the animal care and use committee of the University of Missouri, Columbia.

Rats were weighed using a simple weighing balance and anesthetized with an appropriate dosage of Nembutal (60 mg/kg). Nembutal was given intraperitoneally using a sterile syringe and 28G needle. Rats were maintained warm until a surgical plane of anesthesia was achieved. Anesthesia was assessed by a lack of response to noise and a lack of toe/tail pinching and corneal reflexes. The scrotum of the rat was then shaved using an electric razor to remove excess hair. An incision was made from the bottom of the scrotum to expose the testis with its surrounding cremaster muscle. Excess connective tissue was removed by blunt dissection using fine curved forceps. Arterioles were identified on the cremaster muscle covering the testes and an incision made in an area which has the least branches of the blood vessels. The cremaster muscle was opened by a

longitudinal incision after which the ligament attaching the testis was disrupted leaving the cremaster muscle exposed as a thin sheet. During this procedure the tissue was periodically irrigated with cold saline (0.9%) solution. The muscle was then excised and placed in a dissection chamber containing isolated vessel dissection buffer maintained at -5° C. Recipe of the dissection buffer is given as follows: 3 mM MOPS, 145mM NaCl, 5 mM KCl, 2.5 mM CaCl2, 1 mM MgSO4, 1 mM NaH2PO4, 0.02 mM EDTA, 2 mM pyruvate, 5 mM glucose, and 1% endotoxin and fatty acid free albumin [23, 64].

For microdissection of arteriolar segments the muscle was pinned for viability to a layer of silastic elastomer at the base of the dissection chamber. Segments of the first order (feed) arteriole (1A) of about 2-3mm in length were dissected using sharp forceps and ultra fine spring scissors [65, 66]. Vessel segments were chosen to have no side branches.

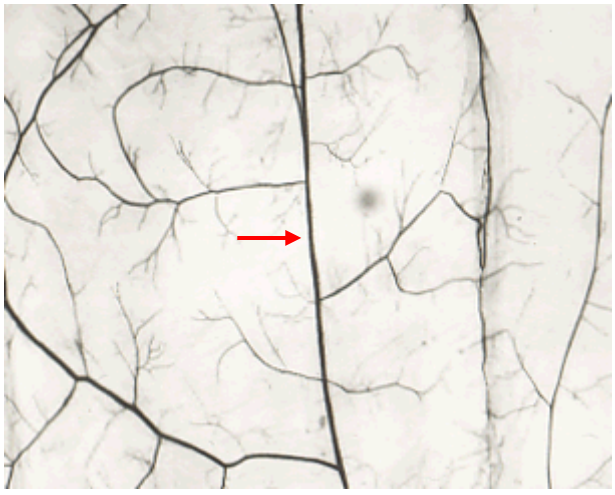

Figure 19: Cremaster tissue as would be positioned on the base of the chamber for dissection. Arrow indicates segments that would likely be suitable for dissection and cannulation.

These segments were then cannulated onto glass pipettes (tips 60-80μm in diameter) which were mounted on a micromanipulator-controlled stage and positioned in a superfusion chamber (5 ml). The chamber was filled with Krebs-bicarbonate buffer solution containing 111 mM NaCl, 25.7 mM NaHCO3, 4.9 mM KCl, 2 mM 5 CaCl2, 1.2 mM MgSO4, 1.2 mM KH2PO4, 11.5 mM glucose, and 10 mM HEPES [23]. The vessel segments were secured tightly at both ends using monofilament silk sutures (10-0) (Alcon Surgicals). Polyethylene tubing on the distal end of the cannulation pipettes was connected to three way stopcocks to allow connection to an appropriate pressure head.

Figure 20: Freshly dissected arteriole, cannulated onto glass pipettes.

On cannulation the vessel stage was positioned on the inverted microscope. One pipette was connected to a pressure reservoir whose height can be adjustable from 40-120mm Hg. The pressure from the reservoir is linearly distributed across the vessel and acts as a physiological parameter [23]. The other end is closed using the 3 way stopcock so that vessels could be studied under pressurized conditions but in the absence of flow. Pressure was calibrated, and marked on the height column, using a sphygmomanometer. The

pressure was continuously monitored using a pressure transducer connected in series with the pressure column. At all times care was taken to avoid air bubbles in the entire fluidic pathway containing the pipettes, vessel and the tubing.

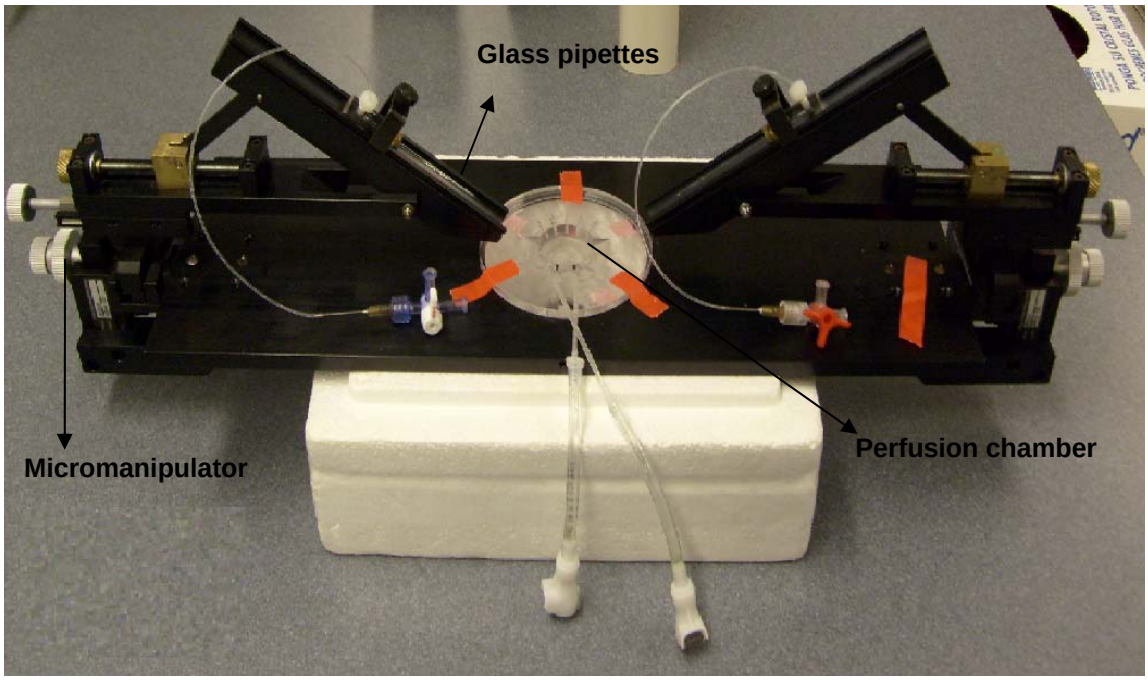

Figure 21: Cannulation chamber for freshly dissected arterioles. Glass pipettes will be filled air-bubble free Kreb's buffer and adjusted to the bottom of the cover slip in the perfusion chamber using the micromanipulator.

The bath was continuously superfused (approximately 2-4 ml/min) with Kreb's bicarbonate buffer and its temperature maintained at constant 34°C using a heating coil. Temperature of the bath is monitored using a detector which works on the principle of thermo electric effect. The pH of the buffer under these conditions would be 7.40. An overflow suction system was connected to the bath to complete the superfusion circuit.

Once the vessel was setup on the inverted microscope, it was first tested for leaks. Pressure was applied at one end starting from 40mm Hg, and increased in the order of

70, 100, 120mm Hg [67]. At every pressure change, the vessel is pressurized and stretched to its optimum length (judged as the length required to prevent lateral bowing on a further increase in pressure). If there was any leak in the system, the leak would be repaired and the preparation rechecked for leaks. If there were no leaks, the pressure was lowered to 70mm Hg (in vivo conditions) then the temperature of the bath was slowly increased to 34°C from room temperature. During a 60 mins equilibration period the vessels typically gained spontaneous myogenic tone. Vessels not gaining tone, or continuing to have leaks, were discarded.

5.1.1 Manufacture of Glass Pipettes:

Six inch borosilicate glass capillaries (Harvard Apparatus with internal and external diameters of the order 0.94mm and 1.2mm respectively) were initially pulled to a fine tip using a Sachs-Flaming Micropipette puller (Model# PC-84). The program was looped for 17 times with each cycle providing heating, pulling and subsequent cooling.

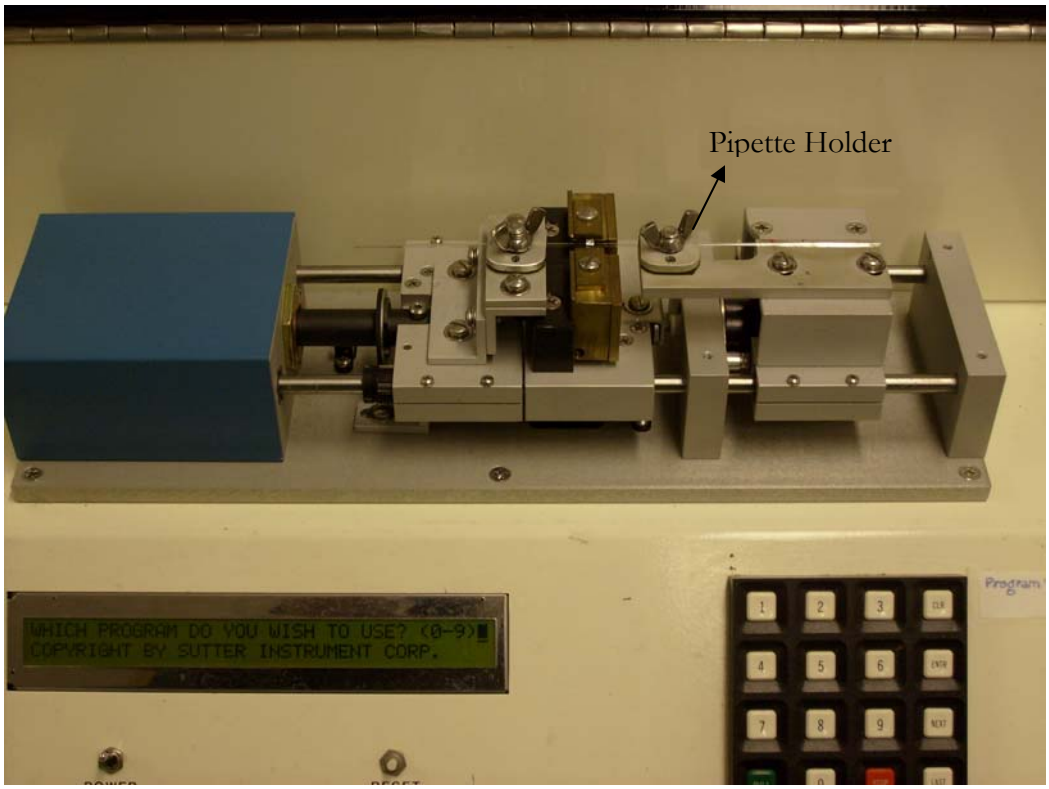

Figure 22: Micropipette Puller. Glass pipette fixed firmly on the holders would be heated and pulled according to a program stored in the memory of the system.

The pipette was then placed in the chunk of a microforge (Stoetling Inc.) and heated to form a hook at the end of the pulled pipette as shown in Figure 22. A light weight was attached to the hook to assist in drawing the tip out as the glass was heated. Pipettes were drawn out to give a tip diameter of approximately 40-60um. The tip was fire polished by heating gently so that the tip was not abrasive to the vessel during cannulation.

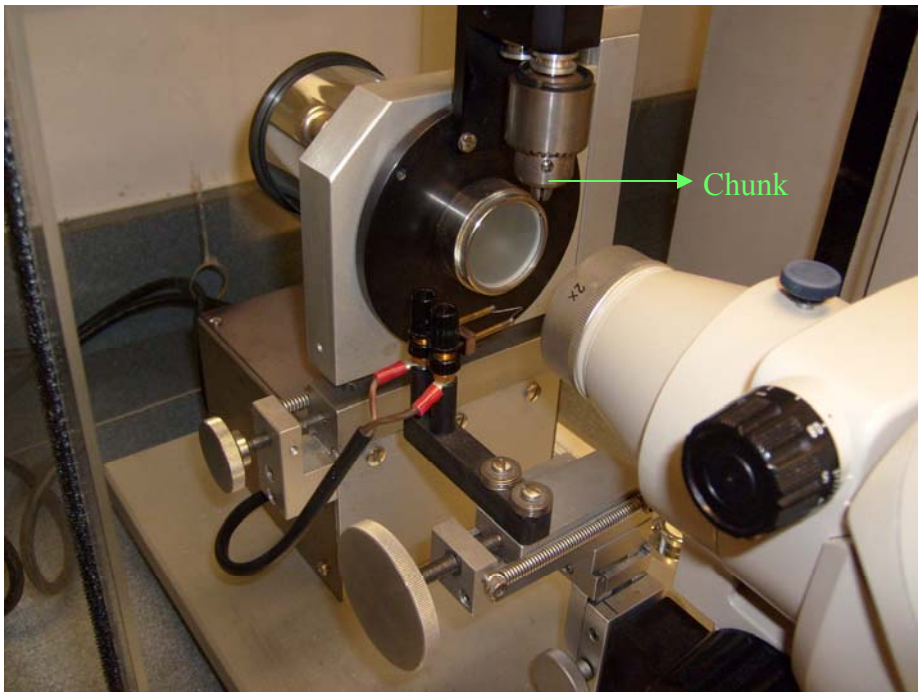

Figure 23: Microforge for shaping the pipettes. Pipettes placed in the chunk, were heated using the filament and shaped.

5.1.2 Cannulation of Vessels:

In preparation for cannulation the pipettes filled with Kreb's bicarbonate buffer, were inserted into a pipette holder and placed on the cannulation chamber. Care was taken to avoid no air bubble in the entire fluidic path. Presence of an air bubble may either disrupt the endothelium or affect the ability of the vessel to gain spontaneous myogenic tone. The pipettes were carefully adjusted toward the base of the cover slip in the chamber. Vessel segments were drawn onto the glass cannula using micro-fine forceps. Monofilament sutures from 'Alcon Surgical', thickness 0.1 Metric were then used to secure vessel segments to each glass cannula.

5.1.3 Measurement of Arteriolar Dimensions:

Measurement of vessel diameter and relating it with other physiological processes is one of the major aims of the project. To accomplish this, an electronic video calipers were used. This system generates lines on the monitor which can be moved in accordance with changes in the vessel diameter. A remote control was used to track the diameter changes observed on a monitor connected to the analog output of the video calipers. Another output from the calipers was given to a POWERLAB Analog-Digital converter. This device communicates with the PC in recording the changes LIVE through the use of compatible software CHART 6.1. A camera attached to the bottom port collected light at wavelength >690nm and makes it feasible to see the diameter changes.

5.2 Loading of Fluorescent Indicators:

For the experiments FRET indicators CC2-DMPE, $DisBAC_4(3)$, and Ca^{2+} indicator Fluo-4AM for measuring membrane potential and intracellular Calcium are used. CC2-DMPE binds to the cellular membrane and the oxonol which is the more negatively charged dye resides in the cytoplasm. Stock solutions of the dyes are made and stored at -20°C. A 5 mM CC2-DMPE aliquot and a 3mM $DisBAC_4(3)$aliquot are taken out of the freezer and brought into room temperature.

The 5mL dye solution (4980uL of Kreb's buffer, 10uL of 0.1% Pluronic acid, 5uL of CC2-DMPE(5mM) and 5uL of $DisBAC_4(3)$ (3mM)) freshly prepared replaces the

contents of the bath. Bicarbonate buffer in the bath was removed carefully and the superfusion is stopped and the heater was turned down for 1 hour. The dye was poured in the bath and the vessel was allowed to incubate for a period of 1 hour at room temperature and at possible no light. After 1 hour of incubation, dye in the bath was removed and the superfusion was turned ON along with the heater. Excess loading solution was washed from the bath for 30 mins and the vessel was allowed to regain tone in preparation of experiments.

When the FRET dyes were made, a mixture of both of them was prepared and loaded simultaneously. The FRET dyes were allowed to wash off, and the vessel should gain its tone and then the Fluo4-AM loading solution (4920uL of Kreb's buffer, 50uL of 0.1% Pluronic acid, 23uL of ($DMSO^{+}$10mg of Fluo4-AM), and 10uL of 100uM Probenecid) replaces the solution in the bath. Another 1 hour of incubation period and washing, and then the vessel will be prepared for membrane potential and Ca^{2+} imaging.

5.3 Procedure for Isolating Vascular Smooth Muscle Cells of Cremaster Tissue:

1) A longest possible arteriole segment of the cremaster tissue was dissected and separated into 10 equal segments and placed in a disposable borosilicate glass culture tube containing of 2mL of low Ca^{2+} buffer for 30 min.

2) Low Ca^{2+} buffer was gently removed from culture tube without disturbing the vessels. Primary digestion buffer consisting of 800uL of low Ca^{2+} buffer, 1mg of dithioerythritol (DITH) powder and 100uL of papain was added into the culture tube and incubated for a period of 30 mins at 37°C.

3) Primary digestion buffer was gently removed and secondary digestion buffer consisting of 800uL of low Ca^{2+} buffer, 1.7mg of elastase, 50uL of collagenase and 50uL of soybean trypsin inhibitor was added and incubated for 12 mins at 34°C.

4) After incubation the secondary digestion buffer was removed and 2mL of low Ca^{2+} buffer was added allowed to equilibrate for a period of 10 mins.

5) A pasteur pipette was fire polished until the ends are rounded.

6) The low Ca^{2+} buffer was gently removed and another 2mL of low Ca^{2+} buffer was added to the vessels and titurated with the fire polished pipette for five times.

5.4 Procedure for Isolating Vascular Smooth Muscle Cells of Cerebral Tissue:

1. A longest possible arteriole segment of the cremaster tissue was dissected and separated into 10 equal segments and placed in a disposable borosilicate glass culture tube consisting of 2mL of low Ca^{2+} buffer for 30 min.
2. Low Ca^{2+} buffer was gently removed from culture tube disturbing the vessels. Primary digestion buffer consisting of 800uL of low Ca^{2+} buffer, 1mg of dithioerythritol (DITH) powder and 100uL of papain was added into the culture tube and incubated for a period of 24 mins at 37°C.

3. Primary digestion buffer was gently removed and secondary digestion buffer consisting of 800uL of low Ca^{2+} buffer, 1.7mg of elastase, 50uL of collagenase and 50uL of soybean trypsin inhibitor was added and incubated for 9 mins at 34°C.
4. After incubation the secondary digestion buffer was removed and 2mL of low Ca^{2+} buffer was added allowed to equilibrate for a period of 10 mins.
5. A pasteur pipette was fire polished until the ends are rounded.
6. The low Ca^{2+} buffer was gently removed and another 2mL of low Ca^{2+} buffer was added to the vessels and titurated with the fire polished pipette for five times.

5.5 Conformation of Fluorescence Studies Using the System:

Initially fluorescently labeled rat brain slices and fluorescent beads were tested to verify the ability of the system to detect changes in fluorescence. Several issues with a newly built system including, chromatic parfocality in the Quadview optics, parfocality alignment in the multiple ports of the microscope, laser alignments for optimal power transmission were examined and corrected where necessary.

Several studies were performed on freshly isolated cremaster and cerebral smooth muscle cells (SMC), cultured SMC isolated and cannulated arterioles for the ability of the system to detect the fluorescence occurring in them. FRET images of cells were collected in the donor and acceptor emission channels in multiple loaded cells. Changes in the

fluorescence emission in the donor and acceptor emission channels in the Quadview mode were collected at certain constant acquisition parameters (intensity of laser illumination, exposure time, gain of the camera, objective lens) and stimulations and the results of these fluorescence values were analyzed and graphed.

5.6 FRET Based Em Measurements in Isolated Cells:

Freshly isolated cremaster and cerebral smooth muscle cells, and cultured smooth muscle cells and were loaded with the coumarin (5uM) and oxonol (3uM) dyes in an 8-well chamber (volume of a well was 1mL). After 1 hour of incubation and washing, the cells were illuminated with 405nm, and the resulting FRET signals are recorded. Time control for cells was performed to indicate that the ratiometric signal was constant for a period of time (3 mins). To test the ability of the FRET system to detect changes in Em, cells were stimulated with KCl which causes depolarization and contraction. Resulting change in fluorescence were tracked continuously for 3 mins.

CHAPTER 6

EXPERIMENTAL PROTOCOLS

6.1 Toxicity of Indicators-Effects on Freshly Isolated Vessels:

After cannulation vessels were allowed to gain spontaneous myogenic tone. Concentration- response relationships to Acetlycholine (ACh) and Norepinephrine (NE) were taken before and after loading with the various dyes. Similarly, actute myogenic responsiveness (as measured by responses to pressure steps) was assessed pre and post dye loading. Acetylcholine is a vasodilator which acts on the endothelial cells, releasing vasodilator factors including NO (Nitric Oxide) and EDHF (Endothelium derived hyperpolarizing factor). Norepinephrine constricts the arterioles by a direct action on VSM mediated through its binding to alpha adrenoreceptors. Varying concentrations of these vasoactive factors (10-9M – 10-5M) were prepared by serial dilutions (Figure 24) and added to the bath in an increasing order of concentration.

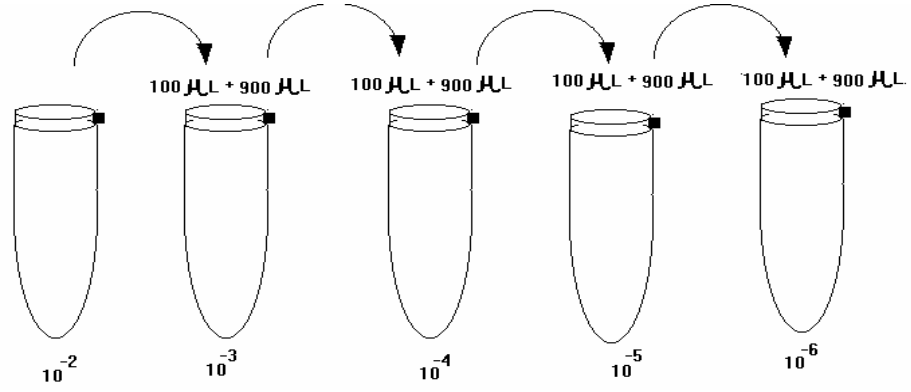

Figure 24: Figure showing the preparation of various concentrations of vasoagonists norepinephrine and acetylcholine using serial dilutions.

Superfusion of the Krebb's bicarbonate buffer was stopped when a response to a given concentration of a vasoactive agent was studied. Vessel diameter was tracked continually for a period of 10 mins. Superfusion was resumed and the vessel was washed for a period of 10 mins to remove the previously added dose. The vessel would be back to its basal tone after a few mins of washing. Data obtained was analyzed and a graph with percentile changes in diameter with respect to the doses was plotted. For normalization of the data, the diameter at 70mm Hg in the presence or absence of an agent was divided by the passive diameter, measured after superfusion in '0' Ca^{2+} buffer. Experiments were performed for individual dyes, CC2-DMPE, $DisBAC_2(3)$, and combined loading. Studies were extended by loading the vessels with another fluorophore, a calcium indicator Fluo4-AM. Loading of Fluo4-AM alone was considered unnecessary as it is a commonly used indicator for calcium measurements in several types of cells and arterioles [68].

Experiments were also conducted based on the vessel's response to pressure step. The vessel was allowed to establish its basal tone by setting the pressure at 70mmHg. A

pressure step response was taken by dropping the pressure to 50mm Hg. Baseline tracking of the vessel's diameter was performed for 10 mins and the pressure was raised to 100mm Hg. As above the data obtained was normalized to the diameter under passive conditions and averaged to obtain group data.

6.2 Toxicity Studies of the Dyes on Vascular Smooth Muscle Cells:

Cultured cremaster smooth muscle cells produced through several passages (<10)were confluent. Cells were grown in an eight well plate as shown in the Figure 25.

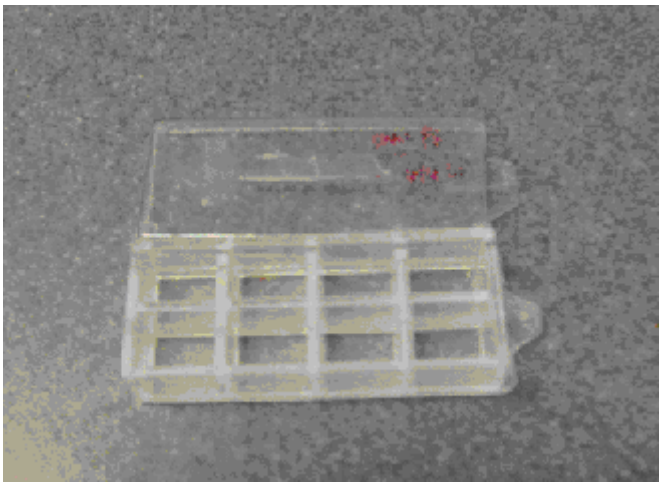

Figure 25: 8 well (volume of each well was 1ml) plate used for growing cells for fluorescence studies.

These cells were maintained in a tissue culture incubator (5% CO2, 34°C) until used. Fresh dye solutions were prepared prior to the loading toxicity experiments. Cells taken out of the incubation chamber were washed in Krebb's buffer and loaded with the dye

solution (5uM CC2-DMPE and 3uM $DisBAC_4(3)$) prepared. Cells were allowed to load for a period of 1 hour and then washed for three times with Krebs buffer.

To test the viability of the cells, the cells were stained with propidium iodide (PI). Cells in a well were treated with ethanol. Such cells dye and the nuclear membrane becomes permeable to the cytoplasmic PI, which then settles in the nucleus.

CHAPTER 7

DEVELOPMENT OF THE OPTICAL SYSTEM

7.1 Olympus Inverted Microscope IX-71 and Basics of Light Path:

The chosen base for the system was the Olympus IX-71. The IX-71 inverted microscope is a V-shaped optical design which gives superior images with minimal optical losses when compared to its predecessors, shown in Figure 26. Frame stability is improved by constructing with cast ADC-12 aluminum and incorporating an external power supply to reduce heat and thermal expansion. IX-71's frame and design provides access to 9 ports herein multiple devices can be connected. Four ports are used for concurrent access of the principal image. Microscope controls are ergonomically placed for easy access by the user. The IX-71 was also chosen as its manual condenser focusing systems, and objective turret provides a flexible yet comparatively simple optical bench.

Using the basic IX-71, a customized optical setup has been designed in conjunction with Hitschfel Instruments (St. Louis, MO). This sophisticated microscope enables experiments to be performed on intact arterioles or isolated cells in both confocal and widefield modes. For the current project the main aim of the optical setup was to allow near simultaneous measurement of membrane potential and intracellular calcium changes in cells and arterioles. The presence of multiple optical communication ports on the IX-

71 frame facilitated the simultaneous use of multiple cameras for the various measurements.

Figure 26: Olympus IX-71.

Source: Olympusamerica, USA.

FRET based experiments, as used in this project, require highly sophisticated and sensitive instrumentation as the amount of signal generated by the energy transfer is relatively small compared to other fluorescence applications. In the present case the system's setup is further complicated as optics for measuring intracellular Ca^{2+} were also included. The Ca^{2+}-sensitive fluorophore exhibits spectral characteristics overlapping, in

particular, with the chosen FRET acceptor. Hence measurement of the 3 fluorescence emission signals (donor, acceptor and Fluo-4) required an image-splitting device, Quadview (Optical Insights, USA), which separates the complex emission signal leaving the microscope and the spinning disk unit. These signals were then projected onto the face of an intensified CCD along with a portion (approximately 10 – 20%) of the transmitted light image. Along with measurements of Em and Ca^{2+}, an ability to monitor the dimensions of a given specimen was also included. In the case of isolated arterioles this allows continuous tracking and recording of changes in vessel diameter via the bottom port (residual 80% of the transmitted light signal). The portion of the transillumination light transmitted to the ICCD allowed collection of a digital image which could potentially be overlaid with the fluorescence images. A consequence of the complex light path was the need to ensure correct alignment of light paths and parfocality.

To increase the flexibility of the system two alternative laser illumination light paths were provided – the first via a spinning disk confocal unit connected to the right hand side port and the second a wide field option coupled to the back side port of the microscope. As stated above, a transillumination light source was used to illuminate the specimen directly. The transillumination light was passed through a 690nm long pass filter, and 80% of it is directed to the bottom port of the microscope. An inexpensive CCD camera was mounted at the bottom port along with a reduction (0.6X) scaling lens, and the signal passed to a Panasonic Flat Panel monitor (19-inch screen).

The Nipkow confocal spinning disk module (Yokogawa-CSU10) was incorporated for localizing signals within cell membranes and for high speed data collection under confocal mode. The optical path in the spinning disk unit was custom designed for the 405/491 lasers. Light passing through the disk unit was coupled to the Quadview (Optical Insights), wavelength splitting module, by means of C-mount metallic rings which again had custom designed optics (described later). The Quadview module splits the full field of optical view into four quadrants based on the wavelength characteristic of the light. Hence an image describing four different events is captured and represented in the complete field of view of the camera. The optical setup of the microscope is shown in Figure 27.

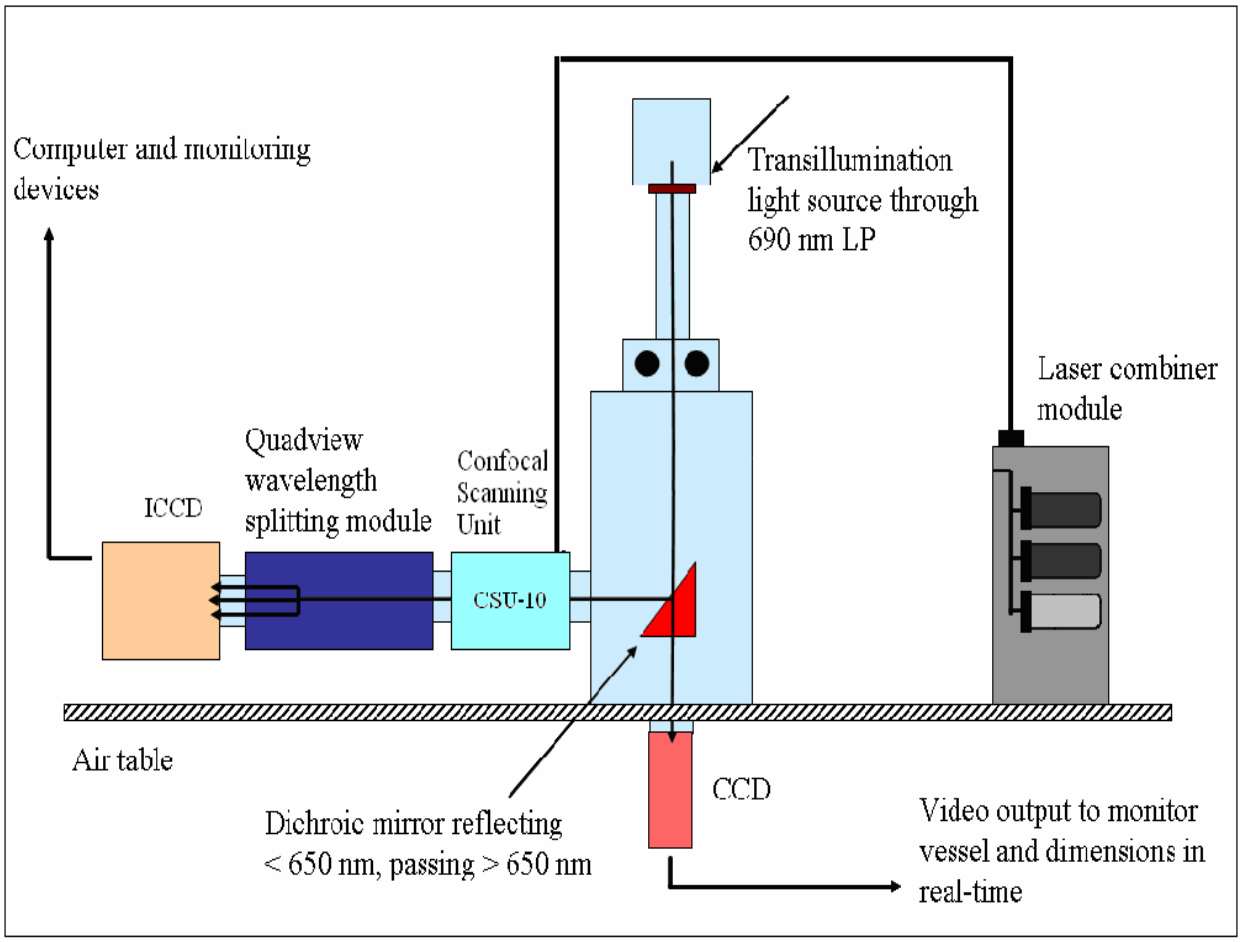

Figure 27: Optical Setup for confocal imaging.

In situations where only a single fluorophore (for example Fluo4-AM for Calcium studies alone) are to be studied the quadview can be operated in "Bypass mode by removal of the emission filter unit. This provides a full field of view and better resolution. An intensified CCD camera (Stanford Photonics XR Mega10-S30) which is highly sensitive and fast is used for fluorescent imaging of the signals.

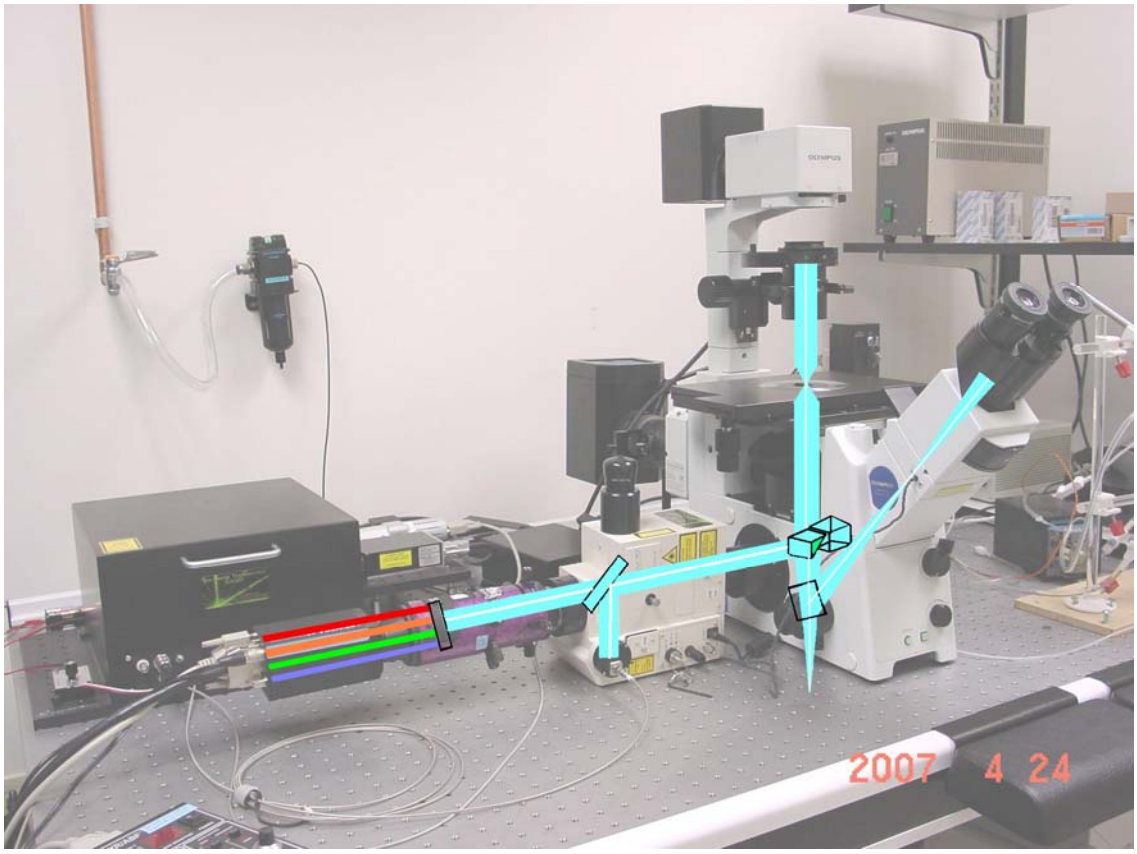

Figure 28: Customized Olympus IX-71. Figure describing the basic entities in the microscope unit and the complex optical path.

7.2 Description of the Bottom port optical path:

A D 690/40-45 filter in the transmitted light path allows the sample to be transilluminated with a specific bandwidth of light (red light). HQ690/40M is an emission filter used to block the laser light 405 and 491nm and transmits the 690nm bright field image to be collected in the Sony CCD camera. The light collected by the bottom port typically passed through a 40x objective which was used for epi-illumination of the specimen. Hence a reduction lens was used in front of the camera to reduce the image size so that a

full image of the specimen was seen on the video monitor. The video monitor image allowed continuous monitoring of the vessel dimension. Video calipers were interfaced between the camera and the monitor, so that the diameter can be continuously tracked and digitally recorded using power lab, and the software Chart and Scope. Flow chart of the optical path for the bottom port is shown in Figure 29

7.3 Description of the Right Side Port:

The Right side port of the Olympus IX-71 was used for fluorescent imaging. Right hand port of the microscope can be defined as the port where laser light was coupled to the spinning disk via an optical fiber, and was used for illuminating the fluorophores in the specimen. Fluorescent light from the specimen traverses back through the objective lens and is reflected off the polychroic in the frame. A dichroic 640DCXXR was employed at the right side port to reflect the 585/40-400nm and 690/40-720 nm transillumination light. This dichroic is placed in between the frame and the spinning disk unit. The optical path of the right side port is shown in Figure 24.

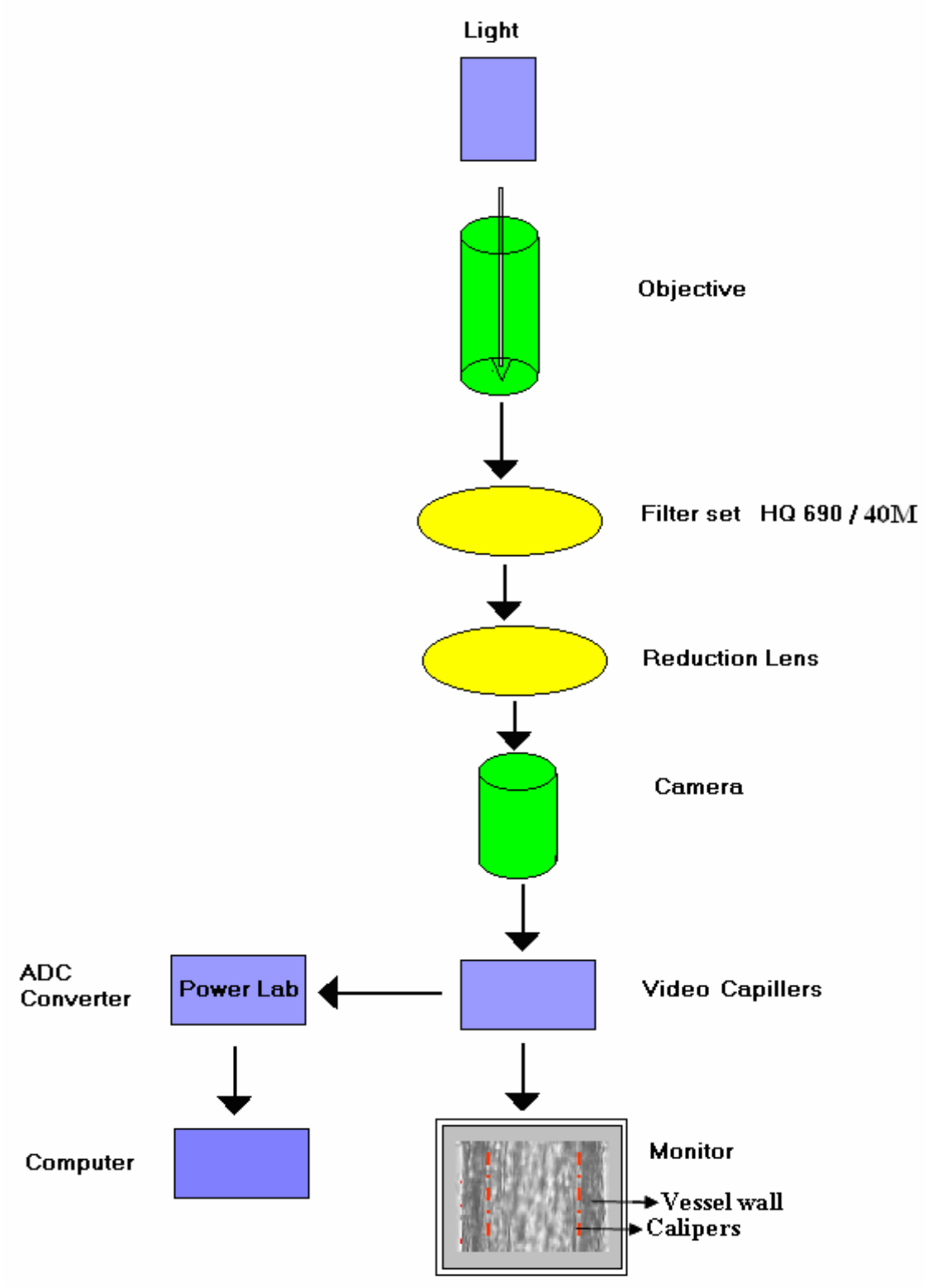

Figure 29: Flow chart of the Optical path for the bottom port.

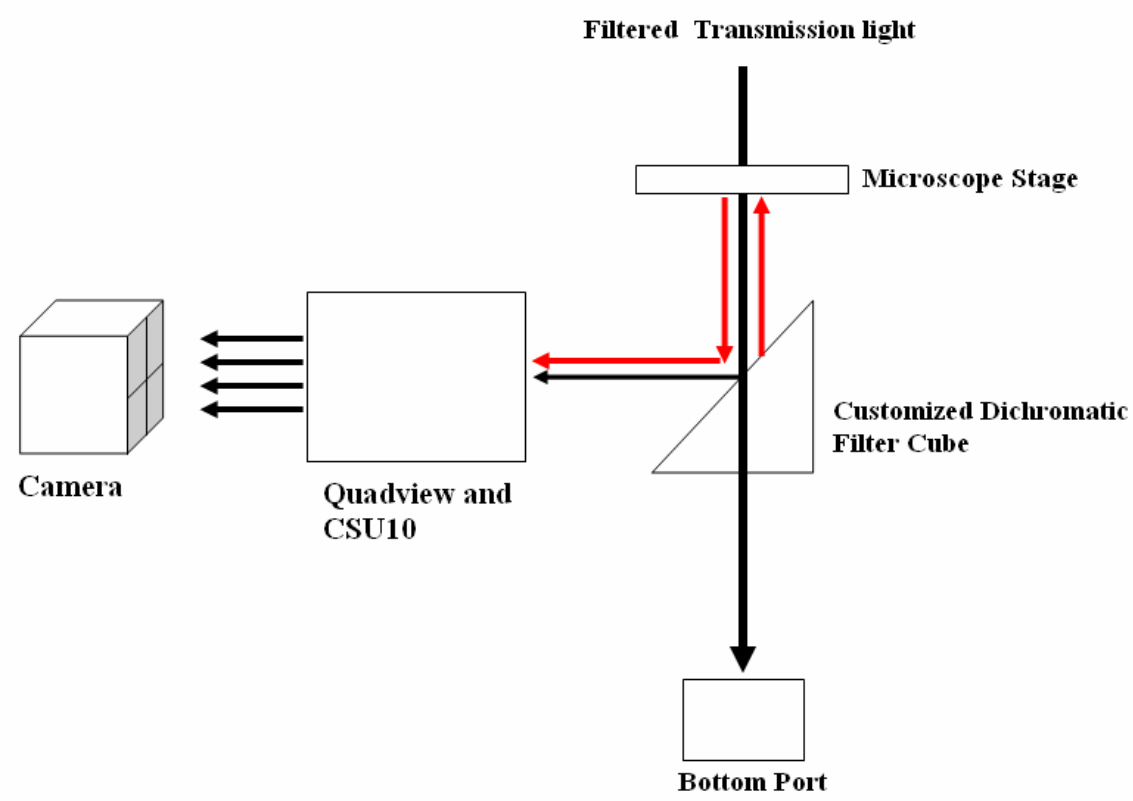

Figure 30: Optical path for the right side port of Olympus IX-71.

7.4 Optical Filters and Dichroic Mirrors:

Filters with specific spectral and physical characteristics are a major requirement for fluorescence microscopy. The requirements vary with the type of application used on the microscope. Because fluorescence requires specific wavelengths both for illumination and detection, separating the light accurately is of primary importance. Due to the development of many dyes, secondary fluorescence increased its prominence, and their spectral characteristics are well defined in the visible spectrum. The shift in the excitation and emission peak wavelengths of a fluorochrome is termed as Stoke's shift. Filters are required in fluorescence microscopy to basically attenuate the excitation light and

selectively distinguish the fluorescent light from the source, background and the autofluorescence signals [69].

Figure 31 shown below depicts the basic filter cube setup and indicating the individual entities in it.

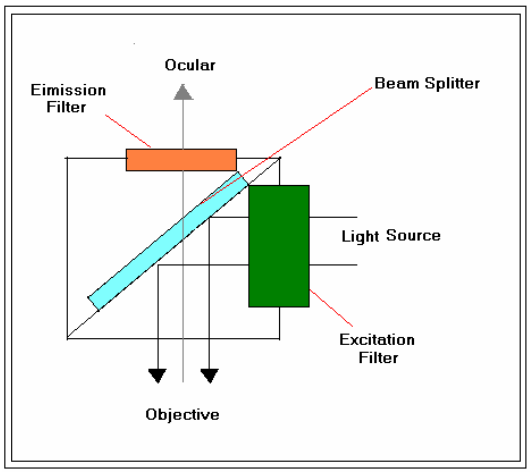

Figure 31: A Basic Filter cube setup showing the arrangement of excitation, emission and dichroic filters and the light path. Dichromatic beam splitter inserted at an angle of 45 degrees to the axis, selectively reflects excitation light and transmits the emission light.

Excitation filters are designed based on the excitation wavelengths of the fluorophores, used to label the specimen. Emission filters selectively transmit the fluorescent light from the fluorophore-labeled specimen, blocking the unwanted light from the excitation sources. The fluorescent light is always of longer wavelength and the emission filters are generally band pass or long pass depending on whether there are multiple fluorophores present in the specimen. A Dichroic beamsplitter also called as the dichroic mirror or dichromatic beam splitter is a filter which is placed at 45 degree angle to the light path of the microscope. This filter reflects light of 1 wavelength and transmits light of higher

wavelength. They are widely used in epiillumination systems and have an efficiency of 90%(~) in both reflecting the excitation and transmitting the emission.

The fluorescent dyes used in the current project are FRET donor (CC2-DMPE), FRET acceptor ($DisBAC_4(3)$) and Ca^{2+} indicator Fluo4-AM. The spectral characteristics of these dyes and their corresponding specifications of the filter sets used in the quadview filter unit are described in the following Table 1. General representation of a filter unit is D X/a-b,where X stands for wavelength, ‘a’ describes the bandwidth, and ‘b’ refers to the diameter of the filter. But the diameter of the filter unit is generally excluded in discussions.

Fluorophore/Process	Excitation Wavelength (nm)	Emission Wavelength (nm)	Quadview Emission Filter	Quadview Dichroic Mirror
FRET				
Donor molecule - CC2-DMPE	405	460	HQ455/30M Block ZQ405/15, 491, 690/40	490DCXR Reflect 400-455/30, Transmit 520/30-720
Acceptor molecule - DiBAC2/4		560 - 620	HQ585/40M Block ZQ405/15, 491, 690/40	640DCXXR Reflect 400-585/40, Transmit 690/40-720
Intracellular Ca^{2+} measurement - Fluo-4	488	520	HQ520/30M Block ZQ405/15, 491, 690/40	545DCXR Reflect 400-520/30, Transmit 585/40-720
Transmitted brightfield image	> 690		HQ690/40M Block ZQ405/15, 491	

Table 1: Description of the filter set designed for the fluorescent dyes used in the current project.

Because the specimen is under epi-illumination and the light from the source is guided through the spinning disk unit, a custom made polychroic "z405/488 trans pc" is used for selective transmission of light. The spectral characteristics of the dichroic are as shown in Figure 32.

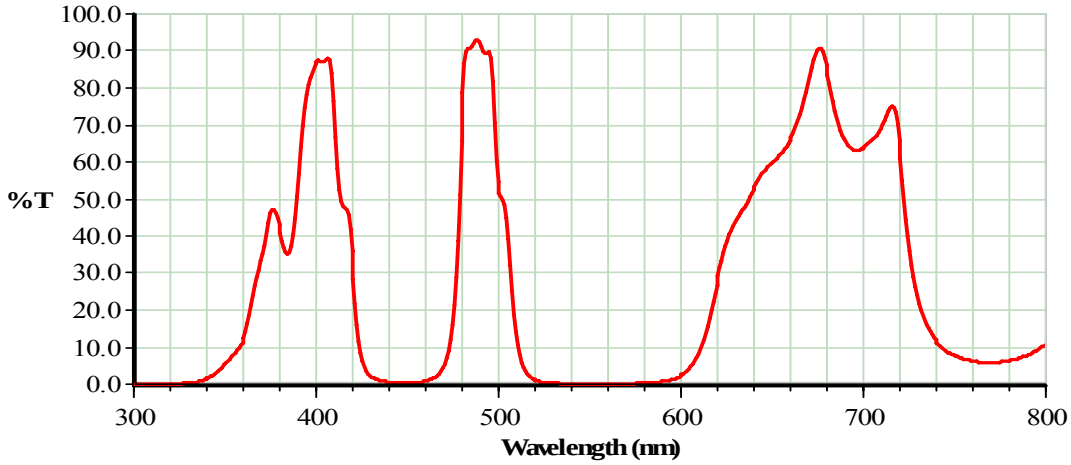

Figure 32: Spectral characteristic of a custom designed polychroic filter used for excitation of the multiple fluorophores CC2-DMPE(405nm), $DisBAC_4(3)$ (488nm) and Fluo4-AM (488nm). %T denotes the peak intensity of transmitted light.

As discussed earlier, the quadview can be operated under bypass mode by removing the unit containing all the emission filters and dichroics. Hence an infinite space was created between the camera and the spinning disk unit. Under these conditions a custom designed dual laser emission filter (HQ540/80nm 25mm) was inserted in the emission path of the CSU-10. Its spectral characteristics are as below in Figure 33. Under this mode of

operation a full field of view (1023/1023 pixel) read out was obtained.

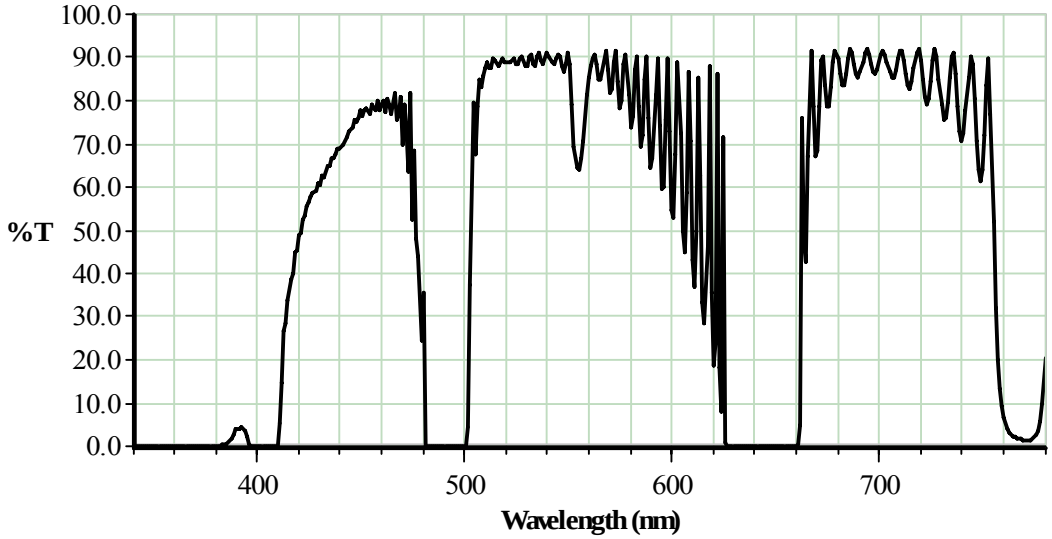

Figure 33: Spectral characteristic of a custom designed polychroic filter used for emission of the multiple fluorophores CC2-DMPE(460nm), $DisBAC_4(3)$ (560nm) and Fluo4-AM (515nm). %T denotes the peak intensity of transmitted light

7.5 Sources of Illumination and Their Control:

Two laser sources were used to excite the fluorophores. Specifications of the Laser sources is described below

1. 491nm Continuous Wave, Green, 100mW, Solid state laser- Cobolt AB Kraftriket.
2. 405nm Continuous wave, violet, 50mW, Diode laser.

A laser combiner module (Solamere Technology group, Salt Lake City, Utah) based on an Acoustic optical tunable filter (AOTF) was used to control the laser illumination and to couple the sources to the microscope via an optical fiber. By exciting the AOTF with a defined frequency of electromagnetic radio waves, its diffraction grating can be controlled, and emission of a particular wavelength of laser light was achieved [69]. The main objective of the project is to perform simultaneous measurement of membrane potential and intracellular calcium, and that is possible with the fast (milli second) switching of lasers by means of the AOTF. Switching of the lasers was incorporated into the system, as there was spectral overlap in the excitation wavelengths of the FRET acceptor and Fluo4. Hence the specimen was sequentially illuminated using the 405nm and 491nm lasers. The image set acquired through this switching of lasers indicates the FRET and Ca^{2+} signaling events and needs to be analyzed based on the excitation signal.

As stated above, a transillumination light source (Halogen 100W) was used to illuminate the specimen directly. The transillumination light was passed through a 690nm long pass filter, and 80% of it is directed to the bottom port of the microscope. An inexpensive Sony CCD camera (Exwave HAD B&W) was mounted at the bottom port along with a reduction (0.6X) scaling lens, and the signal passed to a monitor.

7.6 Confocal Spinning Disk Unit (CSU-10):

CSU was first marketed in 1996, and they are now widely used in biomedical and research laboratories. CSU needs a high speed ICCD camera for collecting light and transducing it to electronic signals compatible with a computer.

CSU employs a Nipkow spinning disk unit, which can scan multiple beams of light passing through a pin-holed disk enabling high speed scanning in opposition to the conventional scanning system. Light is coupled into the unit by means of a fiber optic cable. Divergent light is focused parallel by means of a mirror and a collimating lens. The disk consists of 2 spinning disks, one fabricated with a micro array of lens and the other a pin hole array disk. The beam passes through the micro array of lens and illuminates the sample. Fluorescent light then passes through the pin hole array disk, is deflected through the dichroic mirror in between the disks and is directed to the detector [70].

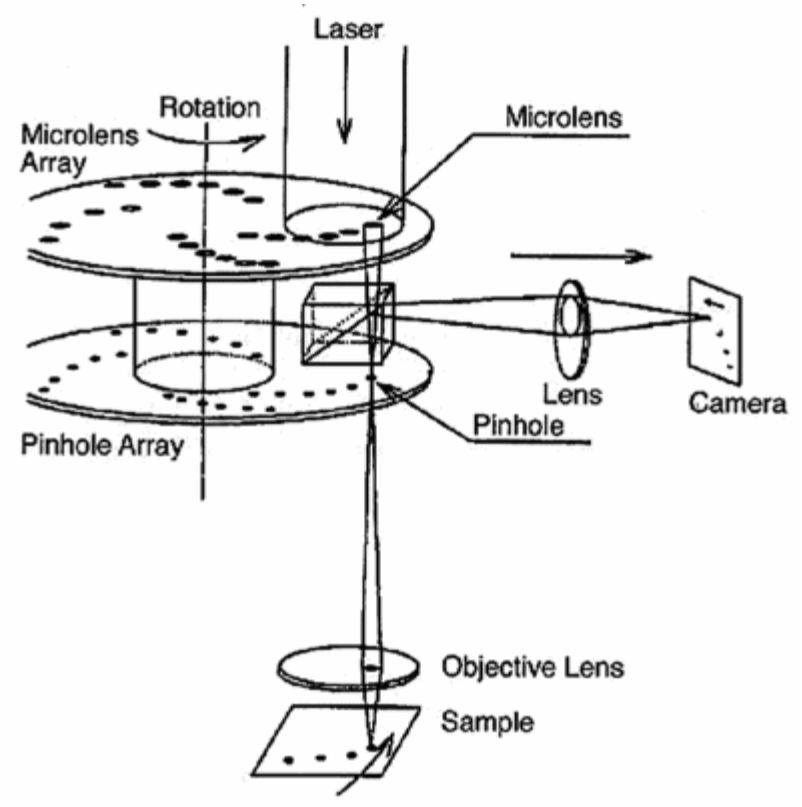

Figure 34: Figure showing the arrangement of the disks and optical path in a basic spinning disk unit.

Source: Video Microscopy. Inoue and Spring, 1997.

Because Nipkow spinning disk device is a high speed scanning device, it needs a camera and a computer equally adaptable for optimal use. An ICCD (XR Mega 10-S30) from Stanford Photonics can monitor the light through the disk, and transfer it to a sophisticated PC. The PC used in the current system was a 2.4GHz processor with 2Giga bytes of Random access memory (RAM) and a 1 Tera Byte RAID fast data storage system. The RAID operates faster than the normal secondary storage devices and provides large storage space (1 Tera Byte hard drive) for the typical bulky data files. A CSU also requires a piezofocussing device for Z-axis control controlled by the computer

if 3-D image stacks are to be collected. The piezo focusing device attaches to the objective and controls it based on the clock signals derived from the PC. This facility was not, however used in our current studies related to measurement of Em.

7.7 Quadview Optics:

Within the Quadview unit there are 4 emission filters and 3 dichroic mirrors (detailed below). These optical elements allow splitting of the complex emission signal into its components and directing the specific emission signals to quadrants of the intensified CCD. Description of the emission filters and dichroics used in the quadview module are already shown in the Table 1.

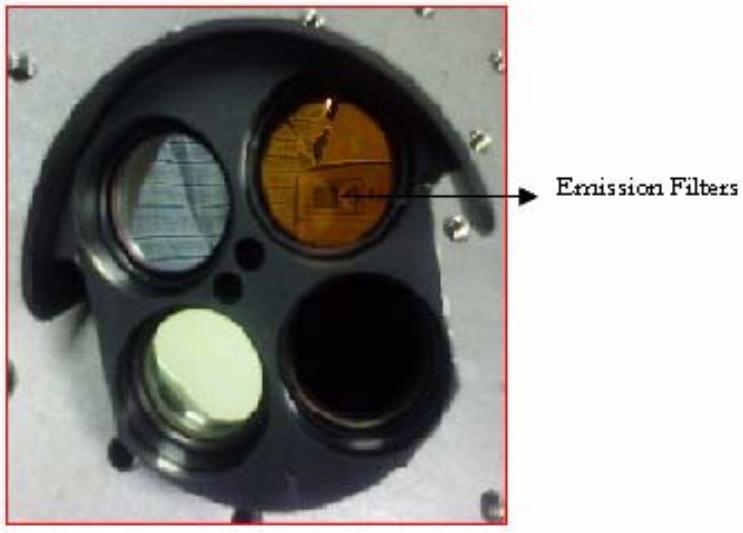

Figure 35: Quadview optics indicating the emission filters for the 4 signals. FRET donor emission, FRET acceptor emission, Fluo4-AM emission, Transilluminated light.

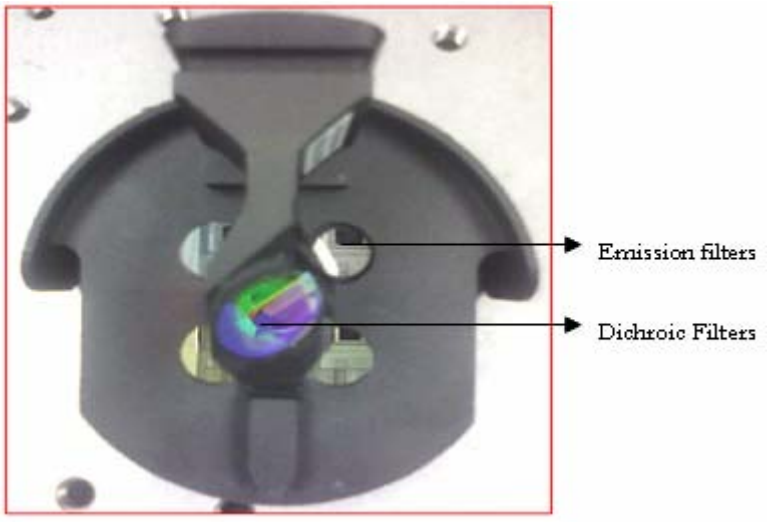

Figure 36: Figure showing the quadview dichroic orientation. Single dichroic filter was shown and the other dichroics are aligned beneath it. Light passes through these dichroics and then is directed to appropriate emission filters.

7.8 High Speed Camera for Fluorescent Imaging

The Stanford Photonics camera used for fluorescence imaging in life science applications is XR/MEGA-10 S30. The device is a mega-pixel CCD (Sony XX285 image sensor) with an attached intensifier and works on the traditional photocathode design principle. It offers a wide spectral range from near IR to 400nm. It is a high speed camera with data collection rates of 15-120 frames/sec.

The key features of the camera S30 can be summarized as follows:

- 1K by 1K resolution 30 frames/sec.
- 512 by 512 (binned 2X2), 60frames/sec.
- 256 by 256 (binned 4X4), 90 frames/sec.
- 1.4K by 104V (binned 4X) for 40% height, 120 frames/sec.

The bit capacity of the camera is 10, and uses Peripheral component interconnect (PCI) for communication with the PC. It comes with a remote handheld controller for gain and mode control. ABF protects the image intensifier tube from unexpected high light exposure. Spectral response of the camera is shown in the Figure 37.

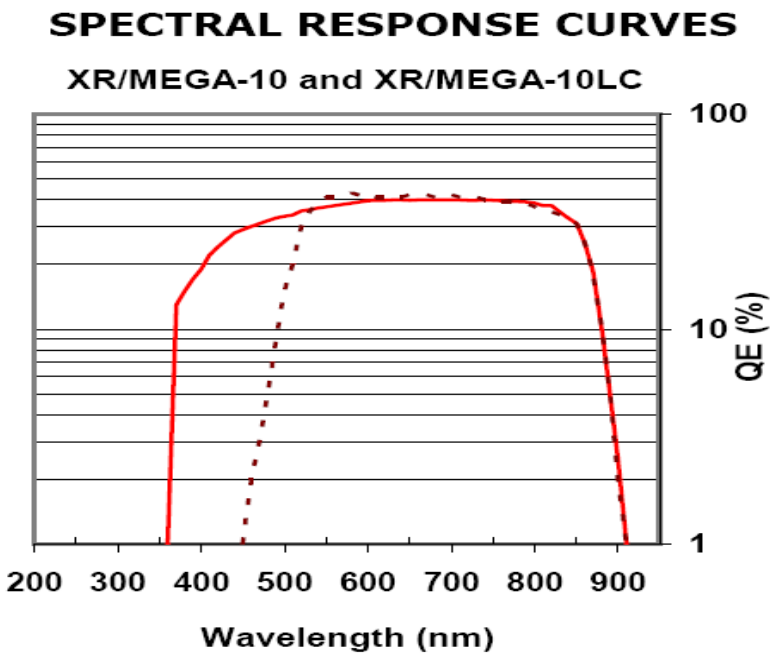

Figure 37: Figure shows the comparison between the two popular cameras XR/MEGA-10 and its predecessor XR/MEGA-10LC. Solid curve indicates the spectral characteristic of XR/MEGA-10 over the extended blue region of the spectrum, advancement to the dotted curve representing the XR/MEGA-10LC. QE represents the quantum efficiency of the cameras.

Source: Stanford Photonics

7.9 Software Control:

Advanced and powerful Image acquisition software "Quad Invivo" is installed in a Windows-XP operated computer. The acquisition window of the imaging software in the computer is divided into 4 quadrants each of 256X256 pixel resolution. The quadrants, if compared to a geometrical co-ordinate system, can be named as follows.

1st Quadrant: Emission of the transillumination light (690nm)

2nd Quadrant: Emission of the Oxonol dye (560nm).

3rd Quadrant: Emission of the Fluo-4AM dye. (515nm).

4th Quadrant: Emission of the Coumarin dye. (460nm)

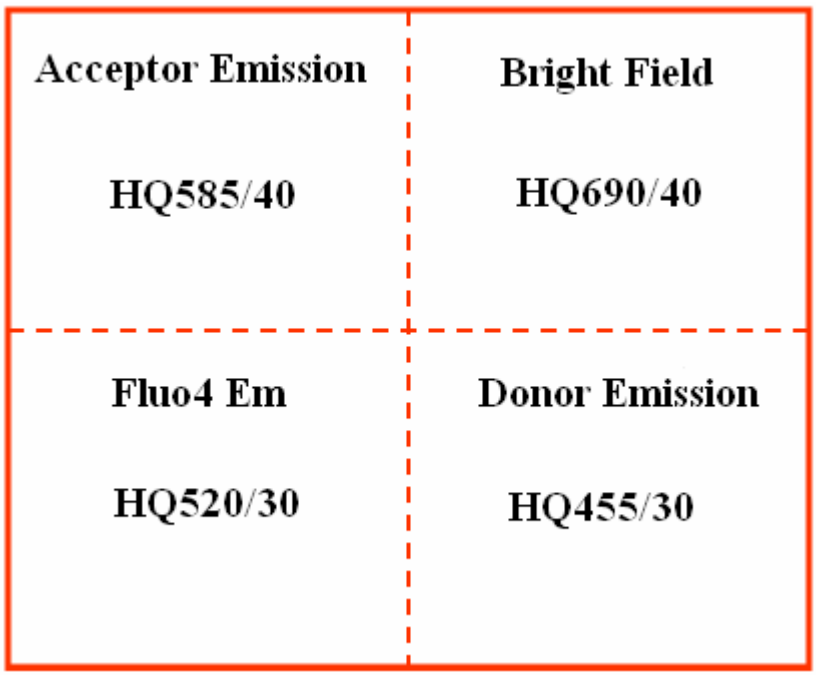

Figure 38: Figure indicating the quadrants and the corresponding emission filters arranged, as seen in the acquisition window.

A 1Tera Byte Raid memory was included for storage of large data files and to assist in rapid collection/storage of image streams. Laser illumination was controlled by an AOTF controller (Solamere Technologies). There are 2 controllers for each of the lasers, and they act as mediators between the computer and lasers in controlling the intensity and exposure time of the beam. Quad In vivo was well designed with all the advanced device drivers, appropriate device settings are to be configured in the software for automatic computer control. An analog to digital controller unit was setup for the system, where in 8 ADC and 3 DAC channels were available for data acquisition. DAC was configured to manage a Piezo controller, which was used to focus the objective for "Z-stack" imaging. ADC channels provide a number of options for monitoring variables such as object dimensions (for example vessel diameter), temperature of superfused solutions, and laser intensity variation.

Off screen image data analysis was performed using the 3D image analysis software Image ProPlus 6.1. This software enables users to write/create macros based on the programming language Visual Basic. These macros act as routines for the commonly performed applications on the acquired data.

CHAPTER 8

RESULTS

8.1 Toxicity Studies

Preliminary experiments were performed on cannulated arterioles, while continuing in the process of designing the confocal microscope. Toxicity studies of the 2 FRET dyes coumarin-labelled phospholipid CC2-DMPE and $DisBAC_4(3)$on the vessels were performed both individually and combined. A set of 4-5 experiments was undertaken for each dye to estimate the exact effect of the dyes on the arterioles. Firstly, concentration response relationships to the vasoconstrictor norepinephrine, and the vasodilator acetylcholine were taken pre and post loading of individual dyes. 5uM CC2-DMPE and 3uM $DisBAC_2(3)$ dye solutions were freshly prepared and added into the bath and the vessels were incubated for a period of one hour at room temperature, turning off the superfusion.

The dye solution was cleared from the bath after 1 hour and then the dye was washed from the vessel for 30 mins turning on the superfusion and the heater. After the vessel regaining tone, concentration responses were taken. For experiments where both dyes were loaded the response to a pressure step from 110-50-100mmHg was also examined.

Before the end of the experiment, passive diameter of the vessel was tracked for 15 mins by superfusing '0' Ca^{2+} buffer into the bath. Data was recorded through Chart and statistically analyzed using the statistical software GraphPad Prism. Graphs obtained for individual and mixed dye combinations are shown in the following figures as follows. Results obtained showed that the FRET dyes were non-toxic and did not affect the myogenic responsiveness of the vessels to vasoagonists and pressure changes.

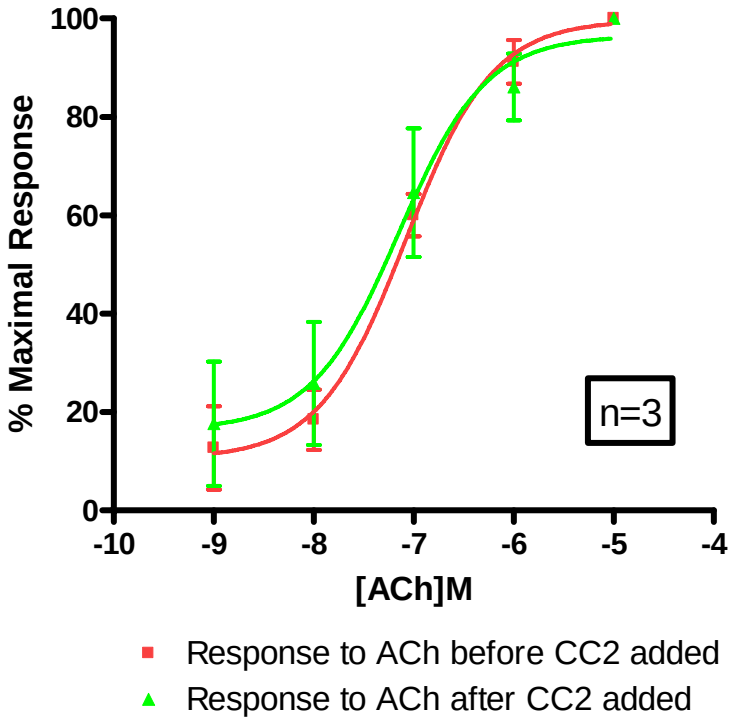

Figure 39: Concentration response to acetlycholine taken before, after CC2 dye loading. Data suggests that the vessels response to vasoactive stimuli did not alter significantly with the fluorophore

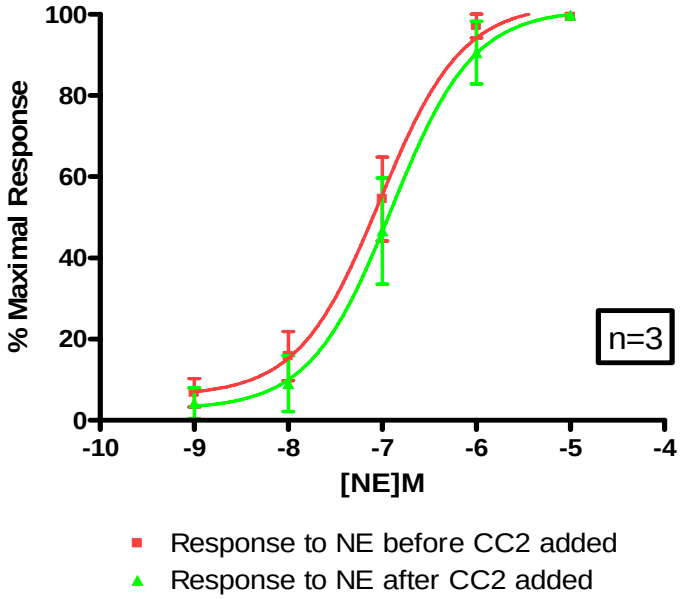

Figure 40: Concentration response to norepinephrine taken before, after CC2 dye loading. Data suggests that the vessels response to vasoactive stimuli did not alter significantly with the fluorophore

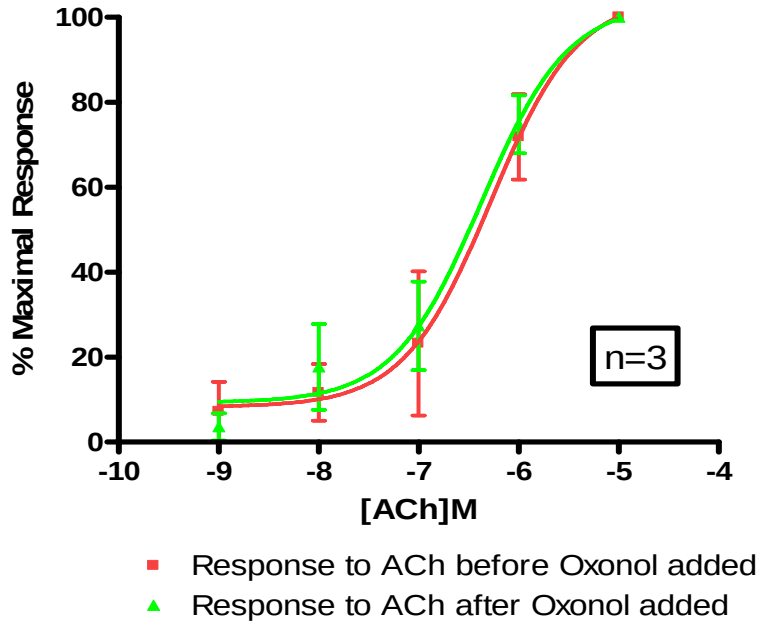

Figure 41: Concentration response to acetlycholine taken before, after oxonol dye loading. Data suggests that the vessels response to vasoactive stimuli did not alter significantly with the fluorophore.

.

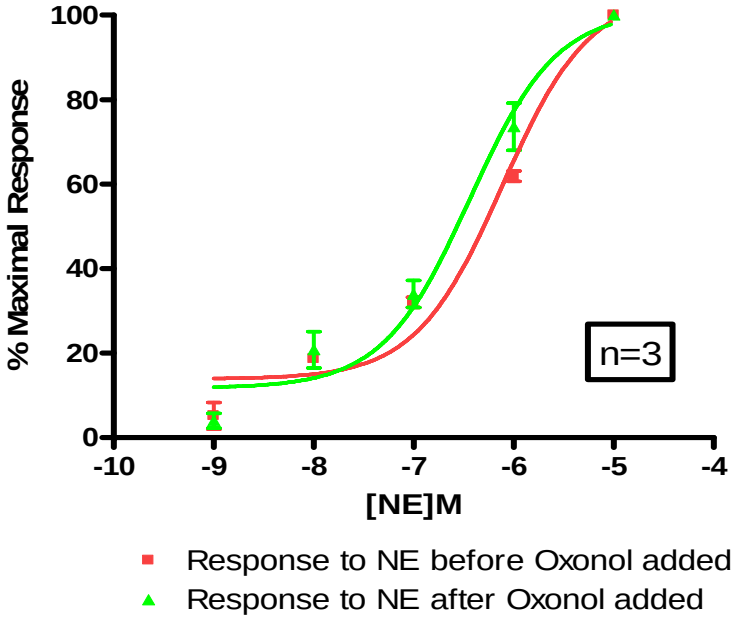

Figure 42: Concentration response to norepinephrine taken before, after FRET dye loading. Data suggests that the vessels response to vasoactive stimuli did not alter significantly with the fluorophore

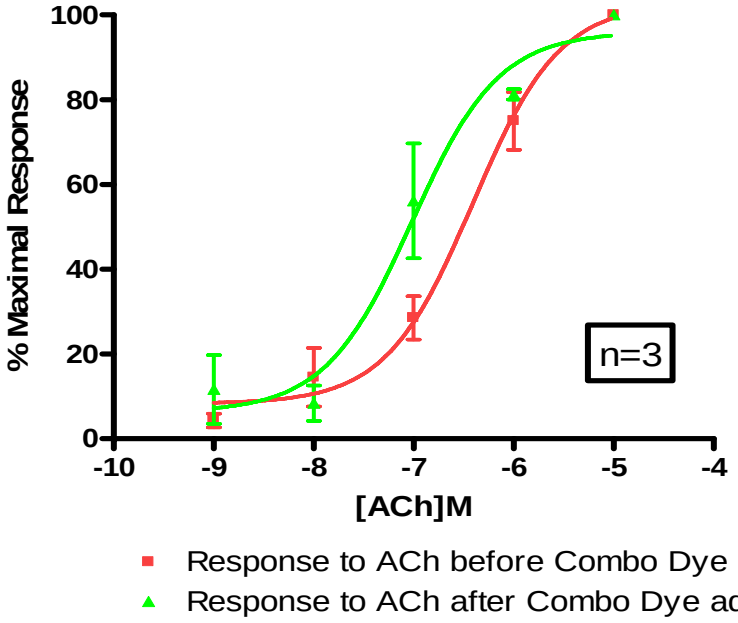

Figure 43: Concentration response to acetlycholine taken before, after FRET dye loading. Data suggests that the vessels response to vasoactive stimuli did not alter significantly with the fluorophore

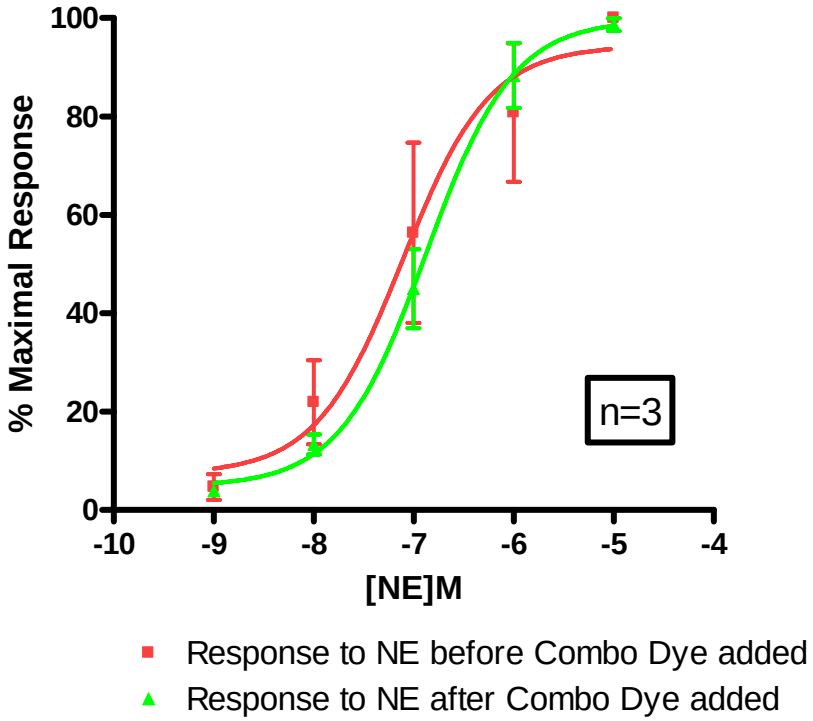

Figure 44: Concentration response to norepinephrine taken before, after FRET dye (CC2-DMPE (5uM) and $DisBAC_2(3)$ (3uM))loading. Data suggests that the vessels response to vasoactive stimuli did not alter significantly after the fluorophore loading.

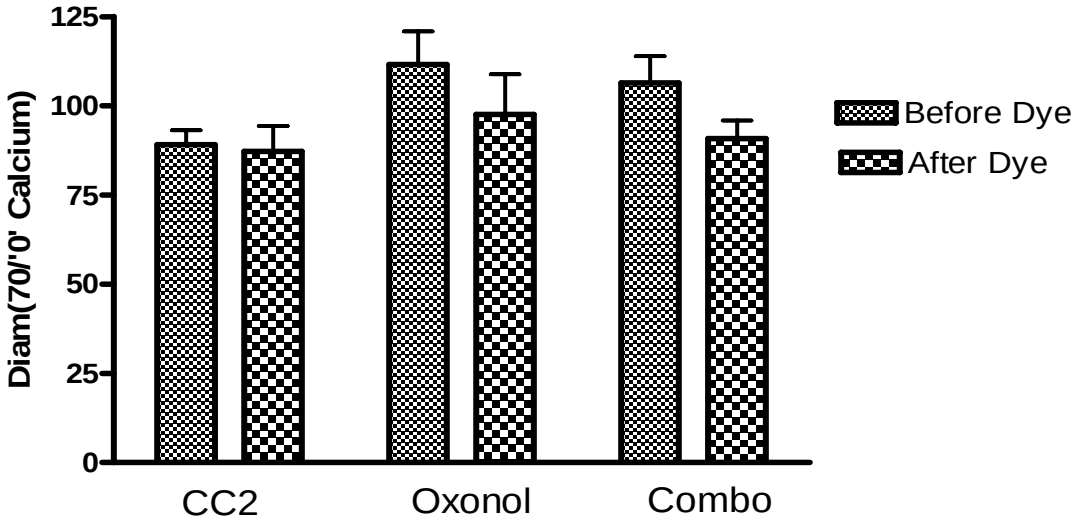

Figure 45: Bar graph representation of the basal myogenic tone of the vessels. Data suggests that vessels maintain their basal diameter after loading of the fluorophores CC2-DMPE (5uM), $DisBAC_2(3)$ (3uM).

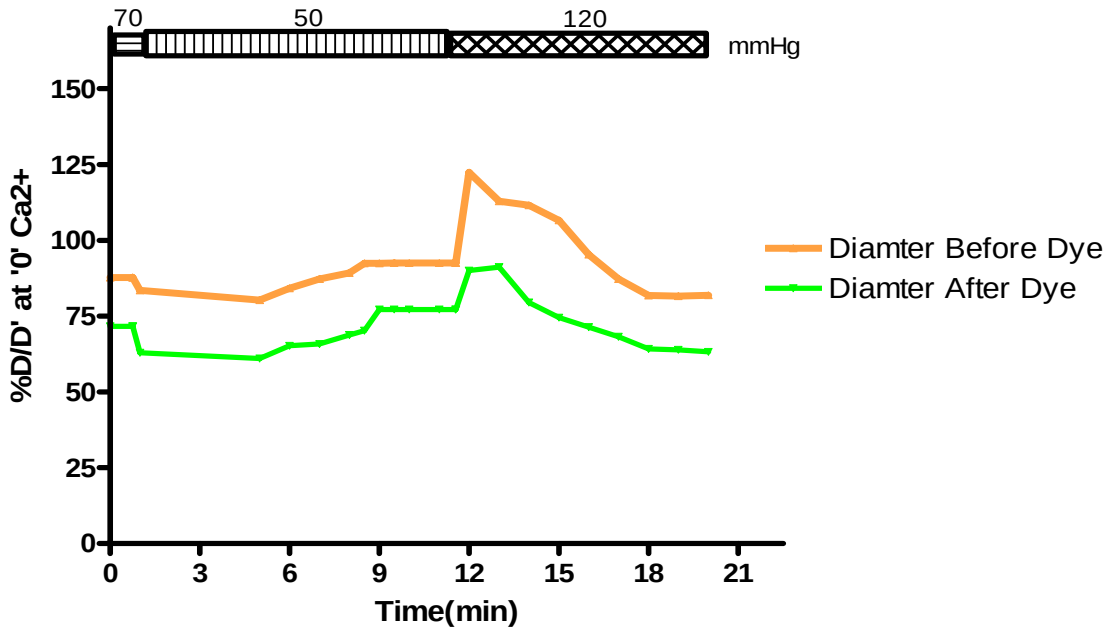

Figure 46: Pressure step response of the vessels before, after the FRET dye (CC2-DMPE (5uM) and $DisBAC_2(3)$ (3uM)). Graph indicates the persistence of myogenic responsiveness of the vessels after loading of the fluorophores.

8.1.1 Toxicity Studies- Loading with Em and Ca^{2+} Indicators:

As stated earlier, the main objective of the project is to measure the membrane potential and intracellular calcium simultaneously. Hence the toxicity studies were extended with loading of the 3rd fluorophore Fluo4-AM. After loading the vessels with FRET dyes, and recording the concentration response curve for acetylcholine, fluo4 was added and the vessels were incubated for 1 hour, similar to the procedure for FRET dyes. The concentration responses to varying acetylcholine were again performed along with the pressure step response. Results of these experiments were analyzed and plotted as shown

below. Graphs in Figure 48 show that the myogenic responsiveness of the vessels in response to the vasoagonists and pressure step did not alter, after addition of the 3 dyes.

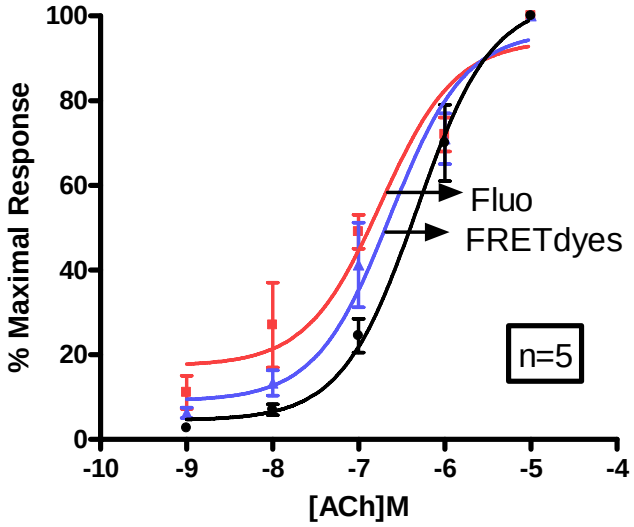

Figure 47: Concentration response to acetlycholine taken before, after FRET dye loading, and after Fluo4. Data suggests that the vessels response to vasoactive stimuli did not alter significantly after the fluorophore loading.

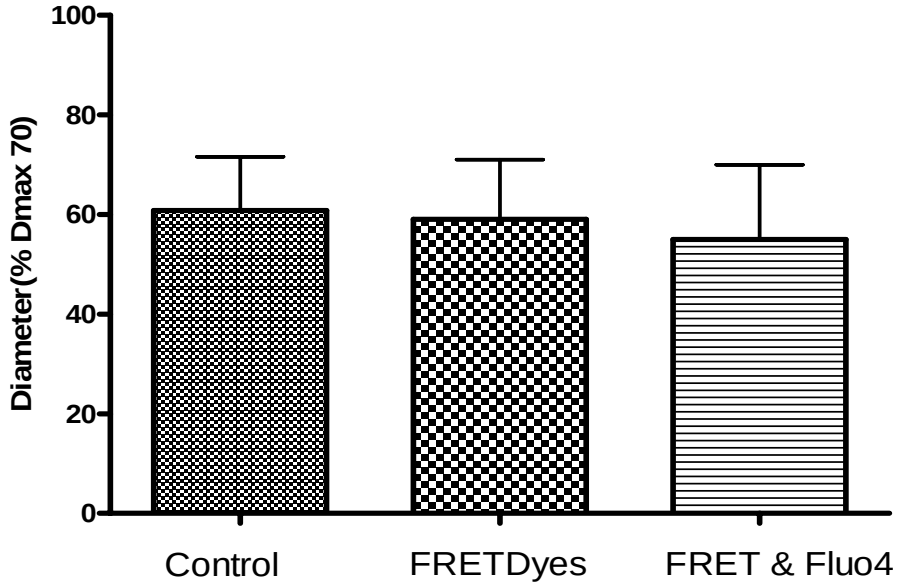

Figure 48: Bar graph representation of the basal myogenic tone of the vessels. Data suggests that vessels maintain their basal diameter after loading of the three fluorophores.

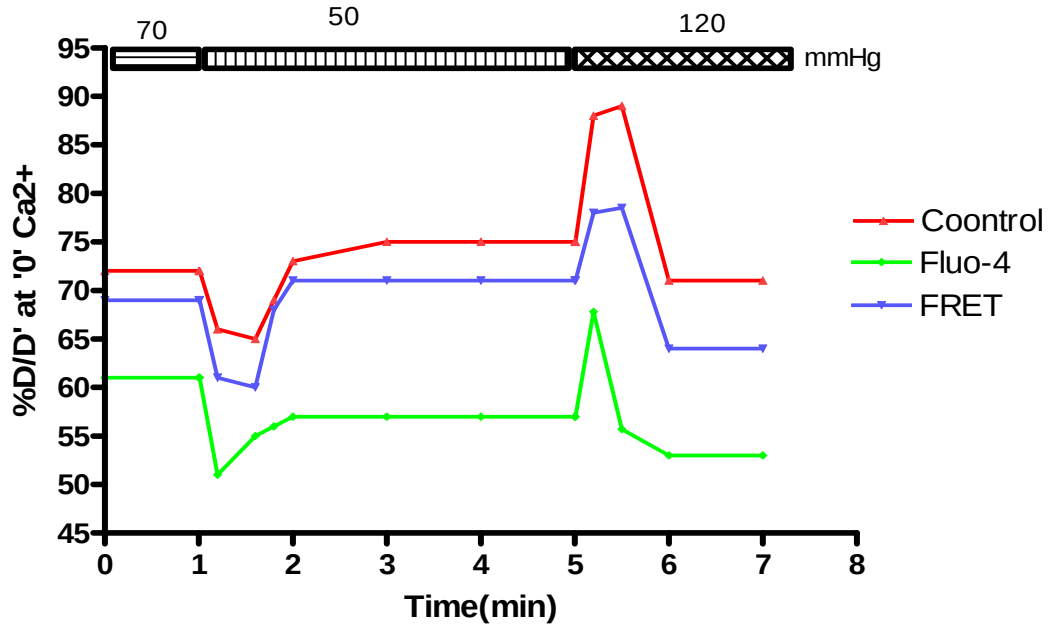

Figure 49: Pressure step response of the vessels before, after the FRET dye (CC2-DMPE (5uM) and $DisBAC_2(3)$ (3uM)), and after Fluo4-AM loading (10uM). Graph indicates the vessels maintain their basal diameter after loading of the three fluorophores.

8.3 Toxicity Studies on Cultured Vascular Smooth Muscle Cells From Cremaster Tissue:

Studies were performed on cultured cremaster smooth muscle cells loaded with CC2 (5uM) and $DisBAC_4(3)$ (3uM) alone and in combination. Cells were loaded with dyes in individual wells and then stained with propidium iodide (PI) in 2 wells, with one of the wells treated with ethanol. PI was illuminated using 540nm light to observe the nuclear staining, indicating the cells were no longer viable. Cells treated with ethanol were compromised with the nuclear membrane being permeable to PI. Cells loaded with the FRET indicators did not stain positively to PI suggesting they remained viable. Figure 51 shows the fluorescent images collected during the experiment.

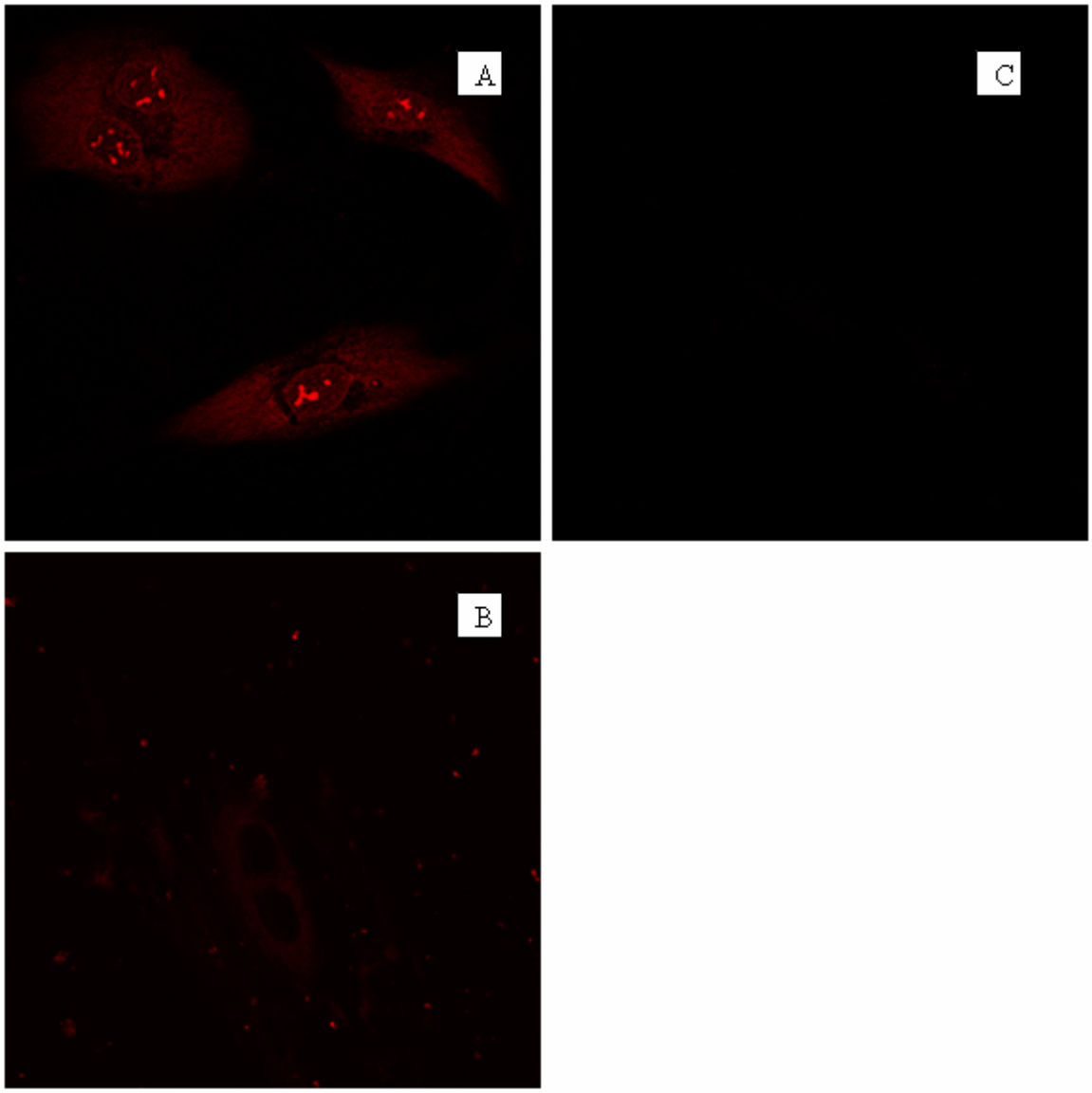

Figure 50: Cells Stained with PI, loaded with FRET dyes. Panel A propridium iodide staining of ethanol treated cells (positive control). Panels B and C; propridium iodide staining of coumarin and oxynol dye-loaded arteriolar smooth muscle cells, respectively. Images were collected on a Zeiss 510 Meta Confocal Microscope

8.2 Spectral Characteristics of the FRET Dyes:

A fluorimeter was used to estimate the spectral characteristics of the fluorescent dyes. This instrument was made available in Prof. Mark Milanick's lab at the Dalton Cardiovascular Research Center. The spectral characteristics (excitation and emission spectra) of the FRET dyes as observed using this instrument are shown below.

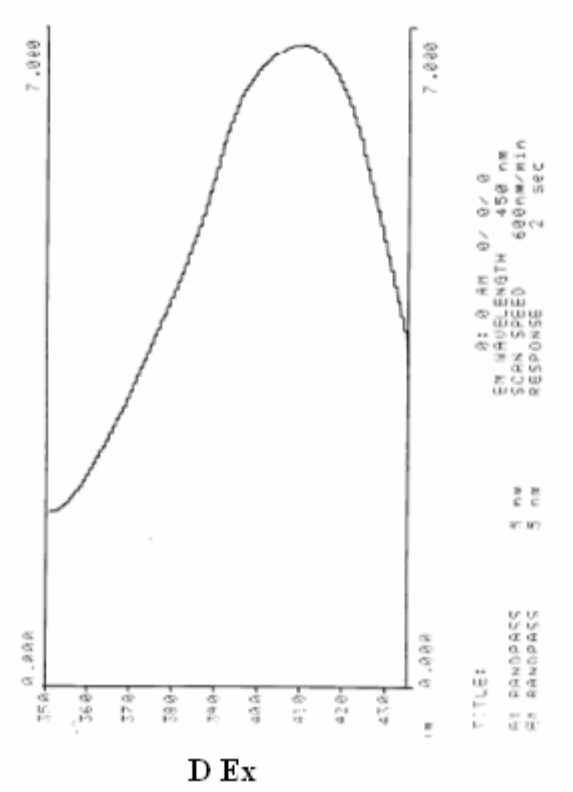

Fig: a

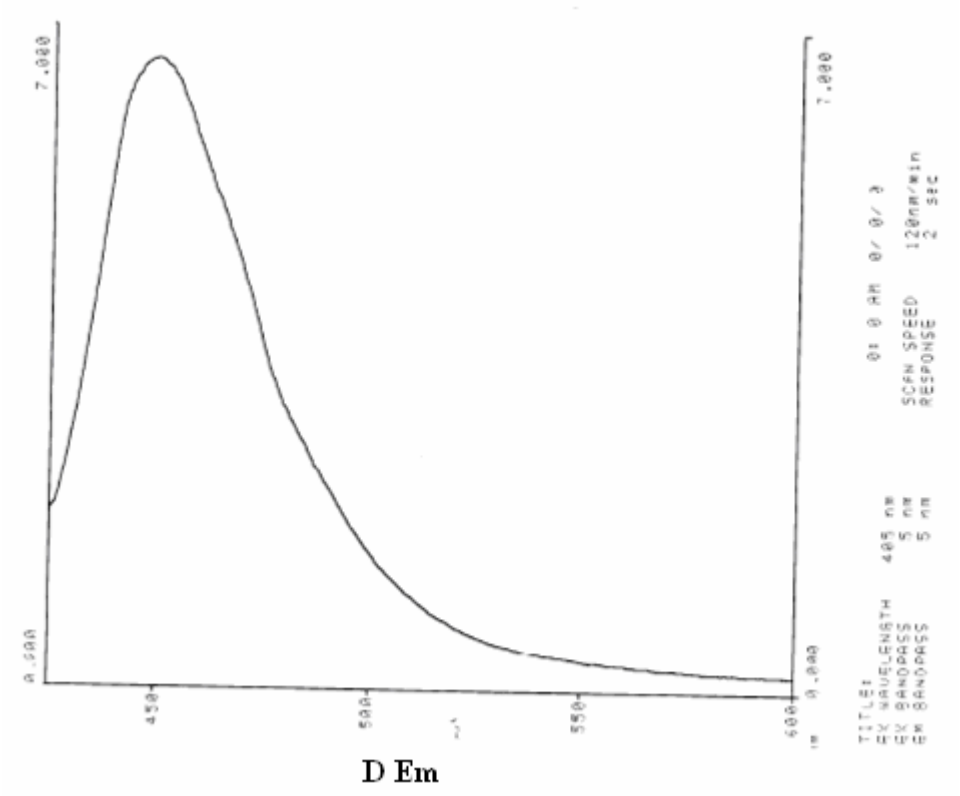
7.000
0.000
7.000
0.000
450
500
550
600
nm
D Em

Fig: b

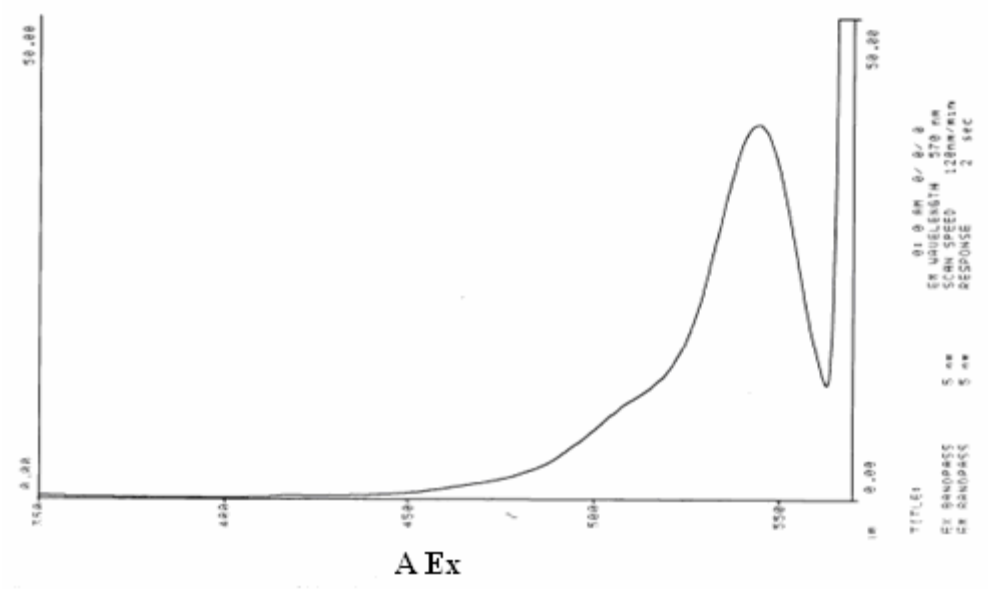
50.00
0.00
50.00
0.00
400
450
500
550
nm
A Ex

Fig:c

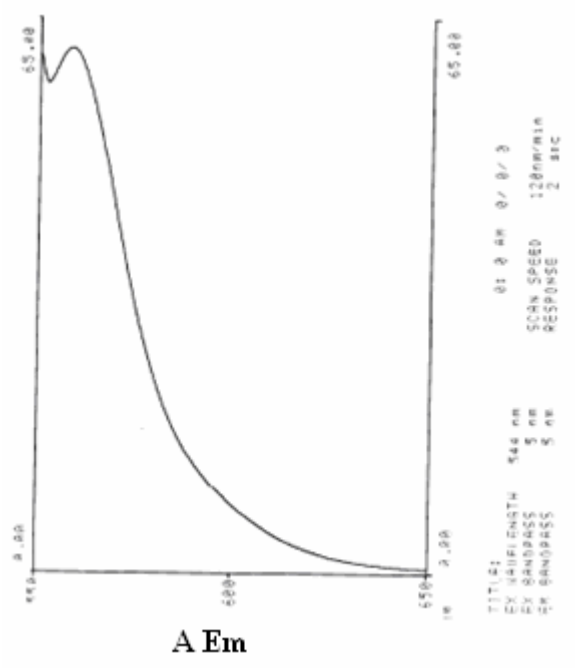

Fig d

Figure 51: Graphs of the spectral characteristics of the FRET dyes CC2-DMPE, and DisBAC3(3) analyzed by a fluorometer. a). CC2-DMPE excitation, b). CC2-DMPE emission, c). DisBAC2(3) excitation and d) DisBAC2(3) emission

.

These results show that the fluorescent dyes CC2-DMPE and $DisBAC_2(3)$ have spectral overlap leading to energy transfer non-radiatively. The large stoke's shift between the two indicators is advantageous in the current project, as another indicator Fluo4-AM was introduced to simultaneously measure global intracellular calcium concentration.

8.4 Demonstration of FRET in Cultured Vascular Smooth Muscle Cells:

These studies were done using a Zeiss 510 Meta dual photon confocal microscope (Cytology Core labs located in the Life Sciences center, Univ. of Missouri-Columbia. Cultured VSM cells loaded with CC2-DMPE were illuminated using the dual photon laser at 790m and images of the stained plasmalemma were collected. A 63x oil immersion objective was used for this demonstration.

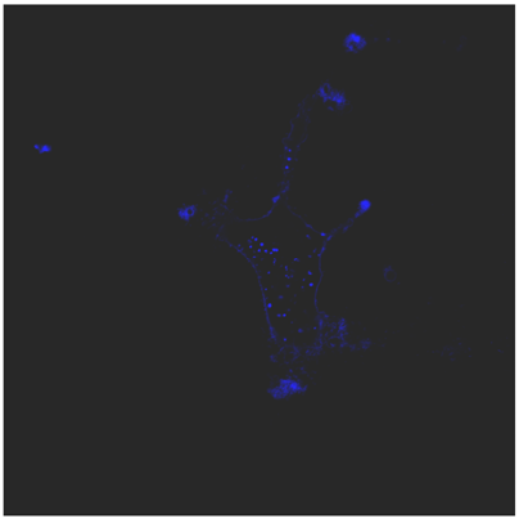

Figure 52: Fluorescent image of a cultured cremaster cell loaded with the FRET donor CC2-DMPE (5uM) dye excited at 790nm(multi photon laser), using a 63X oil immersion objective.

Similarly a 491nm laser was used to illuminate the $DisBAC_2(3)$ dye and the image indicates the diffusion of the oxonol dye into the cell. Results showed that the FRET based indicators can be used on smooth muscle cells for fluorescence studies.

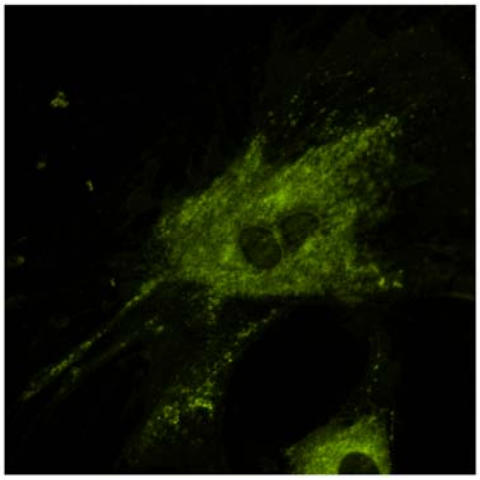

Figure 53: Fluorescent image of a cultured VSM from cremaster muscle loaded with the FRET acceptor-$DisBAC_2(3)$ (3uM) dye excited at 491nm, using a 63X oil immersion objective.

8.5 Parfocalizing the Three Ports of the IX-71 Frame:

The 3 ports of the frame, namely the eyepiece, bottom port and the left hand port were parfocalized for ensuring a consistent view between ports. The order followed in parfocalzing the ports was eyepiece, bottom port and right hand port. A calibration slide was placed on a 40X water objective and was observed through the eye piece to obtain a well focused image. Then using this as a reference, the bottom port was adjusted. A C mount ring was used as a connector for the bottom port and the Sony camera. The C-mount ring was continually rotated to obtain a better image on the monitor, while continuing to maintain a focused image through the eyepiece. Then the left hand port was controlled for equal focal view in the image acquisition window. The CSU-10 connected directly to the port was removed and an optical coupler was used to connect the port and the camera. Position of the dichroic beneath the objective in the frame was adjusted in the z-axis to obtain a best possible image in the acquisition window. Adjusting the right hand

port may result in loss of focal view in the remaining two ports, as the dichroic position is equally important for eyepiece and the bottom port. Hence this process was repeated several times until it was found that equal focal view was seen in all the three ports.

8.6 Quadview Signal Vignetting:

The system employs a Quadview to split the light from transillumination, 460nm, 560nm, 515 nm and to display on the computer. Vignetting is a phenomenon, where the edges of a picture fade gently into the background. Optical signal vignetting was a major issue when the quad view was initially configured. The alignment of the filters and dichroics in the Quadview optics was not optimal and had to be adjusted to eliminate the vignetting. Examples of images with vignetting phenomenon taken with the Quadview are as shown in the Figure 54.

Adjustmenets on the Quadview device align each of the dichroic and the internal mirrors in the X, Y and Z axes. Adjusting the knobs of the Quadview unit, while continuing to monitor for changes in the quadrants of the image acquisition window was performed until each quadrant was optimally aligned with the optical signal spatially distributed along the chip of the camera.

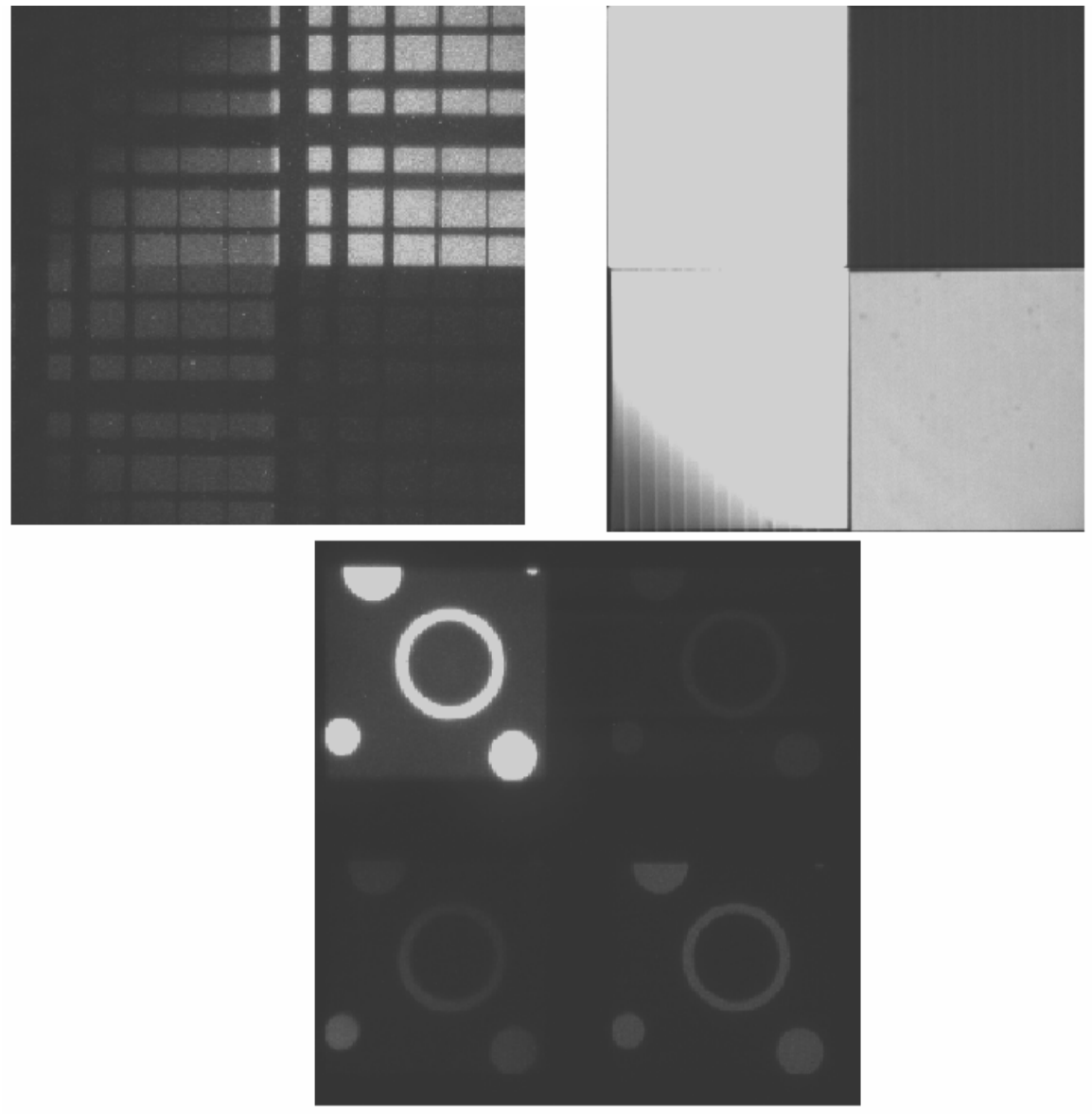

Figure 54: Brightfield quadview images of slides indicating the optical signal vignetting, images were taken with a 20X objective N.A-1.2. Image, top (left and right) represent the vignetting issue in the quadrants. Image, bottom indicates an adjusted quadview image.

8.7 Initial Tests for Fluorescence:

An initial test for fluorescence was performed using fluorescent beads by illuminating them at 491nm via one of the lasers. Cultured SMC stained with CC2-DMPE were illuminated using the 405nm laser. These studies confirmed appropriate excitation by the lasers and the ability to detect the emission signals. The above tests were done in the bypass mode to obtain a full field of view of the specimen. Images of the beads were also obtained through the quadview unit. Fluorescence of the beads was observed only in the 560 and 520 emission channels (2^{nd} and 3^{rd} quadrants according to the notation described earlier) indicating the ability of the quadview optics to spectrally distinguish the light based on wavelength. Images observed are shown in the Figures 55 and 56.

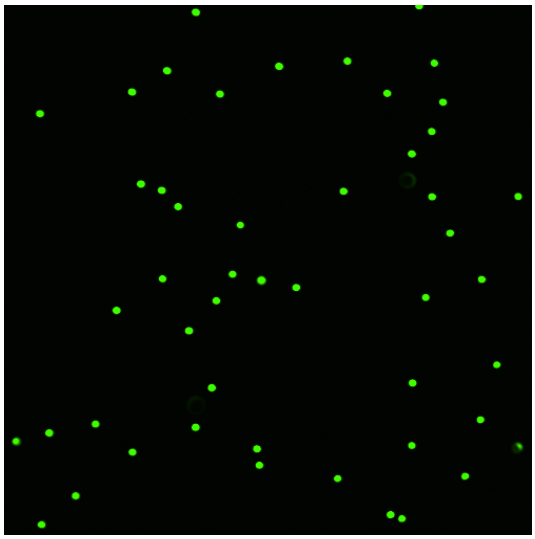

Figure 55: Image of fluorescent beads, excited at 491nm under bypass mode, through a 20X air objective.

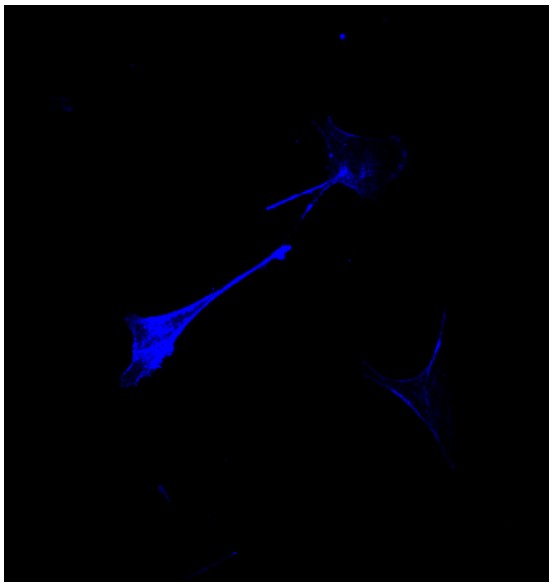

Figure 56: Fluorescent image of cultured cremaster smooth muscle cells stained with Coumarin dye (FRET Donor), excited at 405nm, imaged under bypass mode through a 40X water immersion objective lens.

8.8 Demonstration of FRET Signal on Coumarin/Oxonol Dye-Labeled Freshly Isolated SMC:

Fresh isolated cremaster and cerebral vascular smooth muscle cells loaded with CC2-DMPE (5uM) and $DisBAC_4(3)$ (3uM) were imaged using the developed microscope. Elliptical shaped cells loaded with the coumarin dye alone were identified among the wells and excited with the violet laser-405nm to obtain an image as shown in Figure 57. Quadview unit splits the signal from the CSU-10 into four entities and sends it to the camera. The cell shown in the figure demonstrates the membrane localization of the dye. A brightfield image of the cell is shown in the 1^{st} quadrant of the image, and can be overlaid on the fluorescent signals for diameter and length measurements. Emission of coumarin may bleed through into other quadrants, but may be cancelled using software.

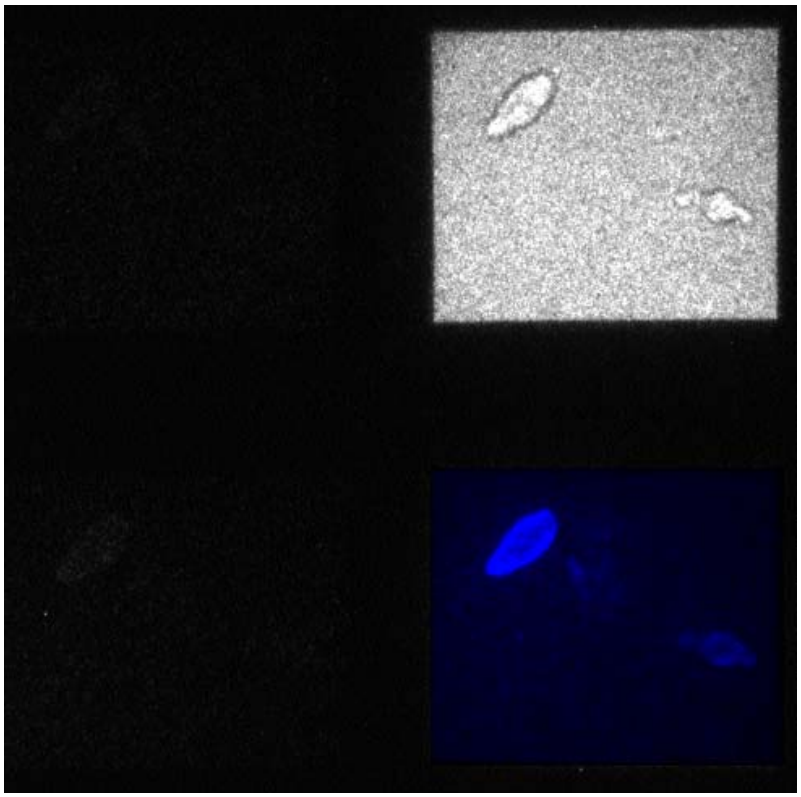

Figure 57: Fluorescent Quadview image of a freshly isolated cremaster smooth muscle cell labeled with CC2-DMPE (5uM), illuminated by a 405nm laser, through a 40X-water immersion objective.

FRET was observed to occur when VSM cells labeled with CC2-DMPE and Oxonol dyes were excited at 405nm. Emission of the coumarin signal excites the oxonol molecules in the cell and leads to its emission as shown in the 2nd quadrant. The intensity of the donor and acceptor emission signal, in part, depends on the membrane potential of the cell. During depolarization, the potential inside the cell tends to be more positive, hence attracting the oxonol molecules, thereby increasing the distance from the coumarin. This leads to increase in the emission of the coumarin dye and decrease in the emission of the oxonol dye. The cell when excited at 491nm laser light fluoresces brighter in the oxonol emission channel, as the diffused oxonol molecules depict independent fluorescence.

Background fluorescence values are subtracted from the obtained signal to get the actual FRET emission signal. Direct excitation of the oxonol dye can be used as a volume marker of the cells.

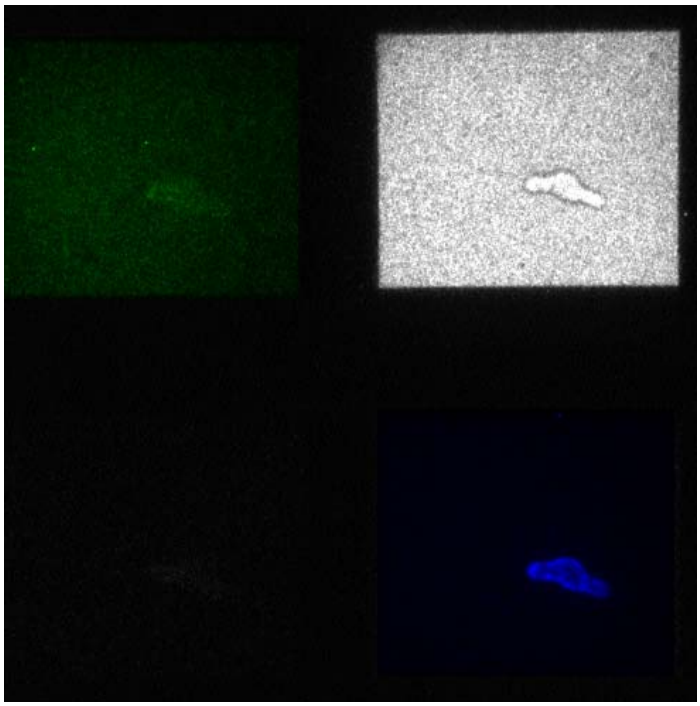

Figure 58: Fluorescent Quadview image of a freshly isolated cremaster smooth muscle cell, loaded with CC2-DMPE (5uM) and DisBAC4(3) (3uM), illuminated at 405nm through a 40X water immersion objective

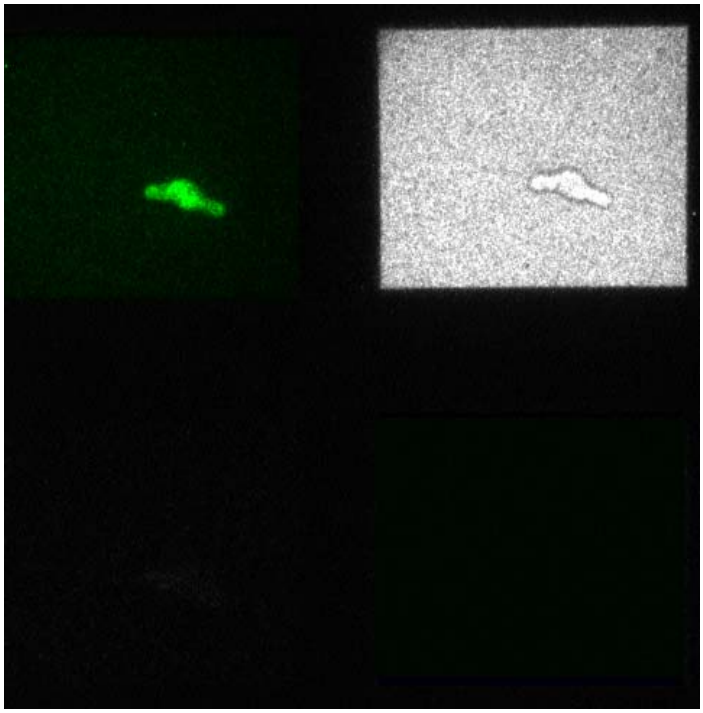

Figure 59: Fluorescent Quadview image of a freshly isolated cremaster smooth muscle cell, loaded with CC2-DMPE (5uM) and DisBAC4(3) (3uM), illuminated at 491nm through a 40X water immersion objective.

8.9 Voltage Sensing by the Em Sensitive FRET Dyes:

Freshly isolated cremaster and cerebral vascular smooth muscle cells were used for these studies. Cells were depolarized using 60mM KCl, and hyperpolarized using 15uM Minoxidil. The cells depolarize and contract when simulated with KCl, hence the fluorescence of the coumarin emission channel increases and oxonol channel decreases, consistent with a change in the membrane potential of the cells. Minoxidil did not cause an apparent hyperpolarization but attenuated the response to a subsequent addition of KCl (n=3). As absolute Em levels of the cells were not known it is uncertain whether the lack of effect of Minoxidil was a function of the initial Em level. Background fluorescence

was subtracted from the 2 emission channels and the data was plotted as the ratio of the coumarin emission to oxonol emission. The data obtained in these set of experiments is shown below. Time control studies were performed at the beginning, halfway through, and at the end of the experiment for cremaster and cerebral cells to show that there is a constant ratiometric signal through out the time period of the experiment. Graded depolarization of the cells was performed by stimulating with varying concentrations of KCl in the cell chamber. A net concentration of the KCl stimuli in the bath was maintained at 30mM, and later 60mM. A step change in voltage sensing was suggested by a proportional change in fluorescence.

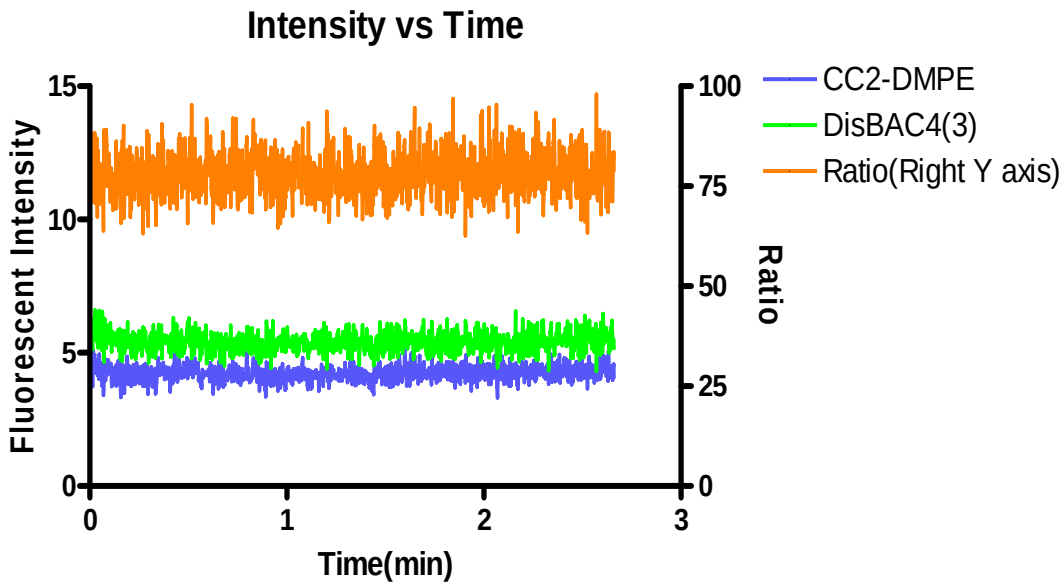

Figure 60: Time control experiment on a VSM cells from cerebral tissue indicating a constant ratiometric signal throughout the time period (3 mins) of the experiment.

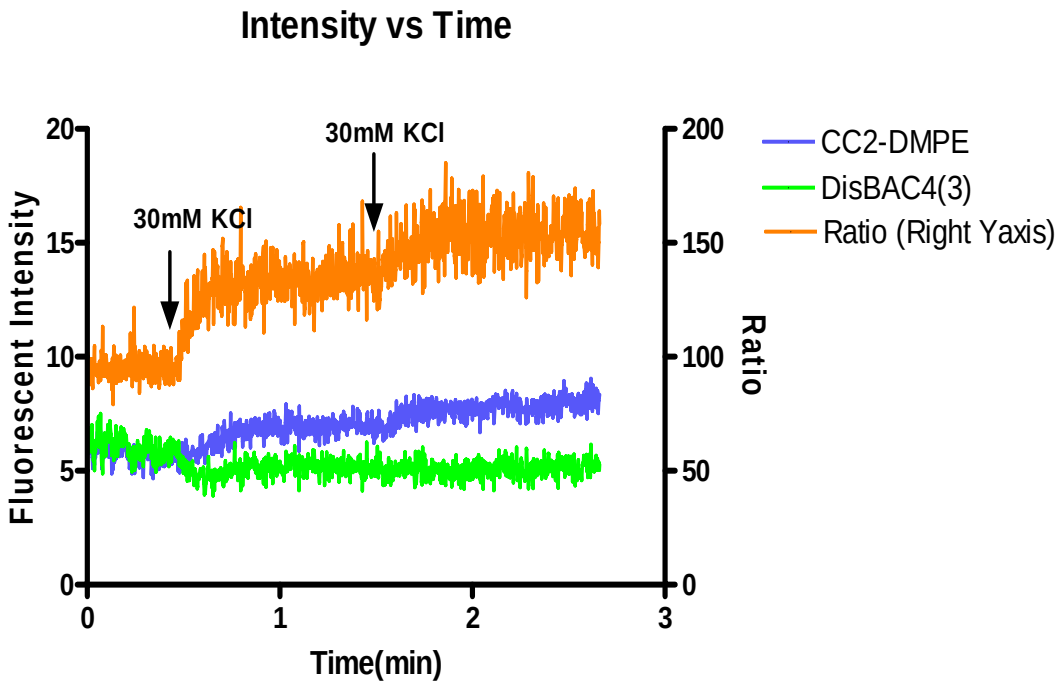

Figure 61: Graph indicating a ratiometric change in the FRET signal for a graded membrane potential change in a VSM cell from cerebral tissue, when stimulated with a depolarizing stimulus of KCl for 3 mins.

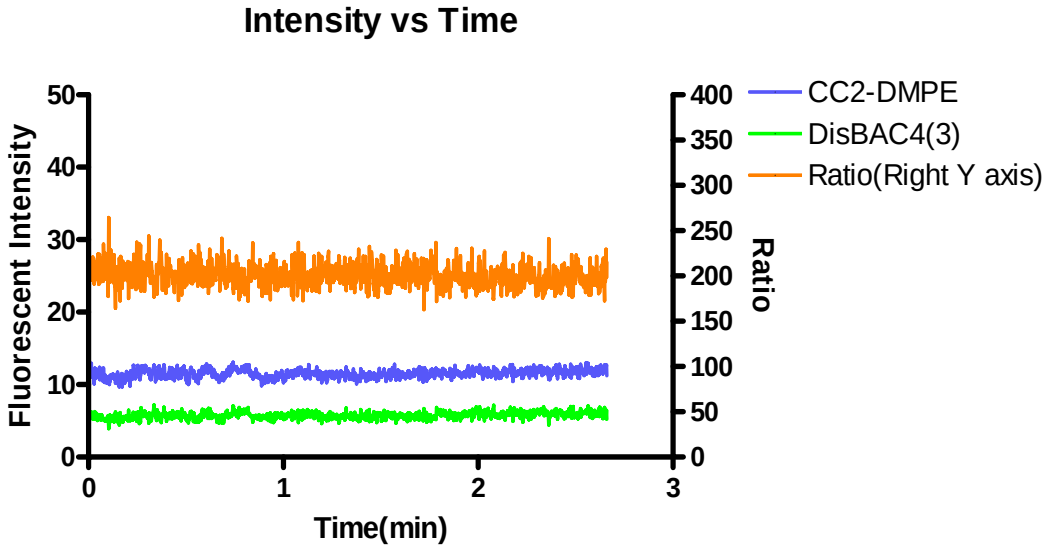

Figure 62: Time control experiment on a VSM of cremaster muscle indicating a constant ratiometric signal throughout the time period (3mins) of the experiment.

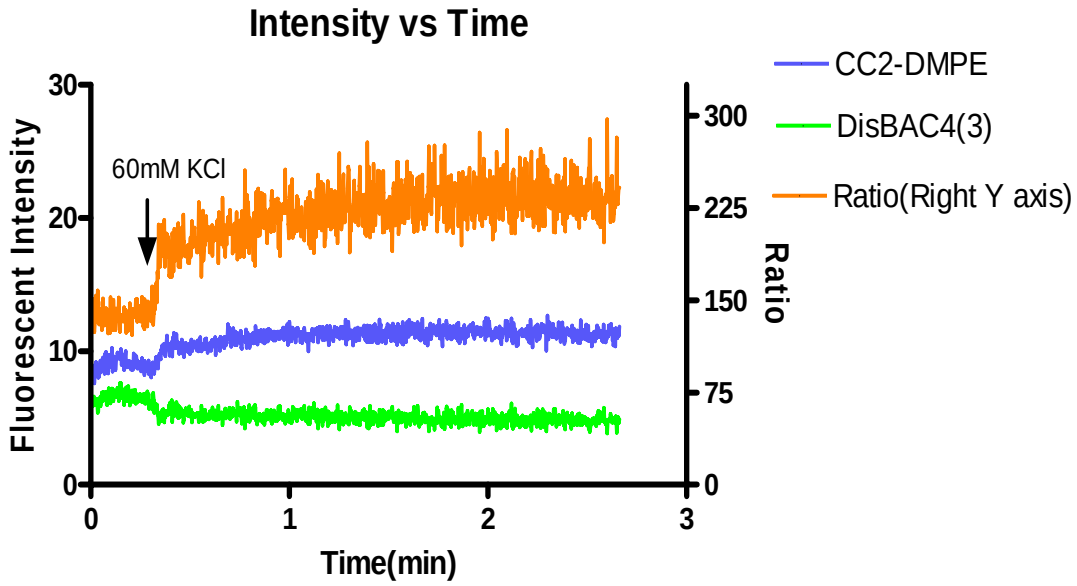

Figure 63: Graph indicating a significant change in the ratiometric FRET signal when VSM of a cremaster muscle subjected to a 60mM KCl depolarization stimuli.

Freshly isolated cerebral and cremaster smooth muscle cells were used for sensing changes in Em using FRET. Data shown below suggests the % change in the fluorescence of VSM cells from cerebral tissue and cremaster muscle when depolarized with a 60mM KCl stimulus

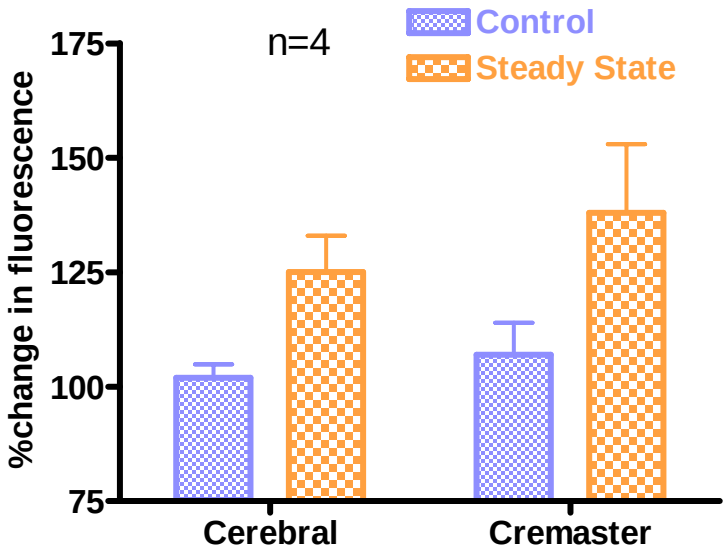

Figure 64: Grouped data of FRET-Em sensing on freshly isolated cerebral and cremaster SMC depolarized with 60mM KCl stimulus.

Smooth muscle cells contract when KCl has its depolarizing effect on the cell. Cell contraction is evident in Figures 65 and 66. Figure 65 shows image of a cell under resting membrane potential loaded with FRET-indicators. Figure 66 shows image of the same cell when depolarized using 60mM KCl.

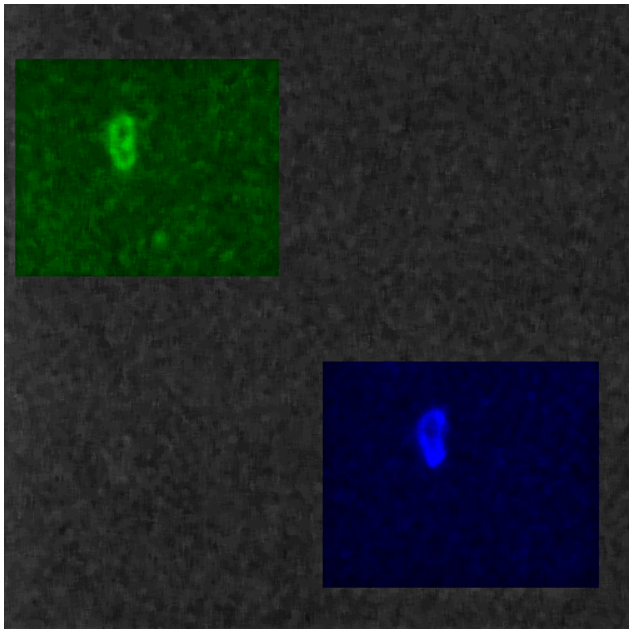

Figure 65: Fluorescent image of a freshly isolated cremaster muscle vascular smooth muscle cell loaded with CC2-DMPE (5uM) and $DisBAC_4(3)$ (3uM) at resting membrane potential

.

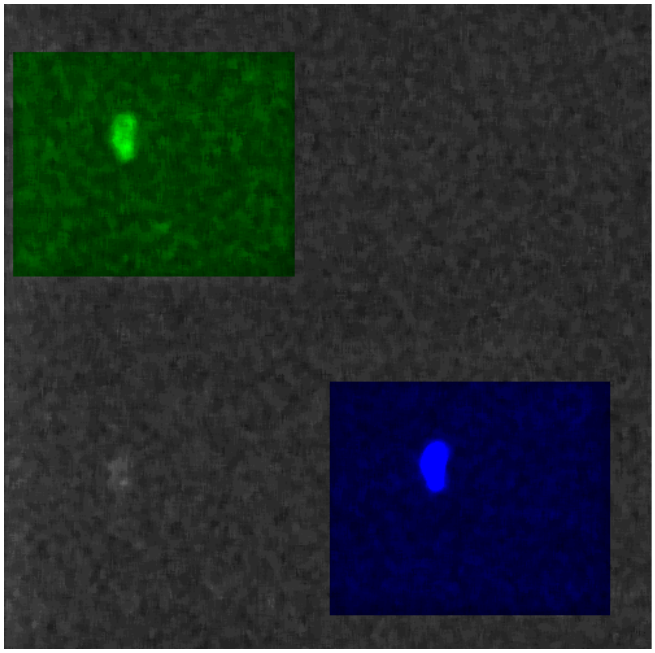

Figure 66: Steady state fluorescent image of a freshly isolated cremaster muscle vascular smooth muscle cell loaded with CC2-DMPE (5uM) and $DisBAC_4(3)$ (3uM) at depolarized state by a KCl stimulus (60mM).

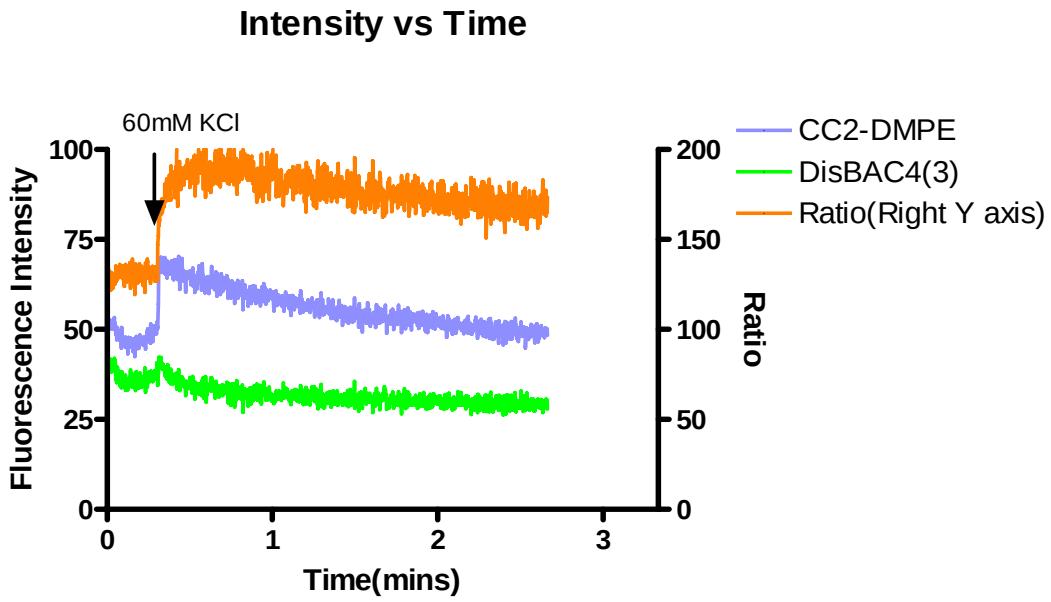

Figure 67: Graph indicating a ratiometric change in the FRET signal for KCl stimuli, on smooth muscle cells treated with Minoxidil, indicating that the depolarization caused initially was not sustained.

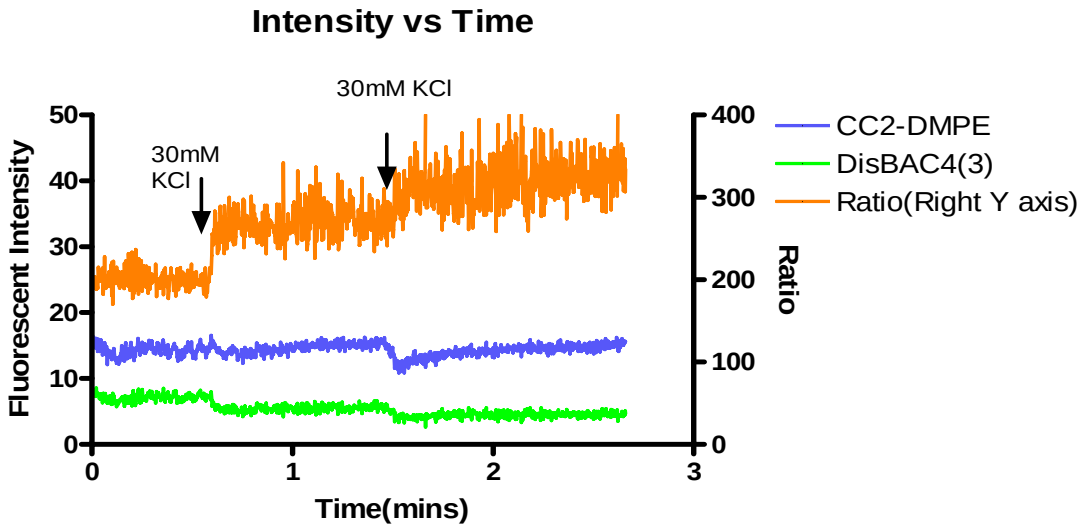

Figure 68: Graph indicating a ratiometric change in the FRET signal for a graded membrane potential change in the cremaster smooth muscle cell, when stimulated with a varying depolarizing stimulus of KCl.

DISCUSSION

The arteriolar myogenic response is critical for local control of microvascular blood flow and pressure [1, 8]. Despite this the roles of a number of the underlying signaling mechanisms remain uncertain. In particular, the exact relationships between transient state events including opening of ion channels, changes in membrane potential and alterations in intracellular calcium have not been fully established. This in part relates to the limitations on current methods used to study these signaling mechanisms. Glass microelectrodes have been reported to measure changes in membrane potential in cannulated arterioles during pressure induced constriction, and agonist stimulation [9]. Data from these studies indicate that while glass electrodes are highly sensitive to Em changes, their use is mostly restricted to steady state measurements. This results from vessel wall movement which results in loss of the impalement, and is thus a major limitation of the technique. Other approaches using conventional fluorescence microscopy have been reported. Such fluorescence-based measurements have also been limited as the indicators typically lack the required signal-to-noise ratio (Eg: di-8-ANEPPS reports 1% change in fluorescence signal/10mV) or time resolution (e.g. carbocyanines and oxonols) [71, 72].

On the basis of the above a promising recent development in the use of fluorescent indicators is the application of FRET techniques to Em measurements [10, 12, 73]. There are many advantages of the FRET-based assays (ratiometric sensing) compared to the

previous indicators. The efficacy of the FRET-indicators CC2-DMPE, and $DisBAC_2(3)$ (or $DisBAC_4(3)$) was previously tested in pancreatic-Beta cells, keratinocytes [59, 60]. In the current project these dyes were tested for toxicity, and were shown to not impact on the viability of VSM cells or the functionality of isolated arterioles.

Specialized optical setup for performing FRET based experiments have been described earlier. These microscopes often require custom designed filters cubes for selectively separating the donor and acceptor fluorescence emissions [12, 50, 51, 59, 60]. Hence a microscope was custom designed to perform Em measurements on smooth muscle cells and arterioles using FRET. Increased complexity in the design came from the ultimate desire to simultaneously/near-simultaneously perform measurements of changes in intracellular calcium and vessel/cell dimensions on the same preparation Significant issues solved in setting up the microscope included parfocalizing multiple ports, correcting signal vignetting in the Quadview optical 'image-splitting' module, and optimizing fluorescence in the emission channels.

Previous studies using confocal iamging on human keratinocytes using FRET reported a sensitivity of approximately 15% change in fluorescence ratio for a 100mV change in Em [11, 60]. This would mean that in studies relevant to myogenic signaling that a change in fluorescence signal may only be in the order of <3% over a physiological range of intraluminal pressures. In the current project, the ability of the system to detect changes in Em when the single cells were stimulated using depolarizing and hyperpolarizing agents is reported. Importantly, our studies were performed on freshly isolated cerebral

and cremaster smooth muscle cells, and cultured cremaster smooth muscle cells and are therefore likely to be relevant to eventual studies to be performed in intact arterioles. Although the studies to date largely represent '*proof of principle*' the signals detected appear greater than that reported for di-8-Anepps and as changes in Em were detected for the depolarizing stimulus provided by 30 mM KCl they are likely to be applicable to studies of myogenic signaling.

In summary, this first usage of FRET-based indicators to report membrane potential changes within smooth muscle cells represents a significant advance in our ability to temporally follow changes in Em and ultimately understand the arteriolar myogenic response in the transient state. In addition, the technology will be more widely applicable and will be of use to many situations where a cellular response is initiated by a change in Em.

CHAPTER 9

CONCLUSIONS

A sophisticated image based method for ultimately investigating the signaling mechanisms involved in the myogenic response of the arterioles has been developed. Introduction of FRET to microvascular studies to measure the membrane potential of smooth muscle cells was performed successfully. The current project suggests we can determine the transient relationship among the prominent variables involved in the signaling mechanisms of the arteriolar myogenic response. A major unresolved aspect in the myogenic signaling cascade is whether pressure induced depolarization in arterioles directly leads to increases in the intracellular calcium through the VDCC's and subsequent development of a contractile force on the lumen of the vessel.

An Olympus IX-71 was custom designed to perform FRET and measure intracellular calcium simultaneously. The design includes two different lasers operated under time multiplexing to illuminate the specimen. A custom designed Quadview module splits the fluorescent light scanned by the spinning disk unit based on wavelength and develops

images which can be directed to a computer by means of an intensified CCD. The images acquired include the details of the events occurring in the cells, and hence were analyzed.

Fluorophores used for FRET and calcium imaging were tested on both single cells and cannulated arterioles to test for any possible toxicity effects and were found to have no apparent adverse effects. Freshly isolated and cultured cremaster smooth muscle cells were stimulated with KCl, a known depolarizing stimuli and a ratiometric change in the fluorescent signal was sensed through the FRET approach. On balance the FRET-ratiometric approach has many potential advantages and relatively high sensitivity compared to the existing methods used for Em measurements in the cells.

CHAPTER 10

FUTURE DIRECTIONS

Our immediate plan is to perform additional optimization experiments of the FRET dye loading. A matrix combination of dyes will be used on cultured and fresh cremaster muscle VSM cells. Efficiency calculations will be performed based on acceptor photobleaching and donor fluorescence in the presence and absence of the acceptor. A fixed concentration combination of dyes is estimated based on the efficiency calculations and will be used for future preparations.

Evidence for dye loading into the smooth muscle cells of arterioles will be shown on vessels gaining tone. Evidence for dye loading will also be estimated on vessels cannulated onto a single long tapered glass pipette. This will allow vessels to be studied in a near isometric state where movement is minimized. Such vessels would not gain the tone as they are not pressurized, but Kreb's buffer will be superfused and temperature of the bath maintained at 34°C.

Em-induced changes in fluorescence under conditions of voltage clamp and raised extracellular K^+ will be used to establish a relation between FRET and Em in smooth

muscle cells and potentially allow calibration. Extension of these studies will be on FRET based measurement of membrane potential in cells and intact arterioles. Ca^{2+} indicator Fluo4-AM will be loaded into the cells and simultaneous detection of Em and cytosolic Ca^{2+} will be performed on cells. Studies will be continued on arterioles for monitoring the changes in arteriolar dimensions due to pressure induced constriction. A relationship among the parameters involved in the arteriolar myogenic response will be estimated.

REFERENCES

1. Davis, M.J. and M.A. Hill, *Signaling mechanisms underlying the vascular myogenic response.* Physiol Rev, 1999. 79(2): p. 387-423.

2. Johnson, P.C., *The Myogenic Response*, in *Handbook of Physiology, The Cardiovascular System, Vascular Smooth Muscle*. 1980. p. 409-442.

3. Johnson, P.C., *Autoregulation of blood flow.* Circ Res, 1986. 59(5): p. 483-95.

4. Davis, M.J. and P.J. Sikes, *Myogenic responses of isolated arterioles: test for a rate-sensitive mechanism.* Am J Physiol, 1990. 259(6 Pt 2): p. H1890-900.

5. Falcone, J.C., M.J. Davis, and G.A. Meininger, *Endothelial independence of myogenic response in isolated skeletal muscle arterioles.* Am J Physiol, 1991. 260(1 Pt 2): p. H130-5.

6. Knot, H.J. and M.T. Nelson, *Regulation of arterial diameter and wall [Ca2+] in cerebral arteries of rat by membrane potential and intravascular pressure.* J Physiol, 1998. 508 (Pt 1): p. 199-209.

7. Jackson, W.F. and K.L. Blair, *Characterization and function of Ca(2+)-activated K+ channels in arteriolar muscle cells.* Am J Physiol, 1998. 274(1 Pt 2): p. H27-34.

8. Jackson, W.F., *Ion channels and vascular tone.* Hypertension, 2000. 35(1 Pt 2): p. 173-8.

9. Kotecha, N. and M.A. Hill, *Myogenic contraction in rat skeletal muscle arterioles: smooth muscle membrane potential and Ca(2+) signaling.* Am J Physiol Heart Circ Physiol, 2005. 289(4): p. H1326-34.

10. Gonzalez, J.E. and R.Y. Tsien, *Improved indicators of cell membrane potential that use fluorescence resonance energy transfer.* Chem Biol, 1997. 4(4): p. 269-77.

11. Cartin, L., K.M. Lounsbury, and M.T. Nelson, *Coupling of Ca(2+) to CREB activation and gene expression in intact cerebral arteries from mouse : roles of ryanodine receptors and voltage-dependent Ca(2+) channels.* Circ Res, 2000. 86(7): p. 760-7.

12. Gonzalez, J.E. and R.Y. Tsien, *Voltage sensing by fluorescence resonance energy transfer in single cells.* Biophys J, 1995. 69(4): p. 1272-80.

13. Mulvany, M.J. and C. Aalkjaer, *Structure and function of small arteries.* Physiol Rev, 1990. 70(4): p. 921-61.

14. Schubert, R. and M.J. Mulvany, *The myogenic response: established facts and attractive hypotheses.* Clin Sci (Lond), 1999. 96(4): p. 313-26.

15. Mulvany, M.J., *Structure and function of small arteries in hypertension.* J Hypertens Suppl, 1990. 8(7): p. S225-32.

16. Lombard, J.H., *Effect of reduced oxygen availability upon myogenic depolarization and contraction of cat middle cerebral artery.* Circ Res, 1986. 58(4): p. 565-9.

17. Meininger, G.A. and M.J. Davis, *Cellular mechanisms involved in the vascular myogenic response.* Am J Physiol, 1992. 263(3 Pt 2): p. H647-59.

18. Hill, M.A., *Invited review: arteriolar smooth muscle mechanotransduction: Ca(2+) signaling pathways underlying myogenic reactivity.* J Appl Physiol, 2001. 91(2): p. 973-83.

19. Bayliss, W.M., *On the local reactions of the arterial wall to changes of internal pressure.* J Physiol, 1902. 28(3): p. 220-31.

20. Selkurt, E.E. and P.C. Johnson, *Effect of acute elevation of portal venous pressure on mesenteric blood volume, interstitial fluid volume and hemodynamics.* Circ Res, 1958. 6(5): p. 592-9.

21. Selkurt, E.E., M.P. Scibetta, and T.E. Cull, *Hemodynamics of intestinal circulation.* Circ Res, 1958. 6(1): p. 92-9.

22. Wiederhielm, C.A., *Effects of temperature and transmural pressure on contractile activity of vascular smooth muscle.* Bibl Anat, 1967. 9: p. 321-7.

23. Duling, B.R., *Methods for isolation, cannulation, and in vitro study of single microvessels.* Am J Physiol, 1981. 241(1): p. H108-116.

24. Hill, M.A. and E.A. Ege, *Active and passive mechanical properties of isolated arterioles from STZ-induced diabetic rats. Effect of aminoguanidine treatment.* Diabetes, 1994. 43(12): p. 1450-6.

25. Nelson, M.T. and J.M. Quayle, *Physiological roles and properties of potassium channels in arterial smooth muscle.* Am J Physiol, 1995. 268(4 Pt 1): p. C799-822.

26. Nelson, M.T., *Relaxation of arterial smooth muscle by calcium sparks.* Science, 1995. 270(5236): p. 633-7.

27. Loutzenhiser, R., L. Chilton, and G. Trottier, *Membrane potential measurements in renal afferent and efferent arterioles: actions of angiotensin II.* Am J Physiol, 1997. 273(2 Pt 2): p. F307-14.

28. Potocnik, S.J., *Effects of mibefradil and nifedipine on arteriolar myogenic responsiveness and intracellular Ca(2+).* Br J Pharmacol, 2000. 131(6): p. 1065-72.

29. Harder, D.R., *Increased sensitivity of cat cerebral arteries to serotonin upon elevation of transmural pressure.* Pflugers Arch, 1988. 411(6): p. 698-700.

30. Welsh, D.G., et al., *Transient receptor potential channels regulate myogenic tone of resistance arteries.* Circ Res, 2002. 90(3): p. 248-50.

31. Earley, S., B.J. Waldron, and J.E. Brayden, *Critical role for transient receptor potential channel TRPM4 in myogenic constriction of cerebral arteries.* Circ Res, 2004. 95(9): p. 922-9.

32. Ganitkevich, V. and G. Isenberg, *Membrane potential modulates inositol 1,4,5-trisphosphate-mediated Ca2+ transients in guinea-pig coronary myocytes.* J Physiol, 1993. 470: p. 35-44.

33. Kukuljan, M., *Membrane potential regulates inositol 1,4,5-trisphosphate-controlled cytoplasmic Ca2+ oscillations in pituitary gonadotrophs.* J Biol Chem, 1994. 269(7): p. 4860-5.

34. Ganitkevich, V. and G. Isenberg, *Ca2+ entry through Na(+)-Ca2+ exchange can trigger Ca2+ release from Ca2+ stores in Na(+)-loaded guinea-pig coronary myocytes.* J Physiol, 1993. 468: p. 225-43.

35. Yamagishi, T., T. Yanagisawa, and N. Taira, *K+ channel openers, cromakalim and Ki4032, inhibit agonist-induced Ca2+ release in canine coronary artery.* Naunyn Schmiedebergs Arch Pharmacol, 1992. 346(6): p. 691-700.

36. Noma, A., *ATP-regulated K+ channels in cardiac muscle.* Nature, 1983. 305(5930): p. 147-8.

37. Jackson, W.F., *Arteriolar tone is determined by activity of ATP-sensitive potassium channels.* Am J Physiol, 1993. 265(5 Pt 2): p. H1797-803.

38. Yamazaki, J., *Functional and molecular expression of volume-regulated chloride channels in canine vascular smooth muscle cells.* J Physiol, 1998. 507 (Pt 3): p. 729-36.

39. Jan, L.Y. and Y.N. Jan, *Voltage-gated and inwardly rectifying potassium channels.* J Physiol, 1997. 505 (Pt 2): p. 267-82.

40. Nichols, C.G. and A.N. Lopatin, *Inward rectifier potassium channels.* Annu Rev Physiol, 1997. 59: p. 171-91.

41. Large, W.A. and Q. Wang, *Characteristics and physiological role of the Ca(2+)-activated Cl- conductance in smooth muscle.* Am J Physiol, 1996. 271(2 Pt 1): p. C435-54.

42. Nelson, M.T., *Chloride channel blockers inhibit myogenic tone in rat cerebral arteries.* J Physiol, 1997. 502 (Pt 2): p. 259-64.

43. Minsky, M., *Memoir in inventing the confocal microscope.* . Scanning 1988. 10: p. 10.

44. Brakenhoff, G., *Confocal Scanning Light Microscopy with High Aperture Immersion Lenses.* Journal of Microscopy, 1979. 117: p. 13.

45. Semwogerere, D., *Confocal Microscopy*, in *Encyclopedia of Biomaterials and Biomedical Engineering*. 2005.

46. Porter, T., *Compositing digital images.* Comput. Graphics, 1984. 18(3): p. 6.

47. Keller, H., *Objective lenses for confocal microscopy.* In Handbook of Biological Confocal Microscopy, 1995. 2: p. 15.

48. Wilson, T., *The role of pinhole in confocal imaging system.* In Handbook of Biological Confocal Microscopy, 1995: p. 15.

49. Becker, P., *Quantitative fluorescence measurements.* Fluorescence Imaging Spectroscopy and Microscopy, 1996: p. 29.

50. Vogel, S.S., C. Thaler, and S.V. Koushik, *Fanciful FRET.* Sci STKE, 2006.(331): p. re2.

51. Jares-Erijman, E.A. and T.M. Jovin, *FRET imaging.* Nat Biotechnol, 2003. 21(11): p. 1387-95.

52. Wallrabe, H. and A. Periasamy, *Imaging protein molecules using FRET and FLIM microscopy.* Curr Opin Biotechnol, 2005. 16(1): p. 19-27.

53. Gonzalez, J.E. and M.P. Maher, *Cellular fluorescent indicators and voltage/ion probe reader (VIPR) tools for ion channel and receptor drug discovery.* Receptors Channels, 2002. 8(5-6): p. 283-95.

54. Szollosi, J., *Applications of fluorescence resonance energy transfer for mapping biological membranes.* J Biotechnol, 2002. 82(3): p. 251-66.

55. Tadakuma, H., *Imaging of single fluorescent molecules using video-rate confocal microscopy.* Biochem Biophys Res Commun, 2001. 287(2): p. 323-7.

56. Sguilla, F.S., A.C. Tedesco, and L.M. Bendhack, *A membrane potential-sensitive dye for vascular smooth muscle cells assays.* Biochem Biophys Res Commun, 2003. 301(1): p. 113-8.

57. Elangovan, M., *Characterization of one- and two-photon excitation fluorescence resonance energy transfer microscopy.* Methods, 2003. 29(1): p. 58-73.

58. Mackenzie, L., *The spatial pattern of atrial cardiomyocyte calcium signalling modulates contraction.* J Cell Sci, 2004. 117(Pt 26): p. 6327-37.

59. Kuznetsov, A., *FRET-based voltage probes for confocal imaging: membrane potential oscillations throughout pancreatic islets*, in *Am J Physiol Cell Physiol*. 2005. p. C224-9.

60. Burgstahler, *Confocal ratiometric voltage imaging of cultured human keratinocytes reveals layer-specific responses to ATP.* Am J Physiol Cell Physiol, 2003. 284(4): p. C944-52.

61. Mandala, M., *The fluorescent cationic dye rhodamine 6G as a probe for membrane potential in bovine aortic endothelial cells.* Anal Biochem, 1999. 274(1): p. 1-6.

62. Flewelling, R.F. and W.L. Hubbell, *The membrane dipole potential in a total membrane potential model. Applications to hydrophobic ion interactions with membranes.* Biophys J, 1986. 49(2): p. 541-52.

63. Huang, C.J., *Characterization of voltage-gated sodium-channel blockers by electrical stimulation and fluorescence detection of membrane potential.* Nat Biotechnol, 2006. 24(4): p. 439-46.

64. Jackson, P.A. and B.R. Duling, *Myogenic response and wall mechanics of arterioles.* Am J Physiol, 1989. 257(4 Pt 2): p. H1147-55.

65. Meininger, G.A., *Calcium measurement in isolated arterioles during myogenic and agonist stimulation.* Am J Physiol, 1991. 261(3 Pt 2): p. H950-9.

66. Zou, H., P.H. Ratz, and M.A. Hill, *Role of myosin phosphorylation and [Ca2+]i in myogenic reactivity and arteriolar tone.* Am J Physiol, 1995. 269(5 Pt 2): p. H1590-6.

67. Meininger, G.A., *Myogenic vasoregulation overrides local metabolic control in resting rat skeletal muscle.* Circ Res, 1987. 60(6): p. 861-70.

68. Duza, T. and I.H. Sarelius, *Localized transient increases in endothelial cell Ca2+ in arterioles in situ: implications for coordination of vascular function.* Am J Physiol Heart Circ Physiol, 2004. 286(6): p. H2322-31.

69. Reichman, *Handbook of Optical Filters for Fluorescence Microscopy.* 2000: p. 37.

70. Kawamura, S., *Confocal Laser Microscope Scanner and CCD Camera.* 2002. 33.

71. Bullen, A., S.S. Patel, and P. Saggau, *High-speed, random-access fluorescence microscopy: I. High-resolution optical recording with voltage-sensitive dyes and ion indicators.* Biophys J, 1997. 73(1): p. 477-91.

72. Bullen, A. and P. Saggau, *High-speed, random-access fluorescence microscopy: II. Fast quantitative measurements with voltage-sensitive dyes.* Biophys J, 1999. 76(4): p. 2272-87.

73. Gonzalez, J.E., *Cell-based assays and instrumentation for screening ion-channel targets.* Drug Discov Today, 1999. 4(9): p. 431-439.